Scuola Internazionale Superiore di Studi Avanzati

Physics Area
Ph.D. Course in Theoretical Particle Physics

Thesis submitted for the degree of Doctor Philosophiae

Matter fields, gravity and Asymptotic Safety

Supervisor:
Prof. Roberto Percacci

Candidate:
Pietro Donà

Academic Year 2013-2014

Contents

Introduction

The unification of Quantum Mechanics (QM) and General Relativity (GR) is still a challenge in contemporary Physics. In spite of the fact that both theories have been formulated and studied for more than a century and that a lot of efforts have been made to combine the principles of the two theories, we do not yet have a consistent Quantum Field Theory (QFT) of Gravitation that describes Planck scale physics in a satisfactory way.

There are many reasons to believe that gravity should be quantised. First of all, one sees that the other three known fundamental forces are taken into account very accurately by quantum theories. In particular, electromagnetism, like gravity, has a macroscopic manifestation which can be described accurately by a classical field theory, but at a microscopic level is described by a QFT. Furthermore, the belief that a unified description of all fundamental interactions must exist demands a quantum picture of gravitation too. Another motivation comes from the existence of spacetime singularities which make classical GR incomplete; some form of discreteness of spacetime at the quantum level would eliminate the ultraviolet (UV) divergences that appear in standard QFTs, providing a physical cutoff for high momenta.

The traditional approach to building a QFT is based on the perturbative quantization of a classical field theory. The physical quantities are expanded in power series of $\hbar$ or of the coupling constants and in order to reabsorb the UV divergences in the action the coupling constants have to be suitably redefined (renormalization). If the attempt is successful a finite, consistent theory is obtained, which only needs a finite number of parameters to be fixed experimentally, and therefore is predictive.

This scheme of perturbative renormalizability had a lot of success with theories that describe physical phenomena in our universe (QED, non-Abelian gauge theories, scalar theories). The amazing experimental precision of the Standard Model indeed shows that perturbation theory is a very powerful tool to solve the problems of a QFT.

Nevertheless, GR does not fit well within this scheme, in fact, it is well-known that performing a perturbative quantisation of the classical GR action

does not lead to a satisfactory QFT.

Explicit calculations show that in flat space the theory is finite at one-loop [1]. However, it was shown in [2], [3] that at the two-loop order appear infinities that require a cubic terms in the curvature to be cancelled. Such terms would lead to divergences proportional to higher powers of curvature and so on, requiring infinitely many renormalisation conditions to be imposed, so that the theory cannot be predictive. In the presence of matter fields, such infinities appear already at the one-loop order.

If a theory is not perturbatively renormalizable, it might be a low-energy effective approximation of a more fundamental theory. This is exactly what happened historically with the Fermi theory and subsequently led to the discovery of the Z and $W^{\pm}$ bosons. It would be tempting to say that this is the case of GR, and that the metric is not a fundamental degree of freedom. The most prominent approach that so far has extended the quantum theory consistently is String Theory [4].

Another common alternative is to think that the issue does not lie in GR but rather in the process of applying the perturbative technique to this theory. The non renormalizability of the theory does not necessarily imply that GR and QM are incompatible. The line of research that has gone the farthest in this direction is Loop Quantum Gravity (LQG) along with its covariant form, the Spin Foam formalism [5].

Before abandoning the QFT picture one should consider whether it is possible to make sense of quantum gravity within some form of non perturbative QFT. This is what will be discussed in this Thesis. The issue we would like to explore here is whether one can give GR the status of a fundamental theory, from which predictions can be extracted for observable quantities at all energy scales, without encountering UV divergences. Among the approaches that maintain the formalism of a continuous QFT, the most promising seems to be Asymptotic Safety, a proposal put forward by S. Weinberg in 1979 [6] and revived in the last two decades.

The essential ingredient of this approach is the existence of an ultraviolet interacting Fixed Point (FP) in the Renormalization Group (RG) flow of gravitational couplings. The existence of the FP guarantees that physical quantities will not blow up when the energy scale tends to ∞. Moreover predictivity can be preserved if all but a finite number of couplings are UV-repulsive at the FP.

In particular in this Thesis some aspects of the renormalization group flow of gravity in presence of fermions are investigated. In the first part we will discuss the sign of the fermionic contribution to the running of Newton's constant, which depends on details of the cutoff. Then we calculate the graviton contributions to the beta functions in the tetrad formalism.

Secondly the compatibility of minimally coupled matter fields with asymptotically safe quantum gravity is discussed. The main novelty is the explicit computation of the graviton and matter anomalous dimension, their inclusion in the beta functions seems to reduce the non-linearity that arises with the standard identification of the graviton anomalous dimension with the background one. Finally another step towards the extension of the truncation to a bimetric computation is taken with the inclusion of the graviton "mass" term.

Outline of the thesis In Chapter 1 we review the basics of the formalism used in the Functional Renormalization Group (FRG), in order to set the notation used throughout this work.

In Chapter 2 the Asymptotic Safety framework is presented and its key properties are discussed.

In Chapter 3 the techniques of FRG are applied to the case of gravity in the Einstein-Hilbert truncation.

In Chapter 4 we discuss the minimal coupling of fermions field to tetrad gravity. We present and solve the sign ambiguity in the choice of the cutoff for fermion fields and we analyze the properties of the fixed point when the fundamental degrees of freedom are carried by a tetrad field.

In Chapter 5 we compute the gravitational anomalous dimension we use them to find constraints on the number of matter fields we can couple to gravity without spoiling asymptotic safety.

Chapter 1

Functional Renormalization Group

In the following we are going to give a very simple introduction to a quantum field theory, through the method of generating functionals. Most of the subsequent concepts we are going to introduce, can of course be refined depending on the subject under study. Our aim is to fix the notations we will use and collect the necessary tools and minimal structures needed for the understanding of the next chapters, avoiding most of the complications.

1.1 Functional formulation of QFT

Let ϕ be a field that take values on a spacetime $\mathcal{M}$; we will build our Quantum Field Theory (QFT) using it as a fundamental building brick. We will assume from now on that the spacetime $\mathcal{M}$ we are working on is Euclidean and in general a Riemaniann manifold, so a notion of distance among points is provided.

It is common knowledge that the QFTs that are useful for describing the physical world are Minkowskian, rather than Euclidean like the one we are building. For this reason we will also always assume that the things we are going to compute will admit a translation, or even a direct interpretation, in terms of some associated Minkowskian field theory. This is generally done in terms of Wick rotations to imaginary time.

We can think of the physical content of a field theory as encoded in the n-point correlation functions of the field ϕ, defined in the following way

$$G^{(n)\mathcal{A}_1,\dots,\mathcal{A}_n} = \left\langle \phi^{\mathcal{A}_1} \cdots \phi^{\mathcal{A}_n} \right\rangle , \tag{1.1}$$

where the labels $\mathcal{A}$ summarize any possible internal indices and a point of

the space-time $\mathcal{M}$. We will assume that when repeated labels (and indices) are present a summation and integration is implied.

We implicitly assume that there is a way to relate the functions $G^{(n)}$ to observable quantities. In general a complete knowledge of the correlation functions imply a complete knowledge of the theory and its physics.

To define the formalism we are still missing the definition of a measure and a probability density. Formally we will denote the measure as $\mathcal{D}\phi$ and the probability density as $\mathcal{P}[\phi]$ and we will use them to weight field configurations.

In particular we ask for the expectation value of a general field configuration $\mathcal{O}[\phi]$ to be computed as

$$\langle \mathcal{O}[\phi] \rangle = \frac{1}{Z} \int \mathcal{D}\phi \mathcal{P}[\phi] \mathcal{O}[\phi]. \tag{1.2}$$

Here Z is a normalization factor for our probability, we will come back to it later. In the same way we can also define the correlation functions

$$\left\langle \phi^{\mathcal{A}_1} \cdots \phi^{\mathcal{A}_n} \right\rangle = \frac{1}{Z} \int \mathcal{D}\phi \mathcal{P}[\phi] \phi^{\mathcal{A}_1} \cdots \phi^{\mathcal{A}_n}. \tag{1.3}$$

Here we may also give a distinction between classical and quantum field theory. In a classical field theory the configuration of ϕ is known once enough boundary conditions are specified and the equations of motion are solved and we call it ϕ_{cl}. In doing so it is obvious that the probability density must be a delta functional $P_{cl} = \delta(\phi - \phi_{cl})$ with respect to the measure $\mathcal{D}\phi$. In the general, quantum, case no particular configuration is picked up by the measure. In our Euclidean formalism the probability is parametrized as

$$P_{quantum}[\phi] = e^{-S[\phi]}. \tag{1.4}$$

Here we introduced the action functional $S[\phi]$ of our theory.

From now on we will address the quantum case, dropping the distinctive label. A systematic way to calculate the correlation functions is obtained introducing a source current J and coupling it to our field ϕ. We start by computing the normalization factor, sometimes also called partition function of the theory

$$Z = \int \mathcal{D}\phi e^{-S[\phi]}. \tag{1.5}$$

Then we modify the partition function by adding to the action a source coupling term making it a functional of the current

$$Z[J] = \int \mathcal{D}\phi e^{-S[\phi] + J_{\mathcal{A}}\phi^{\mathcal{A}}}. \tag{1.6}$$

If we expand $Z[J]$ in a Taylor series around $J = 0$ it becomes obvious that it is a generating functional for the correlations

$$Z[J]/Z = 1 + J_{\mathcal{A}_1}\left\langle \phi^{\mathcal{A}_1}\right\rangle + \frac{1}{2}J_{\mathcal{A}_1}J_{\mathcal{A}_2}\left\langle \phi^{\mathcal{A}_1}\phi^{\mathcal{A}_2}\right\rangle + \cdots$$
$$\Longrightarrow \left\langle \phi^{\mathcal{A}_1}\cdots\phi^{\mathcal{A}_n}\right\rangle = \frac{1}{Z}\frac{\delta^n}{\delta J_{\mathcal{A}_1}\cdots\delta J_{\mathcal{A}_n}}Z[J]\,|_{J=0}. \tag{1.7}$$

In the rest of the thesis we will call the source dependent functional $Z[J]$, the partition function, and Z will be referred just as a normalization factor. At this point we are ready to define another generating functional, which is usually called the generator of connected n-point functions

$$W[J] = \log\, Z[J], \tag{1.8}$$

and they are generated by taking derivatives respect to J.

$$G^{(n)\text{conn, }\mathcal{A}_1,\ldots,\mathcal{A}_n} = \frac{\delta^n}{\delta J_{\mathcal{A}_1}\cdots\delta J_{\mathcal{A}_n}}W[J]\,|_{J=0}. \tag{1.9}$$

1.1.1 A useful example

Before going on with the formal construction of our QFT it is useful to look at an explicit example. Let the action functional be

$$S[\phi] = \frac{1}{2}\phi^{\mathcal{A}}\Delta_{\mathcal{A}\mathcal{B}}\phi^{\mathcal{B}} + V[\phi]. \tag{1.10}$$

These two terms can be seen as a kinetic one plus an interaction via a potential V. In particular we can call $S_0[\phi] = \frac{1}{2}\phi^{\mathcal{A}}\Delta_{\mathcal{A}\mathcal{B}}\phi^{B}$. On flat space-time the kernel Δ represent the propagation of the states of our field. To be more concrete we can further specify Δ to be a local differential operator, say for example $-\partial_\mu\partial^\mu$ or the Dirac operator $\gamma_\mu\partial^\mu$. A general theory with action $S_0[\phi]$ is easily solved if Δ is invertible. To this end just calculate the functional

$$Z_0[J] = \int \mathcal{D}\phi e^{-S_0[\phi]+J_{\mathcal{A}}\phi^{\mathcal{A}}} = C\text{Exp}\left(\frac{1}{2}J_{\mathcal{A}}(\Delta^{-1})^{\mathcal{A}\mathcal{B}}J_{\mathcal{B}}\right). \tag{1.11}$$

where C is a normalization factor that can be neglected because it does not depend on the current. This can be also taken as the formal definition of the gaussian integration over the space of fields.

Now we can try to justify the name "generator of connected n-point functions". We introduce a diagrammatic representation of a generic n-point

function we can derive from (1.11). To do that one has to draw a point for each label $\mathcal{A}_i$ of the field. Having done this, it is sufficient to join a couple of points $(\mathcal{A}, \mathcal{B})$ with a segment any time $(\Delta^{-1})^{\mathcal{AB}}$ appears. The n-point correlation functions for the free theory are said to be disconnected, when n is larger than two, because the segments do not join at any point, so they are all separated. Actually this is rather trivial having introduced no interactions. The only connected function being

$$\left\langle \phi^{\mathcal{A}} \phi^{\mathcal{B}} \right\rangle_0 = \left(\Delta^{-1}\right)^{\mathcal{AB}}, \tag{1.12}$$

that is precisely the building block for all the other correlators. If one looks at the associated functional

$$W_0\left[J\right] = \frac{1}{2} J_{\mathcal{A}} \left(\Delta^{-1}\right)^{\mathcal{AB}} J_{\mathcal{B}}, \tag{1.13}$$

one easily realises that it is the generator of the (only) connected function of the system.

Next we can try to include interactions via a potential $V\left[\phi\right]$. A model like this is not generally explicitly solvable, but still we can manipulate it a little bit. Notice that

$$Z\left[J\right] = \int \mathcal{D}\phi e^{-V[\phi]} e^{-S_0[\phi] + J_{\mathcal{A}}\phi^{\mathcal{A}}} = e^{V\left[\frac{\delta}{\delta J}\right]} Z_0\left[J\right]. \tag{1.14}$$

If the pre-factor e^{-V} is expanded, any term is going to look like a combination of correlations functions of the free theory. The only modifications being vertices, whose number of external lines are determined by the characteristics of $V\left[\phi\right]$.

This procedure sets the groundwork of what is called perturbative expansion. It is possible to show that the n-point correlation functions generated by $W\left[J\right]$ are those of $Z\left[J\right]$ provided one removes all the diagrams that some disconnected segments. This finally explains the reason of the name generator of connected n-point functions. Before concluding this section we need to introduce one final, and perhaps more important, functional. We start considering the J-dependent 1-point function

$$\bar{\phi}^{\mathcal{A}} = \left\langle \phi^{\mathcal{A}} \right\rangle_J, \tag{1.15}$$

that defines the field $\bar{\phi}^{\mathcal{A}}$. It is, under some still unspecified meaning, a quantum "cousin" of $\phi^{\mathcal{A}}$. Obviously $\bar{\phi}^{\mathcal{A}}$ is a functional of the sources $J_{\mathcal{A}}$. We assume it is invertible, leading to $J_{\mathcal{A}} = J_{\mathcal{A}}\left[\bar{\phi}\right]$ and define the Legendre transform

$$\Gamma\left[\bar{\phi}\right] = \bar{\phi}^{\mathcal{A}} J_{\mathcal{A}} - W\left[J\left[\bar{\phi}\right]\right]. \tag{1.16}$$

The transform $\Gamma\left[\bar{\phi}\right]$ is called effective action (EA). It is also a generating functional and its correlators are defined as

$$\Gamma^{(n)}_{\mathcal{A}_1,\ldots,\mathcal{A}_n} = \frac{\delta^n}{\delta\bar{\phi}^{\mathcal{A}_1}\ldots\delta\bar{\phi}^{\mathcal{A}_n}}\Gamma\left[\bar{\phi}\right]. \tag{1.17}$$

The computation of the effective action is often a really complicated task, especially if one does not have theories with many symmetries and spacetime is not two dimensional, or both. The purpose of the next sections is to highlight the technical problems shadowed in the discussion up to now. We will also further extend our definitions, giving up however to some generality as a price of clarity.

1.2 Wilson approach

When we deal with perturbative renormalization of a QFT we think about scale dependent couplings, this is a consequence of the need of renormalization of QFT. We would like to address the issue of scale dependence from the very beginning, introducing scale dependent functionals in such a way this characteristic is built-in in the formalism. This is quite challenging starting from perturbation theory, where the scale emerges in the development.

A systematic attempt to introduce scale dependence in the functionals we constructed before is due to Wilson [7]. For simplicity we begin by considering spacetime to be a flat d-dimensional Euclidean manifold $\mathbb{R}^d$. We shall also take the field ϕ to be a scalar. We have now a natural basis, the momentum basis, to expand the field

$$\phi(x) = \int d^d q \phi_q e^{iqx}, \tag{1.18}$$

and a natural representation for the measure

$$\mathcal{D}\phi(x) = \prod_{q\in\mathbb{R}^d} d\phi_q. \tag{1.19}$$

Therefore following the procedure of the former sections formally the partition function would be

$$Z = \int \prod_{q\in\mathbb{R}^d} d\phi_q e^{-S[\phi]}. \tag{1.20}$$

This is of course ill defined because in explicit calculations it is generally divergent, due to the infinitely many modes the field can have. These divergences come from the unbounded integrations in momentum space. We therefore introduce a cutoff Λ and a certain action $S_\Lambda[\phi]$ such that

$$\int \prod_{q\in\mathbb{R}^d} d\phi_q e^{-S[\phi]} \to \int \prod_{\substack{q\in\mathbb{R}^d,\\ |q|<\Lambda}} d\phi_q e^{-S_\Lambda[\phi]} \equiv Z. \tag{1.21}$$

We introduced the cutoff to work with finite expressions regularizing the divergences in the correlations. We modified the action and the measure at the same time and we further asked that both modifications together match and reproduce the same partition function.

From the point of view of the interpretation it makes sense to think of $S_\Lambda[\phi]$ as a certain ultraviolet (UV) action that contains the information of our theory if large energies are addressed (small scales by the dual relation).

If Λ is a very big scale beyond which we do not know the behavior of the theory, it makes sense to associate it to the UV action of a theory with a hard cutoff. In general we could pick any scale k and perform the same trick to write Z and this is precisely what we are going to do now. We define a new action $S_k[\phi]$ as that particular action for which

$$e^{-S_k[\phi]} = \int \prod_{\substack{q\in\mathbb{R}^d,\\ k<|q|<\Lambda}} d\phi_q e^{-S_\Lambda[\phi]}. \tag{1.22}$$

It is possible to relate $S_k[\phi]$ with $S_\Lambda[\phi]$ by comparison of the two expressions

$$Z = \int \prod_{\substack{q\in\mathbb{R}^d,\\ |q|<k<\Lambda}} d\phi_q e^{-S_k[\phi]}. \tag{1.23}$$

We can interpret $S_\Lambda[\phi]$ as the UV action of a theory possessing a hard cutoff and $S_k[\phi]$ as the result of integrating all the modes in the shell $k < |q| < \Lambda$ towards IR.

We call $S_k[\phi]$ Wilson effective actions. We have constructed a one parameter family of actions labelled by a scale k. These actions are supposed to contain a good description of the physics at the associated scale. A good reason to believe it is that, by definition, only the modes

$$|q| \approx k$$

are active at the given scale and therefore we are, under some approximation, describing their physics. To understand this more precisely it is necessary to refine the technique using a blocking procedure to provide us an actual way to calculate the Wilson effective action.

1.2.1 Blocking

We start to define our blocking procedure by smearing the field over a distribution $\rho_k(x)$. The choice of its shape is not unique. For simplicity we will chose to smear over a sharp cutoff form

$$\rho_k(x) = \int_q \theta(k-q)\, e^{iqx}. \tag{1.24}$$

This choice lets us distinguish between slow (ϕ_-) and fast (ϕ_+) modes

$$\phi_-(x) = \int_y \rho_k(x-y)\,\phi(y) \qquad \text{and} \qquad \phi_+(x) = \phi(x) - \phi_-(x). \tag{1.25}$$

We can now try to evaluate the Wilson effective action $S_k[\phi_-]$

$$e^{-S_k[\phi_-]} = \int \mathcal{D}\phi_+ e^{-S_\Lambda[\phi_- + \phi_+]}. \tag{1.26}$$

It is sufficient to expand quadratically the action $S[\phi]$ in ϕ_+ and perform the gaussian integration to have an approximate result

$$S_k[\phi_-] = S[\phi_-] + \frac{1}{2}\mathrm{Tr}_{k<q}\mathrm{Log}\, S^{(2)}[\phi]\Big|_{\phi=\phi_-} + \cdots, \tag{1.27}$$

where $S^{(2)}$ is the second functional derivative of S.

As it is indicated the trace, that in this case is essentially an integration over the Fourier coefficients, has a lower bound k. This essentially means that we are integrating the fast modes down to the scale we are interested in.

Unfortunately there is no upper bound and, as always happens in QFT these unbounded integrals tend to be divergent and we need to regularize it. For example we may introduce a cutoff Λ and define

$$S_{k,\Lambda}[\phi_-] = S[\phi_-] + \frac{1}{2}\mathrm{Tr}_{k<q<\Lambda}\mathrm{Log}\, S^{(2)}[\phi]\Big|_{\phi=\phi_-} + \cdots. \tag{1.28}$$

We can avoid the regularization procedure deriving an evolution equation for $S_k[\phi_-]$. It is sufficient to perform an infinitesimal step in the integration, to get a result of the form

$$k\partial_k S_k[\phi_-] = \frac{1}{2}\mathrm{TrLog}\left.\frac{\delta^2 S_k[\phi]}{\delta\phi\delta\phi}\right|_{\phi=\phi_-}. \tag{1.29}$$

This is called Wegner-Houghton equation. Once the equation is derived it is necessary to specify the initial condition of the flow and the integration towards lower values of k will automatically give regular results for S_k. The problem of taking the UV limit $\Lambda \to \infty$ is related to the choice of some initial condition of the flow.

1.3 Functional Renormalization Group

It is possible to implement the blocking procedure by modifying the partition function adding an infrared cutoff that depends on some cutoff scale k. In this context k is generally called sliding cutoff scale. We will also try to keep the discussion as general as possible, so we restore the abstract index notation of the field $\phi^{\mathcal{A}}$. We define

$$Z_k[J] = \int \mathcal{D}\phi e^{-S[\phi]+J_{\mathcal{A}}\phi^{\mathcal{A}}-\Delta S_k[\phi]}, \tag{1.30}$$

where we artificially added a new term ΔS_k, called cutoff term [8–10]. The new term is required to vanish for the sliding scale going to zero

$$\Delta S_{k\to 0}[\phi] = 0, \tag{1.31}$$

in such a way to restore the standard partition function $Z_{k\to 0}[J] = Z[J]$. To mimic the blocking procedure of the previous section we have to require the cutoff term to be at most quadratic in the field $\phi^{\mathcal{A}}$:

$$\Delta S_k[\phi] = \frac{1}{2}\phi^{\mathcal{A}} R_{k,\mathcal{AB}}\phi^{\mathcal{B}} \ , \tag{1.32}$$

where $R_{k,\mathcal{AB}}$ is called cutoff function. We will call $\Delta_{\mathcal{AB}}$ some reference operator, it is not necessary that $\Delta_{\mathcal{AB}} = S^{(2)}_{\mathcal{AB}}$ but is fundamental that it will provide a distinction between slow and fast modes of our field $\phi^{\mathcal{A}}$ as we will briefly outline. We will assume that the operator $\Delta_{\mathcal{AB}}$ is diagonalizable with spectrum $\{\lambda_i\}$. Eigenvectors corresponding to eigenvalues $\lambda_i < k$ are called "slow" modes while eigenvectors corresponding to eigenvalues $\lambda_i > k$ are called "fast" modes. The kernel $R_{k,\mathcal{AB}}$ of ΔS_k to be a function of $\Delta_{\mathcal{AB}}$. The quadratic kernel of the theory together with the cutoff term is

$$\Delta_{\mathcal{AB}} + R_{k,\mathcal{AB}}[\Delta] \ , \tag{1.33}$$

and we require to kill mainly the propagation of the slow modes. The sum of the kinetic operator and the cutoff in the eigenvector base reads

$$\Delta_{\mathcal{AB}} + R_{k,\mathcal{AB}}[\Delta] \qquad \longrightarrow \qquad \lambda_i + R_k[\lambda_i] \ . \tag{1.34}$$

Properties of a good cutoff 1. *We want $R_k[\lambda]$ to satisfy the following basic requirements*

(i) it must be continuous and monotonically decreasing in λ and monotonically increasing in k

(ii) it must go rapidly to zero for $\lambda \geq k$, so fast modes are unaffected by coarse-graining. Conversely slow modes will acquire a "mass" that forces their decoupling from spectrum.

(iii) it must tend to a positive (possibly infinite) value for $k \to \infty$ at fixed λ. This ensures that in this limit no modes are propagating.

(iv) it must tend to zero for $k \to 0$. This ensures the limit $Z_{k\to 0}[J] = Z[J]$

In general there is freedom in the choice of the specific shape of R_k and this reflects in some scheme dependence of our averaging technique.

It is useful at this stage to give some example of the most used cutoff functions profiles. One is the so called optimized cutoff [11]

$$R_k(z) = (k^2 - z)\theta(k^2 - z) \ , \tag{1.35}$$

It allows to do almost all the integrals in the traces to be performed analytically. Another one is the exponential cutoff (or more in general a 2 parameter family of shapes)

$$R_k(z) = \frac{z e^{-a(z/k^2)^b}}{1 - e^{-a(z/k^2)^b}} \ . \tag{1.36}$$

to guarantee that condition (iii) is satisfied, one has to assume $b \geq 1$.

We can follow the construction of Section 1.1 using $Z_k[J]$ in exactly the same way we used $Z[J]$ previously, although it has a further k dependence. We first define a modified generator of connected Green's functions

$$W_k[J] = \mathrm{Log} Z_k[J] \ , \tag{1.37}$$

to be compared with (1.8). Both $Z_k[J]$ and $W_k[J]$ generate n-points correlations, which will differ from those generated by $Z[J]$ and $W[J]$ only for a further k dependence. In particular we have the single point correlation (at non-zero source)

$$\bar{\phi}^{\mathcal{A}} = \left\langle \phi^{\mathcal{A}} \right\rangle_{k,J} = \frac{\delta W_k[J]}{\delta J_{\mathcal{A}}} \ . \tag{1.38}$$

For the "average field" $\bar{\phi}$ we used the same notation that was introduced when there was no k dependence (1.15). It is interesting to note that this relation is generally k dependent. This means that when later k derivatives will be performed, we will have to specify the behavior of J and $\bar{\phi}$ under it. In particular, we cannot have them simultaneously constant under k, but we can choose that either the source of the average field are.

We can define a Legendre transform

$$\tilde{\Gamma}_k\left[\bar{\phi}\right] = \bar{\phi}^{\mathcal{A}} J_{\mathcal{A}} - W_k\left[J\left[\bar{\phi}\right]\right] \ , \tag{1.39}$$

where again we have to understand J as a function of $\bar{\phi}$. We will call "Effective Average Action" (EAA) a slight modification of $\tilde{\Gamma}_k$:

$$\Gamma_k\left[\bar{\phi}\right] = \tilde{\Gamma}_k\left[\bar{\phi}\right] - \Delta S_k\left[\bar{\phi}\right] = \bar{\phi}^{\mathcal{A}} J_{\mathcal{A}} - W_k\left[J\left[\bar{\phi}\right]\right] - \Delta S_k\left[\bar{\phi}\right] \ . \tag{1.40}$$

This functional will be our main study subject. Notice that in the limit $k \to 0$ it correspond exactly to the standard Effective Action (1.16).

1.3.1 Functional Equations

The functionals we introduced in the previous section have some interesting scaling properties respect to the sliding scale k, we can describe these properties using some equation we are going to derive in the following [8–10].The first step is to take the derivative of the EAA respect to the renormalization group time $t = \text{Log } k/k_0$.

$$\partial_t \Gamma_k\left[\bar{\phi}\right] = -\partial_t W_k\left[J\right] - \frac{\delta W_k\left[J\right]}{\delta J_{\mathcal{B}}}\partial_t J_{\mathcal{B}} + \bar{\phi}^{\mathcal{B}}\partial_t J_{\mathcal{B}} - \partial_t \Delta S_k\left[\bar{\phi}\right] = \tag{1.41}$$

$$-\partial_t W_k\left[J\right] - \partial_t \Delta S_k\left[\bar{\phi}\right] = -\partial_t W_k\left[J\right] - \frac{1}{2}\partial_t R_{k,\mathcal{A}\mathcal{B}}\bar{\phi}^{\mathcal{A}}\bar{\phi}^{\mathcal{B}} \ . \tag{1.42}$$

Here we used a derivative respect to the sliding scale respect to which $\bar{\phi}$ is constant while the current is not. Next we take the derivative of the partition function

$$\begin{aligned}
\partial_t e^{W_k[J]} &= \int \mathcal{D}\phi \ \left(-\partial_t \Delta S_k\left[\phi\right]\right) e^{-S[\phi]+J_{\mathcal{A}}\phi^{\mathcal{A}}-\Delta S_k[\phi]} \\
&= -\frac{1}{2}\int \mathcal{D}\phi \ \partial_t R_{k,\mathcal{A}\mathcal{B}}\phi^{\mathcal{A}}\phi^{\mathcal{B}} e^{-S[\phi]+J_{\mathcal{A}}\phi^{\mathcal{A}}-\Delta S_k[\phi]} \\
&= -\frac{1}{2}\frac{\delta}{\delta J_{\mathcal{A}}}\partial_t R_{k,\mathcal{A}\mathcal{B}}\frac{\delta}{\delta J_{\mathcal{B}}}\int \mathcal{D}\phi e^{-S[\phi]+J_{\mathcal{A}}\phi^{\mathcal{A}}-\Delta S_k[\phi]} \\
&= -\frac{1}{2}\frac{\delta}{\delta J_{\mathcal{A}}}\partial_t R_{k,\mathcal{A}\mathcal{B}}\frac{\delta}{\delta J_{\mathcal{B}}} e^{W_k[J]} \ ,
\end{aligned} \tag{1.43}$$

performing the derivatives explicitly one gets

$$\partial_t W_k\left[J\right] = -\frac{1}{2}\partial_t R_{k,\mathcal{A}\mathcal{B}}\left(\frac{\delta^2 W_k\left[J\right]}{\delta J_{\mathcal{A}}\delta J_{\mathcal{B}}} + \frac{\delta W_k\left[J\right]}{\delta J_{\mathcal{A}}}\frac{\delta W_k\left[J\right]}{\delta J_{\mathcal{B}}}\right) = \tag{1.44}$$

$$-\frac{1}{2}\partial_t R_{k,\mathcal{A}\mathcal{B}}\left(\frac{\delta^2 W_k\left[J\right]}{\delta J_{\mathcal{A}}\delta J_{\mathcal{B}}} + \bar{\phi}^{\mathcal{A}}\bar{\phi}^{\mathcal{B}}\right) \ . \tag{1.45}$$

Substituting into the expression for $\partial_t \Gamma_k$ we get

$$\partial_t \Gamma_k \left[\bar{\phi}\right] = \frac{1}{2}\partial_t R_{k,\mathcal{AB}} \left(\frac{\delta^2 W_k \left[J\right]}{\delta J_\mathcal{A} \delta J_\mathcal{B}} + \bar{\phi}^\mathcal{A} \bar{\phi}^\mathcal{B} \right) - \partial_t \Delta S_k \left[\bar{\phi}\right] = \frac{1}{2}\partial_t R_{k,\mathcal{AB}} \frac{\delta^2 W_k \left[J\right]}{\delta J_\mathcal{A} \delta J_\mathcal{B}} \ . \tag{1.46}$$

The last step we are missing is to re-express this equation in terms of the EAA itself. The derivative of Γ_k respect to $\bar{\phi}$ is

$$\frac{\delta \Gamma_k \left[\bar{\phi}\right]}{\delta \bar{\phi}^\mathcal{A}} = -\frac{\delta W_k \left[J\right]}{\delta J_\mathcal{B}} \frac{\delta J_\mathcal{B}}{\delta \bar{\phi}^\mathcal{A}} + \frac{\delta J_\mathcal{B}}{\delta \bar{\phi}^\mathcal{A}} \bar{\phi}^\mathcal{B} + J_\mathcal{A} - \frac{\delta \Delta S_k}{\delta \bar{\phi}^\mathcal{A}} = J_\mathcal{A} - R_{k,\mathcal{AB}} \bar{\phi}^\mathcal{B} \ . \tag{1.47}$$

If we take a second derivative and rearrange the terms in the equation we get

$$\begin{aligned} &\frac{\delta J_\mathcal{A}}{\delta \bar{\phi}^\mathcal{B}} = \frac{\delta^2 \Gamma_k \left[\bar{\phi}\right]}{\delta \bar{\phi}^\mathcal{A} \delta \bar{\phi}^\mathcal{B}} + R_{k,\mathcal{AB}} \ \longrightarrow \\ &\frac{\delta^2 W_k \left[J\right]}{\delta J_\mathcal{A} \delta J_\mathcal{B}} = \frac{\delta \bar{\phi}^\mathcal{B}}{\delta J_\mathcal{A}} = \left(\frac{\delta^2 \Gamma_k \left[\bar{\phi}\right]}{\delta \bar{\phi}^\mathcal{A} \delta \bar{\phi}^\mathcal{B}} + R_{k,\mathcal{AB}} \right)^{-1} \equiv G_{k,\mathcal{AB}} \left[\bar{\phi}\right] \ , \end{aligned} \tag{1.48}$$

finally combining the (1.46) with (1.48) we get the so called Functional Renormalization Group Equation (FRGE)

$$\partial_t \Gamma_k \left[\bar{\phi}\right] = \frac{1}{2} \mathrm{Tr} \left[G_k \left[\bar{\phi}\right] \partial_t R_k \right] \ . \tag{1.49}$$

The trace is extended to every index, so it includes integrations over continuous indices. It is interesting to notice that $G_k \left[\bar{\phi}\right]$ has a role of modified propagator in which slow modes are suppressed. As we shall see later one can interpret the FRGE as a 1-loop equation where the modified propagator performs a loop with a single insertion of the derivative of the cutoff term. Indeed, this "1-loop like" structure is very useful from the computational point of view and makes many calculations accessible.

1.3.2 Graphical representation

Before going on with the derivation of the equations for $\partial_t \Gamma_k^{(n)} \left[\bar{\phi}\right]$ it's useful to introduce a graphical representation for the FRGE. We associate a straight line to the propagator $G_{k,\mathcal{AB}}$ and a crossed circle for the cutoff insertion.

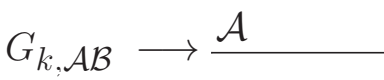

Figure 1.1: Graphical representation of the modified propagator

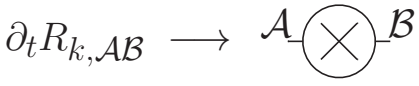

Figure 1.2: Graphical representation of the cutoff function

We represent contraction with the connection of the corresponding elements. With this prescription the FRGE is represented by a loop with a cutoff insertion.

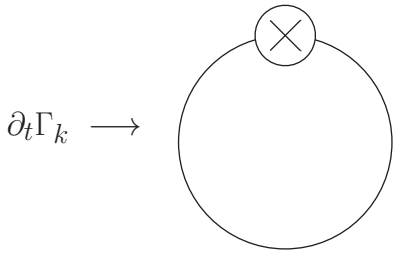

Figure 1.3: Graphical representation of the FRGE

The FRGE is a functional differential equation, therefore contains an enormous amount of information. This can be seen by the fact that it leads to an infinite tower of functional equations for the correlations $\Gamma_k^{(n)}\left[\bar{\phi}\right]$. We start by computing

$$\frac{\delta G_{k,\mathcal{AB}}\left[\bar{\phi}\right]}{\delta\bar{\phi}^{\mathcal{C}}} = \frac{\delta}{\delta\bar{\phi}^{\mathcal{C}}}\left(\frac{\delta^2\Gamma_k\left[\bar{\phi}\right]}{\delta\bar{\phi}^{\mathcal{A}}\delta\bar{\phi}^{\mathcal{B}}} + R_{k,\mathcal{AB}}\right)^{-1} = -G_{k,\mathcal{AD}}\cdot\frac{\delta^3\Gamma_k\left[\bar{\phi}\right]}{\delta\bar{\phi}^{\mathcal{D}}\delta\bar{\phi}^{\mathcal{E}}\delta\bar{\phi}^{\mathcal{C}}}G_{k,\mathcal{EB}}\ . \tag{1.50}$$

Taking a functional derivatives of the FRGE generates interaction vertices like $\frac{\delta^3\Gamma_k\left[\bar{\phi}\right]}{\delta\bar{\phi}^{\mathcal{A}}\delta\bar{\phi}^{\mathcal{B}}\delta\bar{\phi}^{\mathcal{C}}}$ or more in general $\frac{\delta^n\Gamma_k\left[\bar{\phi}\right]}{\delta\bar{\phi}^{\mathcal{A}_1}\ldots\delta\bar{\phi}^{\mathcal{A}_n}}$

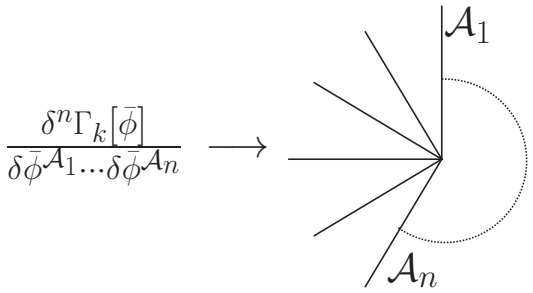

Figure 1.4: Graphical representation of a vertex

At this point computing the functional equation for the n-point function is simple. It is sufficient to take n derivatives of $\partial_t\Gamma_k\left[\bar{\phi}\right]$. Graphically it is sufficient to add n external legs to the FRGE loop (grasping on propagators and vertices) respecting the Leibniz rule and (1.50). We can be more concrete looking to an example that will be useful later, the 2 point function. Taking

the first derivative we have to grasp FRGE loop with a single external leg. Usually we will consider a cutoff function that does not depend on $\bar{\phi}$, the first grasp will act only on the propagator.

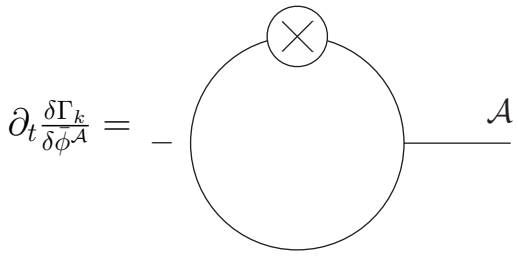

Figure 1.5: Graphical representation of the functional equation for the 1-point function

Then we need to take a second derivative but now we have 3 options: acting on the two propagators or on the three valent vertex.

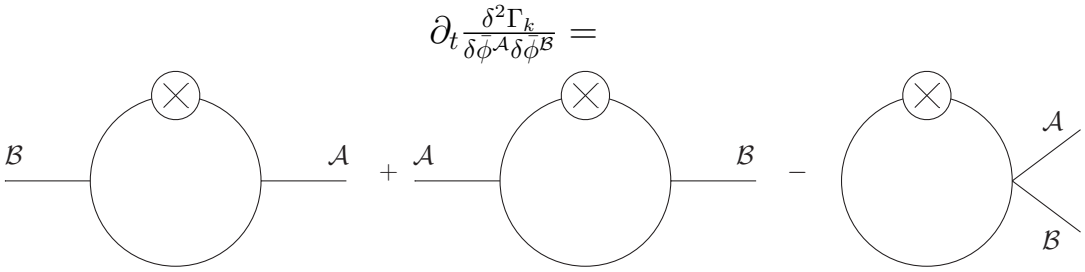

Figure 1.6: Graphical representation of the functional equation for the 2-point function

this collection of diagrams correspond to

$$\begin{aligned}\partial_t \frac{\delta^2 \Gamma_k}{\delta \bar{\phi}^{\mathcal{A}} \delta \bar{\phi}^{\mathcal{B}}} =& \frac{1}{2} \mathrm{Tr} \left[G_k \cdot \frac{\delta^3 \Gamma_k \left[\bar{\phi}\right]}{\delta \bar{\phi}^{\mathcal{A}} \delta \bar{\phi} \delta \bar{\phi}} \cdot G_k \cdot \frac{\delta^3 \Gamma_k \left[\bar{\phi}\right]}{\delta \bar{\phi}^{\mathcal{B}} \delta \bar{\phi} \delta \bar{\phi}} \cdot G_k \cdot \partial_t R_k \right] \\ &+ \frac{1}{2} \mathrm{Tr} \left[G_k \cdot \frac{\delta^3 \Gamma_k \left[\bar{\phi}\right]}{\delta \bar{\phi}^{\mathcal{B}} \delta \bar{\phi} \delta \bar{\phi}} \cdot G_k \cdot \frac{\delta^3 \Gamma_k \left[\bar{\phi}\right]}{\delta \bar{\phi}^{\mathcal{A}} \delta \bar{\phi} \delta \bar{\phi}} \cdot G_k \cdot \partial_t R_k \right] \\ &- \frac{1}{2} \mathrm{Tr} \left[G_k \cdot \frac{\delta^4 \Gamma_k \left[\bar{\phi}\right]}{\delta \bar{\phi}^{\mathcal{A}} \delta \bar{\phi}^{\mathcal{B}} \delta \bar{\phi} \delta \bar{\phi}} \cdot G_k \cdot \partial_t R_k \right] ,\end{aligned} \tag{1.51}$$

where we omitted contracted indices to simplify the notation (each factor is a matrix). By taking further functional derivatives we can obtain similar equations for higher n-point functions.

Chapter 2

The Asymptotic Safety framework

Asymptotic safety is a criterion of consistency for a QFT that generalizes the concepts of perturbative renomalizability and asymptotic freedom.

In this chapter we will define this notion and how practically one studies whether a theory possesses this feature. The discussion will be carried out in general, without restricting ourselves to any specific theory.

For gravity the idea was put forward in 1979 by Steven Weinberg [6], but is well-known in Statistical Mechanics (with the difference that they are not looking at the UV). In the same period there appeared some encouraging results in $2 + \epsilon$ dimensions that showed that the theory of gravity is indeed asymptotically safe [12–14], therefore consistent in the UV regime. The calculations where performed using the standard ϵ expansion, and therefore cannot be immediately generalized to four dimensions, which is the physically interesting case. In the last two decades suitable non-perturbative techniques like FRGE have been developed that allow to attack the problem.

2.0.3 Asymptotic safety

In QFT the couplings are not really constant rather they "run" as the typical scale of the process is varied. In perturbation theory this arises as follows. In order to renormalise the theory one is forced to introduce a mass parameter which acts as a regulator and has no physical meaning. One then has to define the physical, i.e. renormalised Green's functions at a certain renormalisation point, by defining certain coupling constants relative to specific measurement conditions (like momenta of external particles).

In perturbation theory, the RG theory is basically a statement about the independence of physical quantities of the choice of renormalisation point.

This is the content of the Callan-Symanzik equation.

If one changes the renormalisation prescription, the coupling constants will change too, in such a way that the value of physical observable quantities will stay the same. In perturbation theory the RG is mostly used to rearrange the perturbation series and provide a better expansion, since it allows to resum large logarithms.

One also has experimental evidence that constants run, for instance looking at the strong interaction coupling constant measured at particle accelerators. Ultimately, by writing down a suitable effective action, one can evaluate the couplings at the correct energy scale and forget about loop corrections, which will all be included in the renormalised couplings.

Let us see how the RG theory proves to be a powerful method to search for UV singularities. The effective action will be a functional of the classical fields, consisting of a series of monomials, each made up of a combination of the fields compatible with the symmetries of the theory and multiplied by a running coupling. Schematically, we may write

$$\Gamma_k \left[\phi^{\mathcal{A}}\right] = \int \mathrm{d}^d x \sum_i g_i \left(k\right) O_i \left[\phi^{\mathcal{A}}\right] \ , \tag{2.1}$$

where ϕ represents a generic field (we dropped the bar from the notation used in the previous chapter), $O_i \left[\phi^{\mathcal{A}}\right]$, is a generic operator and $g_i \left(k\right)$ is the running coupling defined at the energy scale k.

The constant $g_i \left(k\right)$ will have a certain canonical dimension d_i; let us then define the corresponding dimensionless couplings,

$$\tilde{g}_i \left(k\right) = k^{-d_i} g_i \left(k\right) \ . \tag{2.2}$$

Now, a physical quantity that we want to measure, be it a partial or total cross section, a decay amplitude, or anything else, will be a function of the renormalization scale k, the kinematical parameters of the process (like momenta, angles, etc.) and the running coupling constants. By extracting a suitable power of k, any such on-shell quantity may be written as

$$\tilde{F} = k^D F \left(X, \tilde{g}_i \left(k\right)\right) \ , \tag{2.3}$$

where X stands generically for dimensionless kinematical quantities and their ratios and D is the canonical dimension of F (for instance it is -2 for a total cross section). Equation (2.3) represents the most general expression for a physical quantity; from a consistent theory, we want all such quantities to be finite whatever the energy scale is at which we evaluate the process. We see that, apart from the trivial power like dependence on k, the UV behaviour

of F is controlled by the UV behaviour of the dimensionless constants $\tilde{g}_i$'s. Therefore, if we impose that they approach a FP at infinite energy scale,

$$\lim_{k\to\infty} \tilde{g}_i = \tilde{g}_i^* \ , \tag{2.4}$$

we have a reasonable sufficient condition to make sure that our physical quantities, measured in units of k, will not blow up when the energy scale tends to ∞.

Before going on, we should mention the distinction between the so called essential and inessential couplings. In fact, in (2.1) we have a large freedom to define the coupling constants g_i's. Some of them may be made to disappear from the action if we perform a suitable redefinition of the fields. Given a certain choice of a set of couplings a combinations of them that cannot be eliminated from the action will be called "essential", the remaining ones are "inessential" (or redundant). Mass-shell matrix elements and reaction rates do not depend on the definition of the fields. On the contrary, the off-shell Green's functions will always reflect the way fields are defined, and therefore will also depend on inessential couplings. From a physical QFT, we demand that on-shell quantities possess a good UV behaviour. Since inessential couplings are absent in the general formula (2.3), to apply the asymptotic safety criterion one first has to identify a set of essential couplings and then apply condition (2.4) only to these ones. The focus on on-shell quantities is needed exactly to get rid of inessential couplings. Since this issue is very important in the gravitational context, we discuss it separately in Chapter 3.

The condition that coupling constants approach a FP allow us to make sense of UV divergences. Yet, we have not seen by how many parameters the quantum theory is defined. Like in perturbative renormalizability, we want the theory to be fixed only by a finite number of parameters to be determined experimentally, so that it is predictive. Therefore, we must add to condition (2.4) another suitable criterion.

Suppose we have found a UV attractive FP. In the space of all the flowing actions Γ_k, which is spanned by the (essential) coupling constants $\tilde{g}_i(k)$'s, there will be a subspace consisting of all the trajectories that hit the FP when k goes to infinity.

This subspace forms the UV critical surface $\mathcal{S}_{UV}$. By its very definition, no matter where we start from a specific point in $\mathcal{S}_{UV}$, in the UV regime the RG flow will always bring the action to the FP. If we start outside $\mathcal{S}_{UV}$, instead, the trajectory will in general show divergences (unless we are on the critical surface of another FP, of course). Therefore, the number of parameters that we can freely choose to approach the FP is equal to the dimension of $\mathcal{S}_{UV}$. We must then work out its dimension.

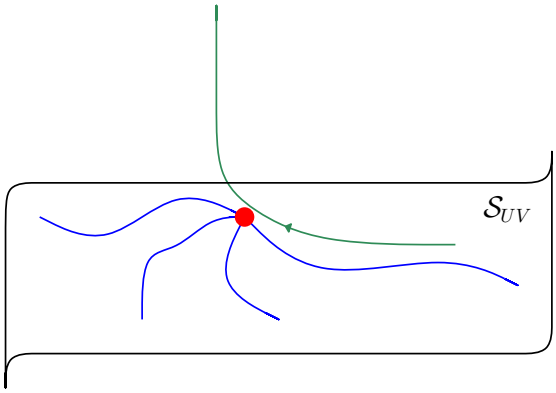

Figure 2.1: Pictorial representation of the UV critical surface in the theory space

2.0.4 Study of the Fixed Point

The easiest way to determine the dimension of $\mathcal{S}_{UV}$ is to study the linearised flow and compute the dimension of the hyperplane tangent to $\mathcal{S}_{UV}$ at the FP. Suppose we have determined the beta functions for the coupling constants:

$$\beta_i\left(\tilde{g}_j\right) = \partial_t \tilde{g}_i(t) \ , \tag{2.5}$$

where t is the RG time we introduced in the previous chapter. We do not specify here how to compute the beta functions; the following applies both to perturbative and non-perturbative approaches. The condition (2.4) implies that at the FP must satisfy

$$\beta_i\left(\tilde{g}_j^*\right) = 0 \ . \tag{2.6}$$

One can expand the flow equations about the FP

$$\beta_i\left(\tilde{g}_j\right) = \beta_i\left(\tilde{g}_j^*\right) + \frac{\partial \beta_i}{\partial \tilde{g}_j}\left(\tilde{g}_j^*\right)\left(\tilde{g}_j - \tilde{g}_j^*\right) + \cdots \ . \tag{2.7}$$

The first term on the right-hand side vanishes by definition of FP, and in a neighbourhood of it we can neglect second order corrections. Introducing the stability matrix $B_{ij} = \frac{\partial \beta_i}{\partial \tilde{g}_j}\left(\tilde{g}_j^*\right)$ we have the linearized flow that reads

$$\beta_i\left(\tilde{g}_j\right) = B_{ij}\left(\tilde{g}_j - \tilde{g}_j^*\right) \ . \tag{2.8}$$

It is an infinite system of first-order differential equations which is easily solved by diagonalizing the stability matrix. Let P be the similarity transformation that diagonalizes it, so that $M^d \equiv PBP^{-1}$ is the matrix of the

eigenvalues. Introduce the eigenvectors $v_i = P_{ij}\left(\tilde{g}_j - \tilde{g}_j^*\right)$, with eigenvalue λ_i, we will call in the following $\theta_i = -\lambda_i$ critical exponent. In general θ_i will be complex, since B is not symmetric a priori. The solution will then be $v_i(t) = C_i \exp(-\theta_i t)$. Going back to the $\tilde{g}_i$'s one finds

$$\tilde{g}_i(t) = P_{ij}^{-1} C_j \exp(-\theta_j t) + \tilde{g}_i^* \ , \tag{2.9}$$

where the C_j's are integration constants which we have to fix so that the $\tilde{g}_i(t)$'s approach the FP in the UV regime, i.e. when $t \to \infty$. If the real part of the critical exponent is negative, the exponential suppresses the contribution from that eigendirection, which will be UV attractive, and we can leave C_i free. If the real part of the critical exponent is positive, instead, condition (2.4) will not be satisfied, so the eigendirection is repulsive and must be eliminated by setting $C_i = 0$. The corresponding operators are named relevant and irrelevant respectively. If an eigenvalue is zero, one has to go beyond the linear approximation to study the attractivity of the FP. We shall not consider this case (as we will see, the non-trivial FP of gravity does not have zero eigenvalues). All in all we conclude that the dimension of $\mathcal{S}_{UV}$ is equal to the number of eigenvalues of the stability matrix with negative real part, which we have to impose to come in a finite number to have a predictive theory. It is easy to see that the existence and attractivity properties of a FP do not depend on the way in which we choose coordinates in the space of all action functionals. The eigenvalues of the stability matrix are universal values representing the critical exponents in Statistical Mechanics.

Now we are in the position of demonstrating the connection between asymptotic safety and perturbative renormalizability. Consider the theory renormalised at the Gaussian FP (GFP), i.e. the FP where all essential couplings vanish. One is then allowed to compute the beta functions perturbatively in the coupling constants. Recalling that we are interested in the dimensionless couplings given by (2.2), one finds

$$\beta_i = -d_i g_i + \text{loop correction} \qquad B_{ij} = -d_i \delta_{ij} + \text{loop correction} \ , \tag{2.10}$$

and evaluated at the GFP it will be diagonal with minus the canonical dimensions as eigenvalues. By the analysis carried out before, we have to rule out the couplings with negative canonical dimension, whereas those with positive dimension are allowed. As for the g_i's that are dimensionless, one should look at the loop corrections (i.e., one has to go beyond the linearised flow) and they represent attractive directions if and only if they satisfy the condition $\beta_i/g_i < 0$. But these conditions represent exactly the standard dimensional arguments for perturbative renormalizability together with asymptotic freedom. So we see that asymptotic safety includes perturbative renormalization

as a very special case. The interesting feature is that when the GFP is not present or does not possess good features, one may look for a non-Gaussian FP (NGFP) about which to renormalise the theory. This is what happens with gravity: the GFP cannot be used because gravity is not perturbatively renormalizable.

Chapter 3

RG Equation for Gravity

It is now time to see how the machinery we developed in the previous two chapter can be applied to the case of gravity. We would like to cast the equation in a form where only the second derivatives of the effective action with respect to the argument of Γ_k are there. We would like to be able to write down, at least formally, the most general form of the effective action, based on symmetry principles. Then we will retain only a suitable truncation thereof in order to perform explicit calculations. Considering the full form of Γ_k is exceedingly complicated. One can make a smart choice for the truncation and try to estimate how accurate are the results by enlarging it. It is crucial to be able to identify the complete Γ_k so that in this way one knows that certain (symmetry-violating) operators are forbidden a priori. This chapter aims to review results already presents in the literature.

3.1 Fixing the notations

We will describe spacetime as a smooth Riemannian manifold $\mathcal{M}$ equipped with a metric $g_{\mu\nu}$. Since the derivative of a vector field does not transform covariantly, we introduce a notion of covariant derivative, expressed in terms of a connection Γ

$$D_\mu V^\nu \equiv \partial_\mu V^\nu + \Gamma^\nu_{\mu\rho} V^\rho \ . \tag{3.1}$$

In this thesis the connection is considered always to be the Levi-Civita connection

$$\Gamma^\nu_{\mu\rho} \equiv \frac{1}{2} g^{\nu\gamma} \left(\partial_\mu g_{\rho\lambda} + \partial_\rho g_{\mu\lambda} - \partial_\lambda g_{\rho\mu} \right) \ , \tag{3.2}$$

where ∂_μ are derivative respect to local coordinates, $g^{\nu\gamma}$ is the inverse metric, and indexes are raised and lowered by the metric. The Riemann curvature

tensor is

$$R^{\lambda}{}_{\mu\nu\rho} \equiv \partial_\rho \Gamma^{\lambda}_{\mu\nu} - \partial_\nu \Gamma^{\lambda}_{\mu\rho} + \Gamma^{\alpha}_{\mu\nu}\Gamma^{\lambda}_{\alpha\rho} - \Gamma^{\alpha}_{\mu\rho}\Gamma^{\lambda}_{\alpha\nu} \ , \tag{3.3}$$

whose contractions give the Ricci tensor $R_{\mu\nu} = R^{\lambda}{}_{\mu\lambda\rho}$ and scalar $R = g^{\mu\nu}R_{\mu\nu}$.

3.2 Background field method

The first issue we will be concerned with is local symmetries. Since the theory we want to deal with is invariant under diffeomorphisms, in order to perform the path-integral quantisation that leads us to the FRGE we have to gauge fix the action and add the corresponding ghost terms. If the gauge-fixing is not carried out in a suitable manner, one may not end up with a gauge invariant quantum effective action, so that the general form of it includes a huge amount of terms that we may not be able to identify. In standard QFT this problem is solved by using a background technique, and this can be extended to the formalism of the effective average action for gauge theories, including gravity [14–16].

Next, one of course wants to be able to compute the traces explicitly. Since now we are interested in curved spaces, the problem is more delicate, since, in general, analytical techniques are not developed to calculate the trace of an arbitrary function of a derivative operator in curved space. Nevertheless, if one is able to have all the covariant derivatives contracted with one another, so that the operators are actually functionals of the Laplacian, then heat-kernel techniques can be easily applied. In order to achieve this, one has to decompose the quantum metric in a suitable way, as we will describe later, and this will restrict the possible projections to a limited class of metrics. The generalization to more complicated spacetimes in not obvious and quite difficult, in this case. We will be mainly interested in the Einstein-Hilbert truncation, for which one can use a maximally symmetric space whose Riemann tensor satisfies

$$R_{\mu\nu\rho\sigma} = \frac{1}{d(d-1)} \left(g_{\mu\rho}g_{\nu\sigma} - g_{\mu\sigma}g_{\nu\rho}\right) R \ , \tag{3.4}$$

corresponding to the metric of a d-dimensional sphere S^d. If one wants to include higher-derivative terms one should consider different spaces to project the FRGE onto. The derivation we present here can be easily generalized, but we specialize our calculations for the Einstein-Hilbert truncation for sake of simplicity.

$$S_{\rm EH} = \frac{1}{16\pi G} \int d^d x \sqrt{g} \left(-R + 2\Lambda\right) \ . \tag{3.5}$$

In order to achieve general covariance in Γ_k, it is convenient to use the background field method [17], splitting the quantum metric $g_{\mu\nu}$, into the sum of a fixed background $\bar{g}_{\mu\nu}$ and a fluctuation $h_{\mu\nu}$.

$$g_{\mu\nu} = \bar{g}_{\mu\nu} + \sqrt{32\pi G_k} h_{\mu\nu} \ . \tag{3.6}$$

Indices will always be raised and lowered with $\bar{g}_{\mu\nu}$. We will refer to the field $h_{\mu\nu}$ as the graviton, even though it is not assumed to be a small perturbation. Next we have to define how background and fluctuation transforms under an infinitesimal change of coordinates $x^\mu \to x^\mu + \epsilon^\mu(x)$.

$$\delta_\epsilon h_{\mu\nu} = \mathcal{L}_\epsilon g_{\mu\nu} = 2 g_{\alpha(\mu} D_{\nu)} \epsilon^\alpha \qquad \delta_\epsilon \bar{g}_{\mu\nu} = 0 \ . \tag{3.7}$$

We will now go through the usual steps of the Faddeev-Popov procedure to gauge-fix the gravitational action and write down the corresponding ghost action. The gauge fixing $S_{\rm gf}$ term and the ghost term $S_{\rm gh}$ can be generically written as follows

$$S_{\rm gf} = \ \tfrac{1}{2\alpha} \int d^d x \sqrt{\bar{g}}\, \bar{g}^{\mu\nu} F_\mu[\bar{g}, h] F_\nu[\bar{g}, h] \tag{3.8}$$

$$S_{gh} = \ - \int d^d x \sqrt{\bar{g}}\ \bar{c}^\mu M_{\mu\nu}[\bar{g}, h] c^\nu \ . \tag{3.9}$$

If we specify the form of the functional F_μ we can compute explicitly the ghost action. We will use an harmonic gauge fixing.

$$F_\mu[\bar{g}, h] = \left(\bar{g}^\beta_\mu \bar{D}^\alpha - \frac{1+\rho}{4} \bar{g}^{\alpha\beta} \bar{D}_\mu \right) h_{\alpha\beta} \ , \tag{3.10}$$

then following the prescription we have

$$M_{\mu\nu}[\bar{g}, h] = 2 \frac{\delta F_\mu[\bar{g}, \delta_\epsilon h]}{\delta \epsilon^\nu} = \frac{\delta F_\mu[\bar{g}, \delta_\epsilon h]}{\delta h_{\alpha\beta}} \frac{\delta_\epsilon h_{\alpha\beta}}{\delta \epsilon^\nu} = \left(\bar{g}^\beta_\mu \bar{D}^\alpha - \frac{1+\rho}{4} \bar{g}^{\alpha\beta} \bar{D}_\mu \right) g_{\nu(\alpha} D_{\beta)} \ . \tag{3.11}$$

Finally the ghost term can be rewritten as

$$\begin{aligned} S_{gh} \ &= \ - \int d^d x \sqrt{\bar{g}}\ \bar{c}_\mu \Big(\bar{g}^{\mu\kappa} \bar{D}^\rho g_{\kappa\nu} D_\rho \\ &+ \ \bar{g}^{\mu\kappa} \bar{D}^\rho g_{\rho\nu} D_\kappa - \frac{1+\rho}{2} \bar{g}^{\rho\sigma} \bar{D}^\mu g_{\rho\nu} D_\sigma \Big) c^\nu \ . \end{aligned} \tag{3.12}$$

The parameters α and ρ are called gauge parameters.

3.3 Evaluation of the beta functions

We will now consider a particular type of truncation, which consists of retaining the bare Einstein-Hilbert action, the gauge-fixing, ghost term and cutoff terms with running coupling constants.

$$\Gamma_k = \Gamma_{\mathrm{EH}k} + \Gamma_{\mathrm{gf}k} + \Gamma_{\mathrm{gh}k} \ , \tag{3.13}$$

where Γ_k looks like exactly the same as their bare counterparts we have defined in the previous section where we promoted the couplings to running ones $G \to G_k$ and $\Lambda \to \Lambda_k$.

Projecting on a maximally symmetric space, it is straightforward to extract the beta functions for G_k and Λ_k. The coupling constants can be extracted as

$$\frac{\Lambda_k}{16\pi G_k} = \frac{1}{2\mathrm{Vol}} \Gamma_k\left[\bar{g}\right]\big|_{R=0} \ , \tag{3.14}$$

$$\frac{1}{16\pi G_k} = -\frac{1}{\mathrm{Vol}} \frac{\partial \Gamma_k\left[\bar{g}\right]}{\partial R}\bigg|_{R=0} \ , \tag{3.15}$$

and their running by differentiating both sides respect to the RG time t. Since to order R there is only one invariant, namely the Ricci scalar, the projection on the spherical background is unambiguous. Suppose we wanted to consider terms of second order in the curvature; for a general background there are three such independent terms, namely R^2, $R_{\mu\nu}R^{\mu\nu}$, and $R_{\mu\nu\rho\sigma}R^{\mu\nu\rho\sigma}$ (even if one can be eliminated using the Gauss-Bonnet identity) and they would all give a term proportional to the curvature squared when projected on the sphere. Therefore, as mentioned before, one must consider more complicated spaces to disentangle the different contributions coming from higher-derivative terms.

The first step to compute the EAA is to compute its quadratic part in the graviton of the (3.13)[1].

$$\Gamma_k^{(2)} = \frac{1}{2}\int d^dx \quad h_{\mu\nu}\Big[(\mathbf{1}-\mathbf{P})\left(-\bar{D}^2 - 2\Lambda_k + \tfrac{4-3d+d^2}{d(d-1)}\bar{R}\right) \\ -\tfrac{d-2}{2}\mathbf{P}\left(-\bar{D}^2 - 2\Lambda_k + \tfrac{d-4}{d}\bar{R}\right)\Big] h_{\rho\sigma} \tag{3.16}$$

Where $\mathbf{1} = 1^{\mu\nu\rho\sigma} = \delta^{\mu(\rho}\delta^{\sigma)\nu}$ and $\mathbf{P} = P^{\mu\nu\rho\sigma} = \frac{1}{d}\delta^{\mu\nu}\delta^{\rho\sigma}$, notice that $\mathbf{P}\cdot\mathbf{P} = \mathbf{P}$. The ghost term is already quadratic in the ghost fields, then it is sufficient to compute it for $g = \bar{g}$ to find its quadratic part. From now on we will

[1]For simplicity we set $\alpha = 1$ and $\rho = d/2 - 1$ which is 1 in $d = 4$

drop the bar form the covariant derivative and from the Ricci scalar and we will always assume they are the one built from the background metric. If it is necessary to explicitly distinguish the background quantities from the complete metric ones the bar will be reintroduced.

3.3.1 Cutoff

The following step to compute the FRGE for gravity is the introduction of the cutoff term

$$\Delta S_k = \frac{1}{2}\int d^d x h_{\mu\nu} R_k^{\mu\nu\rho\sigma} h_{\rho\sigma} - \int d^d x \bar{c}_\mu R_k^{\mathrm{gh}\mu\nu} c_\nu \ . \tag{3.17}$$

The cutoff function R_k appearing here should not be confused with the Riemann tensor. In general we have the freedom to choose the shape and the operator we want to cutoff. Traditionally if the argument of the cutoff function is the Laplacian the cutoff is called of type I, if the argument is the Laplacian plus some multiple of the curvature scalar is called of type II, lastly if the argument include also other couplings is called of type III. We will not talk about type III cutoff in this thesis, for more information about it refer to [18]. Moreover a cutoff is called of type "a" if the graviton is used as fundamental field and type "b" if the graviton is decomposed in irreducible representations of $SO(d+1)$. In the following we will derive explicitly the gravitational beta function ignoring the graviton wave function renormalization factor. We will call this "one loop" approximation.

3.3.2 Cutoff of type Ia

In this section we will finally compute the beta function in the type Ia cutoff case respectively for the graviton and the ghosts.

$$\Delta S_k^{gr} = \frac{1}{2}\int d^d x h_{\mu\nu}\left[(\mathbf{1}-\mathbf{P}) R_k\left(-D^2\right) - \frac{d-2}{2}\mathbf{P} R_k\left(-D^2\right)\right] h_{\rho\sigma} \tag{3.18}$$

$$\Delta S_k^{gh} = -\int d^d x \bar{c}_\mu g^{\mu\nu} R_k c_\nu \ . \tag{3.19}$$

The following step is to compute the modified proparator G_k, thanks to the decomposition in projectors the inversion of the quadratic part of the action is trivial.

$$G_k^{gr} = \left(\Gamma_k^{(2),gr} + R_k\right)^{-1} = 2(\mathbf{1}-\mathbf{P})\frac{1}{-D^2 + R_k(-D^2) - 2\Lambda_k + \frac{4-3d+d^2}{d(d-1)}R} - \frac{4}{d-2}\mathbf{P}\frac{1}{-D^2 + R_k(-D^2) - 2\Lambda_k + \frac{d-4}{d}R} \ ,$$

$$G_k^{gh} = \left(\Gamma_k^{(2),gh} + R_k\right)^{-1} = -\frac{\mathbf{1}_{gh}}{-D^2 + R_k\left(-D^2\right) - R/d} \ .$$

Multiplying with the cutoff term and tracing over spacetime indices one obtains the FRGE

$$\begin{aligned}
\frac{d}{dt}\Gamma_k &= \frac{1}{2}\mathrm{Tr}\left[G_k^{-1}\partial_t R_k\right] = \frac{1}{2}\mathrm{Tr}\left[G_k^{gr\,-1}\partial_t R_k\right] - \mathrm{Tr}\left[G_k^{gh\,-1}\partial_t R_k\right] = && (3.20)\\
&+\frac{1}{2}\mathrm{Tr}\left[\mathbf{1} - \mathbf{P}\frac{\partial_t R_k}{-D^2 + R_k\left(-D^2\right) - 2\Lambda_k + \frac{4-3d+d^2}{d(d-1)}R}\right] && (3.21)\\
&+\frac{1}{2}\mathrm{Tr}\left[\mathbf{P}\frac{\partial_t R_k}{-D^2 + R_k\left(-D^2\right) - 2\Lambda_k + \frac{d-4}{d}R}\right] && (3.22)\\
&-\mathrm{Tr}\left[\mathbf{1}_{gh}\frac{\partial_t R_k}{-D^2 + R_k\left(-D^2\right) - R/d}\right] \ . && (3.23)
\end{aligned}$$

Notice the presence of the total derivative respect to the RG time t instead of the partial derivative that we used in the previous chapters. This meant to reabsorb on the left hand side of the equation terms dependent on the dimension of the fields and Lagrangian. One can now expand to first order in R, and use a heat kernel expansion[2] to obtain

$$\begin{aligned}
\frac{d}{dt}\Gamma_k &= \frac{1}{(4\pi)^{d/2}}\int dx\sqrt{g}\Bigg\{\frac{d\,(d+1)}{4}Q_{\frac{d}{2}}\left[\frac{\partial_t R_k}{z + R_k - 2\Lambda}\right] - dQ_{\frac{d}{2}}\left[\frac{\partial_t R_k}{z + R_k}\right] \\
&+\Bigg(\frac{d\,(d+1)}{24}Q_{\frac{d}{2}-1}\left[\frac{\partial_t R_k}{z + R_k - 2\Lambda}\right] - \frac{d}{6}Q_{\frac{d}{2}-1}\left[\frac{\partial_t R_k}{z + R_k}\right] \qquad (3.24)\\
&-\frac{d\,(d-1)}{4}Q_{\frac{d}{2}}\left[\frac{\partial_t R_k}{\left(z + R_k - 2\Lambda\right)^2}\right] - Q_{\frac{d}{2}}\left[\frac{\partial_t R_k}{\left(z + R_k\right)^2}\right]\Bigg)R + O(R^2)\Bigg\} \ ,
\end{aligned}$$

where $Q_n(W) = \frac{1}{\Gamma(n)}\int_0^\infty dz\, z^{n-1}W(z)$ for any function $W(z)$. We are now ready to extract the beta functions. The first line of (39) gives the beta function of Λ_k/G_k, while the other two lines give the beta function of $1/G_k$. The beta functions (3.14) can be written in the form

$$\begin{aligned}
\partial_t\frac{\Lambda_k}{16\pi G_k} &= \frac{k^d}{16\pi}A_1 \ , && (3.25)\\
-\partial_t\frac{1}{16\pi G_k} &= \frac{k^{d-2}}{16\pi}B_1 \ , && (3.26)
\end{aligned}$$

where A_1 , B_1 are dimensionless functions of Λ, k and of d. One can solve these equations for the dimensionless cosmological constant and newton's constant (2.2) obtaining

[2]For additional details look at the appendix 3.A

$$\partial_t \tilde{\Lambda}_k = -2\tilde{\Lambda}_k + \frac{\tilde{G}_k}{2} A_1 + \tilde{\Lambda}_k \tilde{G}_k B_1 \ , \tag{3.27}$$

$$\partial_t \tilde{G}_k = (d-2)\, \tilde{G}_k + B_1 \tilde{G}_k^2 \ . \tag{3.28}$$

To get an explicit form of the coefficients A and B we need to specify the shape of the cutoff function, with the optimized cutoff (1.35), is

$$A_1 = \frac{1}{(4\pi)^{d/2}\Gamma(\frac{d}{2})} \frac{16\pi(d-3+8\tilde{\Lambda}_k)}{1-2\tilde{\Lambda}_k} \ , \tag{3.29}$$

$$B_1 = \frac{1}{(4\pi)^{d/2}\Gamma(\frac{d}{2})} \frac{-4\pi(-d^3+15d^2-12d+48+(2d^3-14d^2-192)\tilde{\Lambda}_k+(16d^2+192)\tilde{\Lambda}_k^2)}{3d\left(1-2\tilde{\Lambda}_k\right)^2} \ .$$

3.3.3 Cutoff of type Ib

This type of cutoff was introduced in [19]. The fluctuation $h_{\mu\nu}$ and the ghosts are decomposed into their different spin components according to

$$h_{\mu\nu} = h^T_{\mu\nu} + D_\mu \xi_\nu + D_\nu \xi_\mu + D_\mu D_\nu \sigma - \frac{1}{d} g_{\mu\nu} D^2 \sigma + \frac{1}{d} g_{\mu\nu} h \ , \tag{3.30}$$

and

$$C^\mu = c^{T\mu} + D^\mu c \ \ , \bar{C}_\mu = \bar{c}^T_\mu + D_\mu \bar{c} \ , \tag{3.31}$$

where $h^T_{\mu\nu}$ is tranverse and traceless, ξ is a transverse vector, σ and h are scalars, c^T and $\bar{c}^T$ are transverse vectors, and c and $\bar{c}$ are scalars. These fields are subject to the following differential constraints:

$$h^{T\mu}_\mu = 0 \ ; \qquad D^\nu h^T_{\mu\nu} = 0 \ ; \qquad D^\nu \xi_\nu = 0 \ ; D^\mu \bar{c}^T_\mu = 0 \ ; D_\mu c^{T\mu} = 0 \ .$$

Using this decomposition can be advantageous in some cases because it can lead to a partial diagonalization of the kinetic operator and it allows an exact inversion. This is the case for example when the background is a maximally symmetric metric. Then the FRGE can be written down for arbitary gauge α and ρ. Here for simplicity we still restrict ourself to the gauge $\alpha = \rho = 1$ and without making any approximation, the quadratic parts of the action

for each component are

$$\begin{aligned}
\Gamma^{(2)}_{h^T} &= \frac{1}{2}h^T_{\mu\nu}\left[-D^2+\frac{d^2-3d+4}{d(d-1)}R-2\Lambda_k\right]h^{T\mu\nu}\ ;\\
\Gamma^{(2)}_{\xi} &= \left(-D^2-\frac{R}{d}\right)\xi_\mu\left[-D+\frac{d-3}{d}R-2\Lambda_k\right]\xi^\mu\ ;\\
\Gamma^{(2)}_{h} &= -\frac{d-2}{4d}h\left[-D^2+\frac{d-4}{d}R-2\Lambda_k\right]h\ ;\\
\Gamma^{(2)}_{\sigma} &= \frac{d-1}{2d}\left(-D^2\right)\left(-D^2-\frac{R}{d-1}\right)\sigma\left[-D^2+\frac{d-4}{d}R-2\Lambda\right]\sigma\ ;\\
\Gamma^{(2)}_{\bar{c}^Tc^T} &= \bar{c}^T_\mu\left[-D^2+\frac{R}{d}\right]c^{T\mu}\ ;\\
\Gamma^{(2)}_{\bar{c}c} &= -D^2\bar{c}\left[-D^2+\frac{2}{d}R\right]c\ .
\end{aligned}\tag{3.32}$$

The change of variables (3.30) and (3.31) leads to Jacobian determinants involving the operators

$$J_V=-D^2-\frac{R}{d},\ J_S=-D^2\left(-D^2-\frac{R}{d-1}\right),\ J_c=-D^2\ .$$

for the vector, scalar and ghost parts. The inverse propagators (3.32) contain terms with more than two derivatives, we can avoid this by making the field redefinitions

$$\xi_\mu\ \rightarrow\ \sqrt{-D^2-\frac{R}{d}}\,\xi_\mu,\ \sigma\rightarrow\sqrt{-D^2}\sqrt{-D^2-\frac{R}{d-1}}\sigma\ .\tag{3.33}$$

At the same time, such redefinitions also eliminate the Jacobians. These field redefinitions work well for truncations containing up to two powers of curvature, but cause poles for higher truncations as the heat kernel expansion will involve derivatives of the trace arguments. To obtain the FRGE we can now proceed as in the case of cutoff type Ia. Notice that the trace on constrained fields need some care but we will not enter in the details here. Expanding the denominators to first order in R, but keeping the exact dependence on Λ_k as in the case of a type Ia cutoff, and using the Heat

Kernel expansion, one obtains

$$\begin{aligned}\frac{d}{dt}\Gamma_k &= \frac{1}{(4\pi)^{d/2}}\int dx\,\sqrt{g}\Bigg\{\frac{d(d+1)}{4}Q_{\frac{d}{2}}\left(\frac{\partial_t R_k}{z+R_k-2\Lambda}\right)-dQ_{\frac{d}{2}}\left(\frac{\partial_t R_k}{z+R_k}\right) \\ &+R\left[-\frac{d^4-2d^3-d^2-4d+2}{4d(d-1)}Q_{\frac{d}{2}}\left(\frac{\partial_t R_k}{(z+R_k-2\Lambda)^2}\right)-\frac{d+1}{d}Q_{\frac{d}{2}}\left(\frac{\partial_t R_k}{(z+R_k)^2}\right)\right. \\ &\left.+\frac{d^4-13d^2-24d+12}{24d(d-1)}Q_{\frac{d}{2}-1}\left(\frac{\partial_t R_k}{P_k-2\Lambda}\right)-\frac{d^2-6}{6d}Q_{\frac{d}{2}-1}\left(\frac{\partial_t R_k}{z+R_k}\right)\right]+O(R^2)\Bigg\}\,.\end{aligned} \tag{3.34}$$

The beta functions have again the form (3.25); the coefficient A_1 is the same as for the type Ia cutoff but now the coefficient B_1 is

$$\begin{aligned}B_1 &= 4\pi\Big(d(d-1)(d^3-15d^2-36)+24-2(d^5-8d^4-5d^3-72d^2-36d+96)\tilde{\Lambda}_k \\ &-16(d-1)(d^3+6d+12)\tilde{\Lambda}_k^2\Big)\Big/3(4\pi)^{\frac{d}{2}}d^2(d-1)\Gamma\left(\frac{d}{2}\right)(1-2\tilde{\Lambda}_k)^2\end{aligned} \tag{3.35}$$

3.3.4 Cutoff of type IIa

Let us define the following operators acting on gravitons and on ghosts:

$$\begin{aligned}\Delta_h &= (\mathbf{1}-\mathbf{P})\left(-D^2+\frac{4-3d+d^2}{d(d-1)}R\right)-\frac{d-2}{2}\mathbf{P}\left(-D^2+\frac{d-4}{d}R\right) \\ \Delta_{gh} &= -D^2 g^{\mu\nu}-\frac{R}{d}g^{\mu\nu}\end{aligned}$$

The type IIa cutoff is defined by the choice

$$\begin{aligned}\mathbf{R}_k &= \left(\mathbf{1}-\mathbf{P}-\frac{d-2}{2}\mathbf{P}\right)R_k(\Delta_h) \\ R_k^{(gh)\mu\nu} &= g_{\mu\nu}R_k(\Delta_{(gh)})\,,\end{aligned}$$

Collecting all terms and evaluating the traces leads to

$$\begin{aligned}\frac{d}{dt}\Gamma_k &= \frac{1}{(4\pi)^{d/2}}\int dx\,\sqrt{g}\left\{\frac{d(d+1)}{4}Q_{\frac{d}{2}}\left(\frac{\partial_t R_k}{z+R_k-2\Lambda_k}\right)-d\,Q_{\frac{d}{2}}\left(\frac{\partial_t R_k}{z+R_k}\right)\right. \\ &\left.+\left[\frac{d(7-5d)}{24}Q_{\frac{d}{2}-1}\left(\frac{\partial_t R_k}{z+R_k-2\Lambda_k}\right)-\frac{d+6}{6}Q_{\frac{d}{2}-1}\left(\frac{\partial_t R_k}{z+R_k}\right)\right]R+O(R^2)\right\}\,.\end{aligned} \tag{3.36}$$

The beta functions are again of the form (3.25), and the coefficient A_1 is the same as in the case of the cutoffs of type I. The coefficients B_1 is now

$$B_1 = -\frac{4\pi(5d^2-3d+24-8(d+6)\tilde{\Lambda}_k)}{3(4\pi)^{\frac{d}{2}}\Gamma(\frac{d}{2})(1-2\,\tilde{\Lambda}_k)}\,. \tag{3.37}$$

3.3.5 Cutoff of type IIb

This type of cutoff was introduced in [20]. The fluctuation $h_{\mu\nu}$ and the ghosts are decomposed into their different spin components as in the type Ib case. We define the cutoff on each component respectively as a function of the following operators

$$\begin{aligned}
\Delta_{h^T} &= -D^2 + \frac{d^2-3d+4}{d(d-1)}R \qquad & \Delta_\xi &= -D + \frac{d-3}{d}R \\
\Delta_h &= -D^2 + \frac{d-4}{d}R & \Delta_\sigma &= -D^2 + \frac{d-4}{d}R \\
\Delta_{\bar{c}^T c^T} &= -D^2 + \frac{R}{d} & \Delta_{\bar{c}c} &= -D^2 + \frac{2}{d}R\ .
\end{aligned} \tag{3.38}$$

Collecting all terms and evaluating the traces leads to

$$\begin{aligned}
\frac{d}{dt}\Gamma_k \;=\; & \frac{1}{(4\pi)^{d/2}}\int dx\,\sqrt{g}\left\{\frac{d(d+1)}{4}Q_{\frac{d}{2}}\left(\frac{\partial_t R_k}{z+R_k-2\Lambda_k}\right) - d\,Q_{\frac{d}{2}}\left(\frac{\partial_t R_k}{z+R_k}\right)\right. \\
& + \left[-\frac{5d^4-12d^3-5d^2-24d+12}{24(d-1)d}\,Q_{\frac{d}{2}-1}\left(\frac{\partial_t R_k}{z+R_k-2\Lambda_k}\right)\right. \\
& \left.\left. -\frac{d^2-6d-6}{6d}Q_{\frac{d}{2}-1}\left(\frac{\partial_t R_k}{z+R_k}\right)\right]R + O(R^2)\right\}\ .
\end{aligned} \tag{3.39}$$

The beta functions are again of the form (3.25), and the coefficient A_1 is the same as in the case of the cutoffs of type I. The coefficients B_1 is now

$$B_1 \;=\; -\frac{4\pi(5d^2-3d+24-8(d+6)\tilde{\Lambda}_k)}{3(4\pi)^{\frac{d}{2}}\Gamma(\frac{d}{2})(1-2\,\tilde{\Lambda}_k)}\ . \tag{3.40}$$

Notice that the B_1 coefficient is the same as the type IIa case. It is nevertheless interesting to understand the reason for this coincidence, which is independent of the shape of the cutoff function R_k. We will explore it in detail in Chapter 4.

3.3.6 Four dimensions

It's time to be more concrete, let us now consider Einstein's theory with cosmological constant in $d = 4$. The beta functions for $\tilde{\Lambda}_k$ and $\tilde{G}_k$ for various cutoff types have been given in equations (3.27,3.29,3.35,3.37,3.40).
All of these beta functions admit a Gaussian FP at $\tilde{\Lambda}_k = 0$ and $\tilde{G}_k = 0$ and a nontrivial FP at positive values of $\tilde{\Lambda}$ and $\tilde{G}$. Let us discuss the Gaussian FP first. As usual, the critical exponents are equal to 2 and -2, the canonical

mass dimensions of Λ_k and G_k. However, the corresponding eigenvectors are not aligned with the $\tilde{\Lambda}_k$ and $\tilde{G}_k$ axes.
Let us now come to the nontrivial FP. We begin by making for a moment the drastic approximation of expanding A_1 and B_1 in $\tilde{\Lambda}$ and just keeping the leading term ($A_1(\tilde{\Lambda} = 0)$ and $B_1(\tilde{\Lambda} = 0)$). We will call this linearized scheme "perturbative" approximation. Thus we consider again the perturbative Einstein–Hilbert flow. The FP would occur at $\tilde{\Lambda}_k^* = -A_1/4B_1$, $\tilde{G}_k^* = -2/B_1$, it has real critical exponents 2 and 4, equal to the canonical dimensions of the constants $g^{(0)} = 2\Lambda_k/(16\pi G_k)$ and $g^{(2)} = -1/(16\pi G_k)$.
This should not come as a surprise, since the linearized flow matrix for the couplings $g^{(0)}$ and $g^{(2)}$ is diagonal, with eigenvalues equal to their canonical dimensions, and the eigenvalues are invariant under regular coordinate transformations in the space of the couplings.

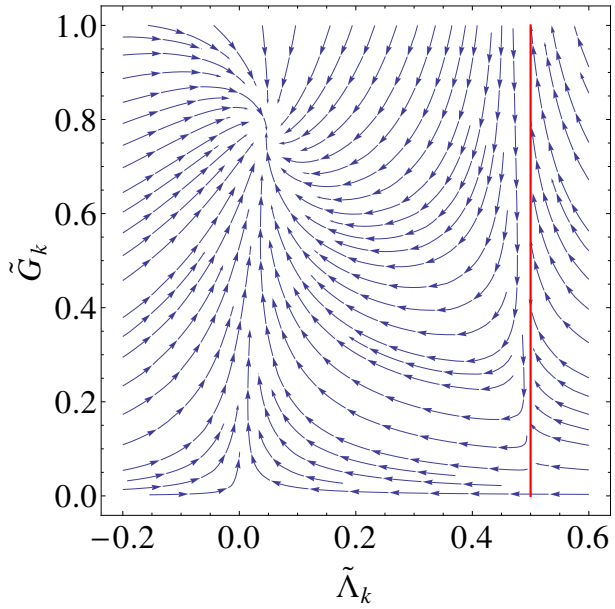

Figure 3.1: The flow near the perturbative region with cutoffs of type IIa. The red thick line on the right is a singularity of the beta functions.

So we see that a nontrivial UV–attractive FP in the $\tilde{\Lambda}_k$–$\tilde{G}_k$ plane appears already at the lowest level of perturbation theory. All the differences between the perturbative and the one loop approximation of Einstein–Hilbert flow are due to the dependence of the constants A_1 and B_1 on $\tilde{\Lambda}_k$ in the one loop one.

In all these calculations the critical exponents at the nontrivial FP always turn out to be a complex conjugate pair, giving rise to a spiralling flow.

Scheme	$\tilde{\Lambda}_*$	$\tilde{G}_*$	$\tilde{\Lambda}_*\tilde{G}_*$	ϑ
Ia	0.1213	1.1718	0.1421	1.868±1.398i
Ib	0.1012	1.1209	0.1134	1.903± 1.099 i
IIa	0.0467	0.7745	0.0362	2.310± 0.382 i
IIb	0.0467	0.7745	0.0362	2.310± 0.382 i

Table 3.1: The nontrivial fixed point for Einstein's theory in $d = 4$ with cosmological constant. To compare with literature we have to stress the fact we are neglecting the graviton anomalous dimensions. This is used called "one loop" computation.

The real part of these critical exponents is positive, corresponding to eigenvalues of the linearized flow matrix with negative real part. Therefore, the nontrivial FP is always UV-attractive in the $\tilde{\Lambda}_k$–$\tilde{G}_k$ plane. Conversely, an infinitesimal perturbation away from the FP will give rise to a renormalization group trajectory that flows towards lower energy scales away from the nontrivial FP. Among these trajectories there is a unique one that connects the nontrivial FP in the ultraviolet to the Gaussian FP in the infrared. This is called the "separatrix".
One noteworthy aspect of the flow equations in the Einstein–Hilbert truncation is the existence of a singularity of the beta functions. There are always choices of $\tilde{\Lambda}_k$ and $\tilde{G}_k$ for which the denominators vanish. The singularities are the boundaries of the shaded region in figure 3.1. Of course the flow exists also beyond these singularities but those points cannot be joined continuously to the flow in the perturbative region near the Gaussian FP, which we know to be a good description of low energy gravity.

When the trajectories emanating from the nontrivial FP approach these singularities, they reach it at finite values of t and the flow cannot be extended to $t \to -\infty$. The presence of these singularities can be interpreted as a failure of the Einstein–Hilbert truncation to capture all features of infrared physics and it is believed that they will be avoided by considering a more complete truncation.

In table 3.1 we collect the main features of the UV–attractive FP for the Einstein–Hilbert truncation with cosmological constant for the different cutoff schemes.

3.A Heat kernel expansion

Here we are going to give a very brief account of the heat kernel expansion we used in this chapter. The heat kernel (HK) is the study of the flow

$$(\partial_z + \Delta)\, K(z) = 0 \tag{3.41}$$

where Δ is a covariant differential operator acting on a section of an unspecified vector bundle V. Let the base manifold be a d-dimensional Riemannian manifold with metric $g_{\mu\nu}$. We restrict our attention to the case in which Δ is of rank 2 and in particular of the form

$$\Delta = \Box + E = -D^2 + E\ . \tag{3.42}$$

We introduced a covariant derivative D, which contains the connection of the bundle, and the box operator defined as $\Box = -D^2 = -g^{\mu\nu} D_\mu D_\nu$. E is a general endomorphism of the bundle. An operator of the form (3.42) is sometimes called "generalized laplacian". The connection itself will be a tensor product of the connection of the bundle and the Christoffel connection of the base manifold. The formal solution of (3.41) is

$$K(s) = e^{-s\Delta} \tag{3.43}$$

It is useful to evaluate the functional trace of the heat kernel

$$\mathrm{Tr}K(s) = \mathrm{tr} \int dx K(s; x, x) \tag{3.44}$$

where tr is the trace over the indices of the bundle and $K(s; y, x)$ solves the differential equation

$$(\partial_s + \Delta_x)\, K(s; y, x) = 0 \tag{3.45}$$

with boundary condition $K(0; y, x) = \delta(x - y)$ (the Dirac delta is for the measure $dx = \sqrt{g} dx$). It turns out that the object $\mathrm{Tr}K(s)$ possesses an expansion in powers of s, that relates to a local expansion in curvatures and powers of the endomorphism E.

This expansion is called Seeley-deWitt expansion and it reads

$$\mathrm{Tr}K(z) = \frac{1}{(4\pi z)^{d/2}} \sum_{n \geq 0} z^n B_{2n}[\Delta] \tag{3.46}$$

The coefficients $B_{2n}[\Delta]$ can be written in terms of other functions $b_{2n}[\Delta]$ defined as

$$B_{2n}[\Delta] = \mathrm{tr} \int dx \sqrt{g}\ b_{2n}[\Delta] \tag{3.47}$$

The new coefficients take values in the endomorphisms of V. The first two b's are

$$b_0[\Delta] = 1 , \tag{3.48}$$
$$b_2[\Delta] = E + R/6 . \tag{3.49}$$

R is the curvature scalar. All the terms in these two expansion, apart for E, are proportional to the identity in the bundle. Once traced with "tr", these will give a result proportional to the dimensionality of the bundle itself.

The expansion (3.46) can be used to calculate the trace of any function of an operator Δ. Suppose now we are interested in calculating the general trace

$$\mathrm{Tr} f[\Delta] \tag{3.50}$$

for arbitrary f. It is convenient to rewrite f in terms of its inverse Laplace transform $\tilde{f}$ and insert it in the trace

$$\mathrm{Tr} f[\Delta] = \mathrm{Tr} \int_0^\infty dz \tilde{f}[z] e^{-z\Delta} = \int_0^\infty dz \tilde{f}[z] \mathrm{Tr} K[z] , \tag{3.51}$$

which shows how to relate any trace with that of the HK.

If we substitute in (3.51) the expansion (3.46), we obtain an expansion with which evaluate the functional trace of $f[\Delta]$.

$$\mathrm{Tr} f[\Delta] = \frac{1}{(4\pi)^{d/2}} \left(Q_{d/2}(f) B_0[\Delta] + Q_{d/2-1}(f) B_2[\Delta] + Q_{d/2-2}(f) B_4[\Delta] + \cdots \right) , \tag{3.52}$$

where

$$Q_m(f) = \int_0^\infty ds s^{-m} \tilde{f}(s) . \tag{3.53}$$

Using the properties of the Laplace transform we can write the functions $Q_m(f)$ in term of f instead if its transform:

$$Q_m(f) = \frac{1}{\Gamma(m)} \int_0^\infty dz z^{m-1} f[z] \qquad \text{for } m \geq 0 \text{ integer} . \tag{3.54}$$

3.B Spectral geometry of differentially constrained fields

In this appendix we specialize the manifold we are working on to be a sphere. Consider the decomposition of a vector field A_μ into its transverse and longitudinal parts:

$$A_\mu \to A^T_\mu + D_\mu \Phi \ .$$

The spectrum of $-D^2$ on vectors is the disjoint union of the spectrum on transverse and longitudinal vectors. The latter can be related to the spectrum of $-D^2 - \frac{R}{d}$ on scalars using the formula

$$-D^2 D_\mu \Phi = -D_\mu \left(D^2 + \frac{R}{d} \right) \Phi \ . \tag{3.55}$$

Therefore one can write for the heat kernel

$$\mathrm{Tr} e^{-s\left(-D^2\right)} \mid_{A_\mu} = \mathrm{Tr} e^{-s\left(-D^2\right)} \mid_{A^T_\mu} + \mathrm{Tr} e^{-s\left(-D^2 - \frac{R}{d}\right)} \mid_{\Phi} - e^{\left(s\frac{R}{d}\right)} \ . \tag{3.56}$$

The last term has to be subtracted because a constant scalar is an eigenfunction of $-D^2 - \frac{R}{d}$ with negative eigenvalue, but does not correspond to an eigenfunction of $-D^2$ on vectors. The spectrum of $-D^2$ on scalars and transverse vectors is obtained from the representation theory of $SO(d+1)$ and is reported in table 3.2.

A similar argument works for symmetric tensors, when using the decomposition (3.30). One can use equation

$$-D^2 \left(D_\mu \xi_\nu + D_\nu \xi_\mu \right) = D_\mu \left(-D^2 - \frac{d+1}{d\,(d-1)} R \right) \xi_\nu + D_\nu \left(-D^2 - \frac{d+1}{d\,(d-1)} R \right) \xi_\mu \ , \tag{3.57}$$

and equation

$$-D^2 \left(D_\mu D_\nu - \frac{1}{d} g_{\mu\nu} D^2 \right) \sigma = \left(D_\mu D_\nu - \frac{1}{d} g_{\mu\nu} D^2 \right) \left(-D^2 - \frac{2}{d-1} R \right) \sigma \ , \tag{3.58}$$

to relate the spectrum of various operators on vectors and scalars to the spectrum of $-D^2$ on tensors. One has to observe that the $d(d+1)/2$ Killing vectors are eigenvectors of $-D^2 - \frac{d+1}{d(d-1)} R$ on vectors but give a vanishing tensor $h_{\mu\nu}$, so they do not contribute to the spectrum of $-D^2$ on tensors. Likewise, a constant scalar and the $d+1$ scalars proportional to the Cartesian coordinates of the embedding $\mathbf{R}^n$, which correspond to the lowest two

Spin s	Eigenvalue $\lambda_l(d,s)$	Multiplicity $D_l(d,s)$
0	$\frac{l(l+d-1)}{d(d-1)}R;\ l=0,1\ldots$	$\frac{(2l+d-1)(l+d-2)!}{l!(d-1)!}$
1	$\frac{l(l+d-1)-1}{d(d-1)}R;\ l=1,2\ldots$	$\frac{l(l+d-1)(2l+d-1)(l+d-3)!}{(d-2)!(l+1)!}$
2	$\frac{l(l+d-1)-2}{d(d-1)}R;\ l=2,3\ldots$	$\frac{(d+1)(d-2)(l+d)(l-1)(2l+d-1)(l+d-3)!}{2(d-1)!(l+1)!}$

Table 3.2: Eigenvalues of the Laplacian on the d-sphere and their multiplicities

eigenvalues of $-D^2-\frac{2}{d-1}R$, also do not contribute to the spectrum of tensors. So one has for the heat kernel on tensors

$$\begin{aligned}\operatorname{Tr} e^{\left(-s\left(-D^2\right)\right)}\Big|_{h_{\mu\nu}} &= \operatorname{Tr} e^{\left(-s\left(-D^2\right)\right)}\Big|_{h^T_{\mu\nu}} + \operatorname{Tr} e^{\left(-s\left(-D^2-\frac{(d+1)R}{d(d-1)}\right)\right)}\Big|_{\xi} \\ &\quad + \operatorname{Tr} e^{\left(-s\left(-D^2\right)\right)}\Big|_{h} + \operatorname{Tr} e^{\left(-s\left(-D^2-\frac{2}{d-1}R\right)\right)}\,|_{\sigma} \\ &\quad - e^{\left(\frac{2}{d-1}sR\right)} - (d+1)\, e^{\left(\frac{1}{d-1}sR\right)} - \frac{d\,(d+1)}{2}\, e^{\left(\frac{2}{d(d-1)}sR\right)}\ .\end{aligned} \tag{3.59}$$

The last exponentials can be expanded in Taylor series as $\sum_{m=0}^{\infty} c_m R^m$ and these terms can be viewed as modifications of the heat kernel coefficients of $-D^2$ acting on the differentially constrained fields. To see where these modifications enter, recall that the volume of the sphere is

$$V_{\mathrm{dS}} = (4\pi)^{\frac{d}{2}} \left(\frac{d\,(d-1)}{R}\right)^{\frac{d}{2}} \frac{\Gamma\left(\frac{d}{2}\right)}{\Gamma\,(d)}\ , \tag{3.60}$$

so that

$$\int \mathrm{d}^d x\sqrt{g}\,\operatorname{Tr} b_n \propto R^{\frac{n-d}{2}}\ . \tag{3.61}$$

This means a coefficient c_m from the Taylor series will contribute to a heat kernel coefficient for which $2m=n-d$. So there are contributions to b_n only for $n\geq d$.

If a computation involve such coefficients, the negative and zero modes of constrained scalar and vector fields have to be excluded from the traces over the constrained fields; this is denoted by one or two primes, depending on the number of excluded modes.

Chapter 4

Fermions in Asymptotic Safety

4.1 Coupling spinors to gravity in brief

Some care is required when coupling spinor fields to gravity. The general procedure involves increasing the number of gravitational degrees of freedom by introducing a d-bein e^a_μ, that is a set of one-forms such that

$$g_{\mu\nu} = e^a_\mu e^b_\nu \delta_{ab} \ . \tag{4.1}$$

We also require the d-bein to have an inverse, so a set of vectors e^μ_a exist such that

$$e^\mu_a e^b_\mu = \delta^b_a \ , \tag{4.2}$$
$$e^\mu_a e^a_\nu = \delta^\mu_\nu \ . \tag{4.3}$$
$$\tag{4.4}$$

These are useful because when adopting them as a basis the metric gets trivialized. The number of degrees of freedom of the d-bein is bigger than that of the metric and it is easy to see it. The metric is a symmetric tensor that in four dimensions has ten independent components, while e^a_μ has sixteen components. A d-bein is therefore a general linear transformation, one is allowed to think of it as a basis transformation on the tangent bundle. Alternatively it can be seen as an isomorphism between the tangent bundle and another bundle with flat metric tensor. Let $\mathcal{M}$ be the Euclidean spacetime manifold and $T\mathcal{M}$ its tangent bundle. Before going on we need to fix some terminology. When resticted to 4 dimensions the d-bein is called vierbain or tetrad. When we will refer to the general formulation of gravity where the fundamental field is thee d-bein we will use the name tetrad formulation even if it is not precise. Further, we call V a vector bundle with fiber $\mathbb{R}^4$. In this

new bundle we can construct a connection $A^a_{\mu b}$ requiring $\nabla_\mu e^a_\nu = 0$ where ∇ is the total covariant derivative on $T\mathcal{M} \oplus V$. This gives its relation to the Christoffel connection on $T\mathcal{M}$

$$A^a_{\mu b} = e^a_\lambda \Gamma^\lambda_{\mu\nu} e^\nu_b + e^a_\lambda \partial_\mu e^\lambda_b \ . \tag{4.5}$$

This new connection can be used to construct a spinor covariant derivative

$$D_\mu \psi = \partial_\mu \psi + \frac{1}{2} A_{\mu,ab} J^{ab} \psi \ . \tag{4.6}$$

where the generators J_{ab} of $O(4)$ rotations in V are obtained from the Clifford algebra $\left\{\gamma^a, \gamma^b\right\} = 2\delta^{ab}$

$$J^{ab} = \frac{1}{4}\left[\gamma^a, \gamma^b\right] \ . \tag{4.7}$$

The $O(4)$ gauge invariance accounts for the additional degrees of freedom of the d-bein and can be gauge fixed in such a way that the vielbeins are symmetric. With this choice they essentially maintain only the degrees of freedom of the metric. Finally we can construct the spinor field action. The conjugate spinor is introduced as usual $\bar{\psi} = \psi^\dagger \gamma^0$ and the Lagrangian is

$$i\bar{\psi}\gamma^a e^\mu_a D_\mu \psi = \bar{\psi} i \not{D} \psi \ . \tag{4.8}$$

It is easily seen that the metric degrees of freedom will enter in three ways in the spinor action, namely in the volume element, the covariant derivative and the inverse d-bein that couples the covariant derivative. This makes the treatment of spinor field in gravitational settings more complicated than that of a scalar.

4.2 Noticing an ambiguity

In the first part of this chapter we will focus on solving one ambiguity present in the literature on the renormalization group for gravity where the scheme dependence is particularly nasty: it is the contribution of fermion fields to the beta function of Newton's constant. This contribution has been computed, for example, in Sec. III of [18]. If there are N_D Dirac fields, it is in 4 dimensions

$$-N_D \frac{1}{2(4\pi)^2} \int d^4x \sqrt{g} \left(\frac{2}{3} Q_1 \left(\frac{\partial_t R_k}{P_k} \right) - Q_2 \left(\frac{\partial_t R_k}{P_k^2} \right) \right) R \ , \tag{4.9}$$

if one uses a type I cutoff and

$$N_D \frac{1}{2(4\pi)^2} \int d^4x \sqrt{g} \, \frac{1}{3} Q_1 \left(\frac{\partial_t R_k}{P_k} \right) R \ , \tag{4.10}$$

if one uses a type II cutoff. Here $P_k(z) = z + R_k(z)$ is the modified propagator. If we use the optimized cutoff (1.35) the contribution of fermions to the relevant term of the beta functional is

$$-\frac{N_D}{96\pi^2}\int d^4x\,\sqrt{g}\,R \qquad \text{for the type I cutoff} \tag{4.11}$$

$$\frac{N_D}{48\pi^2}\int d^4x\,\sqrt{g}\,R \qquad \text{for the type II cutoff.} \tag{4.12}$$

The latter agrees with an earlier independent calculation of the renormalization of G in [21]; the former differs not just in the value of the coefficient but even in the sign. To check that this is not just a quirk of the optimized cutoff, we considered also an exponential cutoff (1.36) and encountered the same problem.

This sign ambiguity is puzzling. Since the beta function of G vanishes for $G = 0$, the sign of G can never change in the course of the RG flow (we disregard here as pathological the case when the inverse of G passes through zero). Therefore, if the physical RG trajectory approaches a fixed point in the UV, the sign of Newton's constant at low energy will be the same as that of Newton's constant at the fixed point. In a model where gravity is induced by minimally coupled fermions, the sign of Newton's constant would depend on the scheme.

One has to be careful in drawing physical conclusions from these calculations: the relation between the coupling G appearing in Γ_k and the physical Newton's constant that is measured in the laboratory may not be as simple as it seems. The functional that obeys an exact RG equation is not a simple functional of a single metric but rather a functional of a background metric and (the expectation value of) the fluctuation of the metric. This functional is not invariant under shifts of the background and fluctuation that keep the sum constant, and therefore there may be several couplings that one could legitimately call "Newton's constant" (for a discussion see [22–24]). The one that we are discussing here is the one that multiplies the Hilbert action constructed from the background metric only, and it is not obvious that the other ones would behave in the same way. We will come back on this point in the following chapters. To make a completely well–defined statement one should really calculate a physical observable and in such a calculation all ambiguities should disappear. It is therefore possible, in principle, that even the sign difference between the two calculations discussed above may be resolved when one considers physical observables. In this chapter we will argue for a different and simpler solution of the issue, namely that only the type II cutoff gives a result with the physically correct sign.

As an aside, we will also calculate the contribution to the beta functions

of the cosmological constant and Newton constant due to Euclidean Kähler fermions in four dimensions. Kähler fermions are a way of describing fermion fields in terms of Grassmann algebra elements, instead of spinors, and it has the merit that it does not require the use of tetrad fields. We find that one Kähler fermion gives exactly the same contribution as four Dirac spinors, and that the same sign issue is present.

4.2.1 Kähler fermions

Before discussing in detail the issue of the cutoff scheme with ordinary spinor fermions, we would like to point out that precisely the same problem arises also in another representation of fermionic matter.

As is well known, in any dimension the Grassmann and the Clifford algebras are isomorphic as vector spaces. This is the basis for a representation of fermion fields as inhomogeneous differential forms [25–27]. Such fields are called Kähler fermions. In this representation the analogue of the Dirac operator is the first order operator $d + \delta$, where d is the exterior derivative and δ is its adjoint. Note that the use of tetrads is not required. We would like to compare the contribution of Kähler fermions to the gravitational beta functions to the one of ordinary spinor fermions. In particular we would like to see whether the same sign issue arises when different cutoff types are used. Since the details of the calculation are strongly dimension dependent, we shall restrict our attention to the case $d = 4$.

An inhomogeneous complex differential form Φ can be expanded as

$$\begin{aligned}\Phi &= \varphi(x) + \varphi_\mu(x)dx^\mu + \frac{1}{2!}\varphi_{\mu\nu}(x)dx^\mu \wedge dx^\nu + \\ &\quad \frac{1}{3!}\varphi_{\mu\nu\rho}(x)dx^\mu \wedge dx^\nu \wedge dx^\rho + \frac{1}{4!}\varphi_{\mu\nu\rho\sigma}(x)dx^\mu \wedge dx^\nu \wedge dx^\rho \wedge dx^\sigma \ .\end{aligned} \tag{4.13}$$

We can map the 3- and 4-form via Hodge duality into a 1- and 0-form respectively. The field Φ thus describes a scalar, a pseudoscalar, a vector, a pseudovector and an antisymmetric tensor, for a total of 16 complex components. This is an early sign of the fact that one Kähler field is equivalent to four Dirac fields.

The square of the Kähler operator is the Laplacian on forms: $\Delta = (d + \delta)^2 = d\delta + \delta d$. On forms of degree 0, 1 and 2 it is given explicitly by

$$\Delta^{(0)} = -\nabla^2 \ , \tag{4.14}$$

$$\Delta^{(1)\mu}_{\ \nu} = -\nabla^2 \delta^\mu_\nu + R^\mu_{\ \ \nu} \ , \tag{4.15}$$

$$\Delta^{(2)\gamma\sigma}_{\alpha\beta} = -\nabla^2 \mathbf{1}_{\alpha\beta}{}^{\gamma\sigma} + R_\alpha{}^\gamma \delta_\beta{}^\sigma - R_\beta{}^\gamma \delta_\alpha{}^\sigma - 2R_\alpha{}^\gamma{}_\beta{}^\sigma \ . \tag{4.16}$$

In a maximally symmetric space (3.4) the operators defined above reduce to

$$\Delta_\nu^{(1)\mu} = \left(-\nabla^2 + \frac{1}{4}R\right)\delta_\nu^\mu \ , \tag{4.17}$$

$$\Delta_{\alpha\beta}^{(2)\gamma\sigma} = \left(-\nabla^2 + \frac{1}{3}R\right)\mathbf{1}_{\alpha\beta}{}^{\gamma\sigma} \ . \tag{4.18}$$

The FRGE for a Kähler fermion within the Einstein-Hilbert truncation with a type II cutoff is

$$\begin{aligned}\frac{d\Gamma_k}{dt} =& -2\,\frac{1}{2}\mathrm{Tr}_{(0)}\left(\frac{\partial_t R_k(\Delta^{(0)})}{P_k(\Delta^{(0)})}\right) - 2\,\frac{1}{2}\mathrm{Tr}_{(1)}\left(\frac{\partial_t R_k(\Delta^{(1)})}{P_k(\Delta^{(1)})}\right) - \frac{1}{2}\mathrm{Tr}_{(2)}\left(\frac{\partial_t R_k(\Delta^{(2)})}{P_k(\Delta^{(2)})}\right) \\ =& 4\cdot\frac{1}{2}\frac{1}{(4\pi)^2}\int d^4x\,\sqrt{g}\left[-4\,Q_2\left(\frac{\partial_t R_k}{P_k}\right) + \frac{1}{3}R\ , Q_1\left(\frac{\partial_t R_k}{P_k}\right)\right] \ .\end{aligned} \tag{4.19}$$

For a type I cutoff we find instead:

$$\begin{aligned}\frac{d\Gamma_k}{dt} =& -2\cdot\frac{1}{2}\mathrm{Tr}_{(0)}\left(\frac{\partial_t R_k(-\nabla^2)}{P_k(-\nabla^2)}\right) - 2\cdot\frac{1}{2}\mathrm{Tr}_{(1)}\left(\frac{\partial_t R_k(-\nabla^2)}{P_k(-\nabla^2)+\frac{R}{4}}\right) - \frac{1}{2}\mathrm{Tr}_{(2)}\left(\frac{\partial_t R_k(-\nabla^2)}{P_k(-\nabla^2)+\frac{R}{3}}\right) \\ =& 4\cdot\frac{1}{2}\frac{1}{(4\pi)^2}\int d^4x\,\sqrt{g}\left[-4\,Q_2\left(\frac{\partial_t R_k}{P_k}\right) - R\left(\frac{2}{3}\,Q_1\left(\frac{\partial_t R_k}{P_k}\right) - Q_2\left(\frac{\partial_t R_k}{P_k^2}\right)\right)\right] \ .\end{aligned} \tag{4.20}$$

Evaluating the Q functionals (3.54) for the cutoff (1.35) we get

$$\text{type II:}\quad \frac{d\Gamma_k}{dt} = 4\cdot\frac{1}{2}\frac{1}{(4\pi)^2}\int d^4x\,\sqrt{g}\left[-4\,k^4 + \frac{2}{3}R\,k^2\right] \tag{4.21}$$

$$\text{type I:}\quad \frac{d\Gamma_k}{dt} = 4\cdot\frac{1}{2}\frac{1}{(4\pi)^2}\int d^4x\,\sqrt{g}\left[-4\,k^4 - \frac{1}{3}R\,k^2\right] \ . \tag{4.22}$$

In both cases the effect of one Kähler fermion is seen to match exactly the result of four spinors ($N_D = 4$). This should not induce one to believe that spinors and Kähler fermions are equivalent: in fact, their contributions to the curvature squared terms are quite different. Nevertheless, the puzzling sign issue of the R term that afflicts spinor fermions is present in this case too.

4.2.2 Cutoff choice for fermions

We now return to ordinary Dirac spinor fields and we reexamine in more detail their contribution to the gravitational effective action and beta functions. For the sake of generality we will now work in arbitrary dimension

d. The standard way of defining the effective action for a fermion field that is minimally coupled to gravity is to exploit the properties of the logarithm and write

$$\Gamma = -\mathrm{Tr}\log(|\not{D}|) = -\frac{1}{2}\mathrm{Tr}\log(\not{D}^2) = -\frac{1}{2}\mathrm{Tr}\log\left(-\nabla^2 + \frac{R}{4}\right) \ . \tag{4.23}$$

The corresponding one-loop EAA can then be defined as

$$\Gamma_k = -\frac{1}{2}\mathrm{Tr}\log\left(-\nabla^2 + \frac{R}{4} + R_k\right) \ . \tag{4.24}$$

In the definition of this functional one encounters the same ambiguities that we have mentioned in Section 3.3.1 for the gravitational systems. In addition to the shape of the cutoff function R_k, one seems to also have the freedom of choosing the argument of this function to be either $-\nabla^2$ (type I cutoff) or $-\nabla^2 + \frac{R}{4}$ (type II cutoff). The former choice has been made in [19, 28–31], the latter in [32]. Taking the derivative respect to the RG time t and defining $P_k(z) = z + R_k(z)$, one has

$$\frac{d\Gamma_k}{dt} = -\frac{1}{2}\mathrm{Tr}\frac{\partial_t R_k(-\nabla^2)}{P_k(-\nabla^2) + \frac{R}{4}} \qquad \text{for a type I cutoff,} \tag{4.25}$$

$$\frac{d\Gamma_k}{dt} = -\frac{1}{2}\mathrm{Tr}\frac{\partial_t R_k(-\nabla^2 + \frac{R}{4})}{P_k(-\nabla^2 + \frac{R}{4})} \qquad \text{for a type II cutoff.} \tag{4.26}$$

The first few terms in the curvature expansion of these traces can be evaluated, for any background, using heat kernel methods (see Appendix 3.A). However, for a spherical background, the spectrum of the Dirac operator is known explicitly, and the same traces can also be computed directly as spectral sums.

4.2.3 Heat kernel evaluation

With a type I cutoff, the trace (4.25) giving contribution of N_D Dirac spinors to the FRGE is

$$\frac{d\Gamma_k}{dt} = -\frac{N_D}{2}\frac{2^{[d/2]}}{(4\pi)^{d/2}}\int d^dx\,\sqrt{g}\left[Q_{\frac{d}{2}}\left(\frac{\partial_t R_k}{P_k}\right) + \left(\frac{1}{6}Q_{\frac{d}{2}-1}\left(\frac{\partial_t R_k}{P_k}\right) - \frac{1}{4}Q_{\frac{d}{2}}\left(\frac{\partial_t R_k}{P_k^2}\right)\right)R + \dots\right] . \tag{4.27}$$

Here $2^{[d/2]}$ (where $[x]$ is the integer part of x) is the dimension of the representation. The first term proportional to R is proportional to the heat kernel coefficient $b_2(-\nabla^2)$, and the second comes from the expansion of the

denominator in (4.25). Evaluating the Q functionals with the cutoff (1.35) we obtain

$$\frac{d\Gamma_k}{dt} = -\frac{1}{\Gamma\left(\frac{d}{2}+1\right)}\frac{2^{[d/2]}}{(4\pi)^{d/2}}N_D\int d^dx\,\sqrt{g}\left[k^d+\frac{d-3}{12}k^{d-2}R\right]\ . \tag{4.28}$$

Evaluating (4.26) with the same techniques yields

$$\frac{d\Gamma_k}{dt} = -\frac{N_D}{2}\frac{2^{[d/2]}}{(4\pi)^{d/2}}\int d^dx\,\sqrt{g}\left[Q_{\frac{d}{2}}\left(\frac{\partial_t R_k}{P_k}\right)-\frac{1}{12}R\,Q_{\frac{d}{2}-1}\left(\frac{\partial_t R_k}{P_k}\right)+\ldots\right], \tag{4.29}$$

where the term proportional to R comes entirely from the heat kernel coefficient $b_2\left(-\nabla^2+\frac{R}{4}\right)$. Evaluating with the cutoff (1.35) we obtain

$$\frac{d\Gamma_k}{dt} = -\frac{1}{\Gamma\left(\frac{d}{2}+1\right)}\frac{2^{[d/2]}}{(4\pi)^{d/2}}N_D\int d^dx\,\sqrt{g}\left[k^d-\frac{d}{24}k^{d-2}R\right]\ . \tag{4.30}$$

In $d=4$ this yields the results quoted in Sec. I. We see that the sign issue is present in any dimension $d>3$.

4.2.4 Spectral sums on S^d

The heat kernel calculation of the preceding subsection can be done in an arbitrary background. On the other hand, in the case of the spherical background we know explicitly the spectrum of the Dirac operator: the eigenvalues and multiplicities are

$$\lambda_n^{\pm} = \pm\sqrt{\frac{R}{d(d-1)}}\left(\frac{d}{2}+n\right)\ ,\qquad m_n = 2^{\left[\frac{d}{2}\right]}\left(\begin{array}{c} n+d-1 \\ n \end{array}\right)\ ,\qquad n=0,1,\ldots\ . \tag{4.31}$$

With this information one can compute the trace of any function of the Dirac operator as $\mathrm{Tr}\,f(\not{D}) = \sum_{n=0}^{\infty} m_n f(\lambda_n)$. We will now evaluate the right hand side (r.h.s.) of the FRGE by imposing a cutoff on the eigenvalues of the Dirac operator. The one-loop EAA can be defined directly in terms of the Dirac operator as

$$\Gamma_k = -\mathrm{tr}\log\left(|\not{D}| + R_k^D(|\not{D}|)\right)\ , \tag{4.32}$$

where the cutoff R_k^D has to be a function of the modulus of the Dirac operator, since we want to suppress the modes depending on the wavelength of the corresponding eigenfunctions. This is also needed for reasons of convergence. Since the operator is first order, the conditions that R_k^D has to satisfy are

similar to (i) to (iv) of (1), except for the replacement of q^2 and k^2 by λ_n and k respectively. For the explicit evaluation, we will use the optimized profile

$$R_k^D(z) = (k-z)\theta(k-z) \ , \quad (z>0) \ . \tag{4.33}$$

Then we have

$$\mathrm{Tr}\left[\frac{\partial_t R_k^D(|\not{D}|)}{P_k^D(|\not{D}|)}\right] = \sum_n m_n \frac{\partial_t R_k^D(|\lambda_n|)}{P_k^D(|\lambda_n|)} = \sum_{\pm}\sum_n m_n \theta(k-|\lambda_n|) \ . \tag{4.34}$$

The sum can be computed using the Euler-Maclaurin formula.

$$\begin{aligned}\sum_{i=0}^{n} F(i) &= \int_0^n F(x)\,dx - B_1\cdot(F(n)+F(0)) + \\ &\sum_{k=1}^{p}\frac{B_{2k}}{(2k)!}\left(F^{(2k-1)}(n)-F^{(2k-1)}(0)\right) + \text{remainder}\end{aligned} \tag{4.35}$$

where B_i are the Bernoulli numbers. After collecting a volume contribution, the only terms we need to compute are the zeroth and first power of R.

Note that only the integral depends on R, and therefore, in dimensions $d>2$ for the terms that we are interested in it is enough to compute the integral.

Since the volume of the d sphere is $V(d) = \frac{2}{d!}\Gamma\left(\frac{d}{2}+1\right)(4\pi)^{d/2}\left(\frac{(d-1)d}{R}\right)^{d/2}$ we only have to isolate the terms in the integral proportional to $R^{-d/2}$ and $R^{1-d/2}$

$$2\,2^{\left[\frac{d}{2}\right]}\int_0^{k\sqrt{\frac{d(d-1)}{R}}-\frac{d}{2}} \mathrm{d}n\ \begin{pmatrix} n+d-1 \\ n \end{pmatrix} = 2\,\frac{2^{\left[\frac{d}{2}\right]}}{(d-1)!}\int_0^{k\sqrt{\frac{d(d-1)}{R}}-\frac{d}{2}} \mathrm{d}n\ (n+d-1)\cdots(n+1) \ , \tag{4.36}$$

changing variables $n \to n' - d/2$

$$2\frac{2^{\left[\frac{d}{2}\right]}}{(d-1)!}\int_{\frac{d}{2}}^{k\sqrt{\frac{d(d-1)}{R}}} \mathrm{d}n'\ \left(n'+\frac{d}{2}-1\right)\cdots\left(n'-\left(\frac{d}{2}-1\right)\right) \ , \tag{4.37}$$

the terms we are interested in come from the integral of the two highest order power of n'

$$\left(n'+\frac{d}{2}-1\right)\cdots\left(n'-\left(\frac{d}{2}-1\right)\right) = n'^{d-1} - n'^{d-3}\sum_{k=1}^{\left[\frac{d-1}{2}\right]}\left(\frac{d}{2}-k\right)^2 + \cdots \ , \tag{4.38}$$

we can rewrite the sum $\sum_{k=1}^{\left[\frac{d-1}{2}\right]}\left(\frac{d}{2}-k\right)^2=\frac{1}{24}d\,(d-1)\,(d-2)$, and perform the integral

$$\begin{aligned}\mathrm{Tr}\left[\frac{\partial_t R_k}{P_k}\right] &= 2\frac{2^{\left[\frac{d}{2}\right]}}{(d-1)!}\frac{1}{d}\left(k\sqrt{\frac{d(d-1)}{R}}\right)^d \\ &\quad -2\frac{2^{\left[\frac{d}{2}\right]}}{(d-1)!}\frac{1}{d-2}\left(k\sqrt{\frac{d(d-1)}{R}}\right)^{d-2}\frac{1}{24}d\,(d-1)\,(d-2)+\cdots\end{aligned} \tag{4.39}$$

Collecting the volume of S^d we obtain

$$\frac{d\Gamma_k}{dt}=-\mathrm{Tr}\left[\frac{\partial_t R_k}{P_k}\right]=-\frac{1}{\Gamma\left(\frac{d}{2}+1\right)}\frac{2^{\left[\frac{d}{2}\right]}}{(4\pi)^{\frac{d}{2}}}V(d)\left(k^d-\frac{d}{24}k^{d-2}R+O\left(R^2\right)\right)\,. \tag{4.40}$$

The result is

$$\frac{d\Gamma_k}{dt}=-\mathrm{Tr}\left[\frac{\partial_t R_k^D}{P_k^D}\right]=-\frac{1}{\Gamma\left(\frac{d}{2}+1\right)}\frac{2^{\left[\frac{d}{2}\right]}}{(4\pi)^{\frac{d}{2}}}V(d)\left(k^d-\frac{d}{24}k^{d-2}R+O\left(R^2\right)\right)\,, \tag{4.41}$$

where $V(d)$ is the volume of the d sphere. This agrees exactly with (4.30), which was obtained with the type II cutoff. It can be checked in the same way that the agreement extends also to the next order in the curvature expansion.

4.2.5 Solving the ambiguity

Note that computing the r.h.s. of the FRGE with a spectral sum is a much more direct procedure, since it avoids going through the square root of the square of the Dirac operator, and also avoids having to use the Laplace transform and the heat kernel. It is therefore also a more reliable procedure when there are ambiguities. The agreement of the spectral sum with the type II heat kernel calculation is a useful consistency check and suggests that the latter gives the correct result, whereas the type I cutoff does not.

If so, it remains to understand why the type I cutoff should not be admissible in this case. One can get some hint by thinking of what this cutoff does in terms of eigenvalues of the Dirac operator. We begin by noting that

(4.32) can be rewritten as follows [1]:

$$\begin{aligned}\Gamma_k &= -\frac{1}{2}\mathrm{tr}\log\left(|\not{D}| + R_k^D(|\not{D}|)\right)^2 \qquad (4.42)\\ &= -\frac{1}{2}\mathrm{tr}\log\left(-\nabla^2 + \frac{R}{4} + 2|\not{D}|R_k^D(|\not{D}|) + R_k^D(|\not{D}|)^2\right) .\end{aligned}$$

One can compare this with (4.24). Note that the cutoff R_k in that formula could be a function of different operators which, on a sphere, differ by a constant shift. For the present purposes it is convenient to think of it as a function of $\not{D}^2$. Calling $\bar{R}_k$ this function and calling $z = |\not{D}|$, we have

$$\bar{R}_k(z^2) = 2zR_k^D(z) + R_k^D(z)^2 . \qquad (4.43)$$

We can solve this relation to get

$$R_k^D(z) = -z + \sqrt{z^2 + \bar{R}_k(z^2)} , \qquad (4.44)$$

so for any cutoff imposed at the level of (4.24) one can reverse engineer an effective cutoff to be imposed at the level of (4.32) that will give the same result.

In general, this cutoff may fail to satisfy the required conditions, in particular condition (iv) of (1). For a type II cutoff, R_k in (4.24) is a function of z^2, so $\bar{R}_k(z^2) = R_k(z^2)$. This implies that $\bar{R}_0(z^2) = 0$ and thus also $R_0^D(z) = 0$ for all $z > 0$. For a type I cutoff, on the other hand, this may not be the case, as we will show in the following examples.

Consider first the optimized cutoffs. In the type II case one has $\bar{R}_k(z^2) = (k^2 - z^2)\theta(k^2 - z^2)$ and one finds that in this case the corresponding cutoff $R_k^D(z)$ given by (4.44) is also optimized, and precisely of the form (4.33). This is a way of understanding why the two calculations give the same result. In the case of a type I cutoff, we have instead $\bar{R}_k(z^2) = (k^2 - z^2 + R/4)\theta(k^2 - z^2 + R/4)$, whence one derives

$$R_k^D(z) = \left(\sqrt{k^2 + \frac{R}{4}} - z\right)\theta\left(\sqrt{k^2 + \frac{R}{4}} - z\right) . \qquad (4.45)$$

This does not tend uniformly to zero when $k \to 0$. In the case of an exponential type II cutoff with $\bar{R}_k = R_k$ given by (1.36), we have

$$R_k^D(z) = -z + \frac{z}{\sqrt{1 - e^{-a(z^2/k^2)^b}}} , \qquad (4.46)$$

[1] This is a formal relation because the functional Γ_k is ill–defined, but one can write a corresponding relation for $\frac{d}{dt}\Gamma_k$, with the same result.

which has all the desired properties. On the other hand for an exponential type I cutoff with $\bar{R}_k$ given by (1.36),

$$R_k^D(z) = -z + \sqrt{z^2 + \left(z^2 - \frac{R}{4}\right) \frac{e^{-a\left(z^2-\frac{R}{4}\right)^b/k^{2b}}}{1 - e^{-a\left(z^2-\frac{R}{4}\right)^b/k^{2b}}}} \ . \tag{4.47}$$

For b odd, and in particular for the most natural case $b = 1$, this function does not tend uniformly to zero when $k \to 0$ and therefore condition (iv) is not satisfied. [2]

An analogue reasoning can be also made for Kähler fermions, by applying the cutoff directly on the operator $d+\delta$ one recover exactly the type II cutoff result.

These arguments lend support to the view that only the type II cutoff gives the physically correct result. Of course not all results obtained from the type I cutoff have to be wrong; for example, the leading term (renormalizing the cosmological constant) and, in $d = 4$, the curvature squared terms are the same using the two cutoffs. These, however, are just the "universal" quantities that do not depend on the choice of the cutoff. We believe that for the generic dimensionful, nonuniversal quantities, the results obtained via a type I cutoff should not be trusted.

[2]Note that in the limit $k \to 0$ the function R_k^D is nonzero only for $z < \sqrt{R/4}$. Since the smallest eigenvalue of the Dirac operator is $\sqrt{R/3}$, it remains true that $\lim_{k\to 0} \Gamma_k = \Gamma$.

4.3 Tetrad gravity

When spinors are coupled to gravity an additional question arises regarding the field carrying the gravitational degrees of freedom. In [19, 28, 29], where the contribution of graviton loops was added to that of matter fields, as well as in [33–35] where scalars and fermions were interacting with gravity, the carrier of the gravitational degrees of freedom was the metric. It has been pointed out in [36] that in the presence of fermions it may be more natural to use the d-bein. Even if one chooses a Lorentz gauge where the antisymmetric part of the d-bein fluctuation is suppressed, the two calculations are not the same, because one has to work off shell and the Hessian in the tetrad formalism contains some additional terms proportional to the equations of motion. The calculations in [36], which used a type Ia cutoff in the $\alpha = 1$ gauge, show that a fixed point is still present, but is less stable than in the metric formulation. We will very briefly review their result in the following. In this thesis we present the computation of the gravitational contributions in the tetrad formalism, using type b cutoffs (both Ib and IIb); this allows us to analyze the off–shell α dependence. The results will be found to be somewhat closer to those of the metric formalism than those found in [36] (which we have independently verified), but they still present a stronger dependence on the scheme and on the gauge parameter.

4.3.1 Hessian and gauge fixing

The ansatz we make for the effective average action is the standard Einstein–Hilbert truncation (3.13) where the metric is represented in terms of d-beins that are considered the fundamental degrees of freedom. If we decompose in background plus fluctuation both $g_{\mu\nu} \equiv \bar{g}_{\mu\nu} + h_{\mu\nu}$ and $e^a{}_\mu \equiv \bar{e}^a{}_\mu + \varepsilon^a{}_\mu$ we have the relation

$$h_{\mu\nu} = 2\varepsilon_{(\mu\nu)} + \varepsilon_{(\mu}{}^\rho \varepsilon_{\nu)\rho} \tag{4.48}$$

where Latin indices on ε have been transformed to Greek ones by contraction with $\bar{e}$. Now substituting this formula in the Taylor expansion of the action in terms of metric fluctuations we find:

$$\Gamma^{EH}(e) = \Gamma^{EH}(\bar{e}) + \int \frac{\delta\Gamma^{EH}}{\delta g_{\mu\nu}} 2\varepsilon_{\mu\nu} + \zeta \int \frac{\delta\Gamma^{EH}}{\delta g_{\mu\nu}} \varepsilon_\mu{}^\rho \varepsilon_{\nu\rho} + \frac{1}{2} \int\int \frac{\delta\Gamma^{EH}}{\delta g_{\mu\nu}\delta g_{\rho\sigma}} 4\,\varepsilon_{\mu\nu}\varepsilon_{\rho\sigma} + \dots \,. \tag{4.49}$$

In the third term we have introduced by hand a factor $0 \leq \zeta \leq 1$ that interpolates continuously between the pure metric formalism ($\zeta = 0$, $h_{\mu\nu} = 2\varepsilon_{(\mu\nu)}$) and the tetrad formalism ($\zeta = 1$). We see that the part of the action

quadratic in ε differs from the one in the metric formalism by terms proportional to the equations of motion. Since in the derivation of the beta functions it is essential to work off shell, we cannot ignore these terms.

The gauge fixing terms for diffeomorphisms and local Lorentz transformations are

$$\Gamma_k^{GF}[e,\bar{e}] = \frac{1}{2\alpha}\int \mathrm{d}^d x\sqrt{\bar{g}}\bar{g}^{\mu\nu}F_\mu F_\nu + \frac{1}{2\alpha_L}\int \mathrm{d}^d x\sqrt{\bar{g}}\, G^{ab}G_{ab}\ . \tag{4.50}$$

For diffeomorphisms we choose the condition (3.10) while for the internal $O(d)$ transformation we choose a symmetric vielbein $G^{ab} = \varepsilon^{[ab]}$. We will choose $\alpha_L = 0$ to simplify the computation. This corresponds to a sharp implementation of the Lorentz gauge fixing, where one can simply set $\varepsilon_{[\mu\nu]} = 0$ and suppress the corresponding rows and columns in the Hessian.

We can compute the ghost action in analogous way we did in Section 3.2, notice how the action is not diagonal in the ghost fields.

$$\begin{aligned}\Gamma_k^{gh} = \quad & \int d^d x\sqrt{\bar{g}}\left[\bar{c}_\mu\Big(\bar{g}^{\mu\kappa}\bar{D}^\rho g_{\kappa\nu}D_\rho + \bar{g}^{\mu\kappa}\bar{D}^\rho g_{\rho\nu}D_\kappa - \frac{1+\rho}{2}\bar{g}^{\rho\sigma}\bar{D}^\mu g_{\rho\nu}D_\sigma\Big)c^\nu\right. \\ & +\frac{\mu}{2}\bar{\Sigma}^{\mu\nu}\left(D_\mu\delta^\rho_\nu - D_\nu\delta^\rho_\mu - 2\omega^{IJ\rho}e_{\mu J}e_{\nu I}\right)c_\rho \\ & \left.+2\mu^2\bar{\Sigma}^{\mu\nu}\Sigma_{\mu\nu}\right]\ ,\end{aligned} \tag{4.51}$$

where the mass scale μ has been introduced, following [36], to compensate for the fact that the Lorentz ghosts do not have a kinetic term and give them the same dimension as c_μ.

Next we perform the TT decomposition on the symmetric part of the d-bein fluctuation as we did in Section 3.3.3

$$\varepsilon_{(\mu\nu)} = h^{TT}_{\mu\nu} + D_\mu\xi_\nu + D_\nu\xi_\mu + D_\mu D_\nu\sigma - \frac{1}{d}g_{\mu\nu}D^2\sigma + \frac{1}{d}g_{\mu\nu}h^2\ , \tag{4.52}$$

and the associated field redefinitions for ξ_μ and σ.

With these definitions the quadratic part of the action (3.13) is

$$\Gamma^{(2)}_{h^T h^T} = \frac{1}{2}\int \sqrt{g}\; h^{T\mu\nu}\left[-D^2 + \left(\frac{d\,(d-3)+4}{d\,(d-1)} - \zeta\frac{d-2}{2d}\right)R - (2-\zeta)\Lambda\right] h^T_{\mu\nu}\;; \tag{4.53}$$

$$\Gamma^{(2)}_{\xi\xi} = \frac{1}{\alpha}\int \sqrt{g}\; \xi^{\nu}\left[-D^2 + \left(\frac{\alpha\,(d-2)-1}{d} - \zeta\alpha\frac{d-2}{2d}\right)R - \alpha\,(2-\zeta)\,\Lambda\right] \xi_{\nu}\;; \tag{4.54}$$

$$\begin{aligned}\Gamma^{(2)}_{\sigma\sigma} =& \frac{(d-1)}{2d}\frac{2\,(d-1)-\alpha\,(d-2)}{\alpha d} \\ &\times \int \sqrt{g}\; \sigma\left[-D^2 + \frac{(d-2)(2-\zeta)\alpha - 4}{2\,(d-1)-\alpha\,(d-2)}R - \frac{\alpha d\,(2-\zeta)}{2\,(d-1)-\alpha\,(d-2)}\Lambda\right]\sigma\;;\end{aligned} \tag{4.55}$$

$$\begin{aligned}\Gamma^{(2)}_{hh} =& \frac{d-2}{4d}\frac{2\,(d^2-3d+2)\,\alpha - 4\rho^2}{d\alpha(d-2)} \\ &\times \int \sqrt{g}\; h\Big[-D^2 + \frac{\alpha(d-2)\,(d-4+\zeta)}{2\,(d^2-3d+2)\,\alpha - 4\rho^2}R - 2\frac{d\alpha\,(d-2+\zeta)}{2\,(d^2-3d+2)\,\alpha - 4\rho^2}\Lambda\Big]h\;;\end{aligned} \tag{4.56}$$

$$\Gamma^{(2)}_{h\sigma} = \frac{-(d-2)\alpha + 2\rho}{d\alpha}\,\frac{(d-1)}{d}\int \sqrt{g}\; h\left(-D^2 - \frac{R}{(d-1)}\right)D^2\sigma\;. \tag{4.57}$$

We notice that for $\rho = \alpha(d-2)/2$ we can get rid of the mixed term. In the rest of the chapter we will work in this "diagonal" gauge. In this case the trace part reduces to

$$\begin{aligned}\Gamma^{(2)}_{hh} \;=\; -\tfrac{1}{2}\tfrac{d-2}{2d}\int \sqrt{g}\, h\Bigg[-D^2 \;&+\frac{d-4+\zeta}{2(d-1)-\alpha(d-2)}R \\ &-\frac{2d}{2(d-1)-\alpha(d-2)}\left(1+\frac{\zeta}{d-2}\right)\Lambda\Bigg]h\;.\end{aligned}$$

After decomposing the diffeomorphism ghost in its transverse and longitudinal parts, and absorbing $\sqrt{-D^2}$ in the latter, the ghost action is the sum of

$$\Gamma^{(2)}_{\bar{c}^T_\nu c^T_\mu} = \int \sqrt{g}\,\bar{c}^T_\nu\left(D^2 + \frac{R}{d}\right)c^T_\mu \qquad \Gamma^{(2)}_{\bar{c}c} = \int \sqrt{g}\,\bar{c}\left(D^2 + 2\frac{R}{d}\right)c\;. \tag{4.58}$$

The Lorentz ghosts do not propagate and following standard perturbative procedure one could neglect them entirely, but we will follow [36] and introduce a cutoff for them too.

4.3.2 Beta functions

Using the same procedure as in Section 3.3 we can compute the expression for $\frac{d}{dt}\Gamma_k$. The main difference between the following and what we presented in Section 3.3 is the extension of the truncation by the addition of the graviton's wave function renormalization. To do that we rescale the graviton $h_{\mu\nu} \to \sqrt{Z}h_{\mu\nu}$. Comparing the terms of order zero and one in R in the FRGE yields

$$\frac{d}{dt}\left(\frac{2\Lambda}{16\pi G}\right) = \frac{k^d}{16\pi}\left(A_1 + \eta A_2\right) \ , \tag{4.59}$$

$$-\frac{d}{dt}\left(\frac{1}{16\pi G}\right) = \frac{k^{d-2}}{16\pi}\left(B_1 + \eta B_2\right) \ , \tag{4.60}$$

where $\eta = \frac{1}{Z}\frac{dZ}{dt}$ and A_i, B_i are in general polynomials in $\tilde{\Lambda} = k^{-2}\Lambda$. To close the beta functions we further identify $\eta \equiv -1/G\frac{dG}{dt}$. From here one can find the beta functions of the dimensionless parameters $\tilde{G} = k^{d-2}G$ and $\tilde{\Lambda}$:

$$\frac{d}{dt}\tilde{G} = (d-2)\tilde{G} + \frac{B_1\tilde{G}^2}{1+\tilde{G}B_2} \tag{4.61}$$

$$\frac{d}{dt}\tilde{\Lambda} = -2\tilde{\Lambda} + \tilde{G}\frac{A_1 + 2B_1\tilde{\Lambda} + \tilde{G}\left(A_1B_2 - A_2B_1\right)}{2\left(1+B_2\tilde{G}\right)} \ . \tag{4.62}$$

In the following two sections we will give explicit results using specific cutoffs.

For numerical results in $d = 4$ we will always use the optimized cutoff (1.35). For a discussion of the dependence on the shape of the function $R_k(z)$ we refer to [36]. We will instead concentrate on the differences between cutoffs of type I vs II and type "a" vs "b". We present here a review of the results the type Ia cutoff, we refer to the extensive discussion in [36] for additional details. We will report in detail the results for the cases Ib and IIb, and highlight the differences with the case Ia.

4.3.3 Type Ib cutoff

First we choose as reference operator, in each spin sector, the "bare" Laplacian $-D^2$. The cutoff is a function $R_k(-D^2)$. This is called a cutoff of type Ib. The calculation of the coefficients A_1, A_2, B_1 and B_2 for arbitrary dimension and cutoff shape is described in Appendix 4.A. Here we just report

the result in $d = 4$ and for the cutoff profile (1.35):

$$A_1 = \frac{1}{2\pi}\left[\frac{5}{1-(2-\zeta)\tilde{\Lambda}} + \frac{3}{1-\alpha(2-\zeta)\tilde{\Lambda}} + \frac{1}{1-\frac{2\alpha(2-\zeta)}{3-\alpha}\tilde{\Lambda}} + \frac{1}{1-\frac{2(2+\zeta)}{3-\alpha}\tilde{\Lambda}} - 8\right] + A^L(\tilde{\mu}) \ , \tag{4.63}$$

$$A_2 = \frac{1}{12\pi}\left[\frac{5}{1-(2-\zeta)\tilde{\Lambda}} + \frac{3}{1-\alpha(2-\zeta)\tilde{\Lambda}} + \frac{1}{1-\frac{2\alpha(2-\zeta)}{3-\alpha}\tilde{\Lambda}} + \frac{1}{1-\frac{2(2+\zeta)}{3-\alpha}\tilde{\Lambda}}\right] \ , \tag{4.64}$$

$$\begin{aligned} B_1 =& \frac{1}{24\pi}\Bigg[-\frac{20}{1-(2-\zeta)\tilde{\Lambda}} - \frac{5\,(8-3\zeta)}{(1-(2-\zeta)\tilde{\Lambda})^2} + \frac{6}{1-\alpha(2-\zeta)\tilde{\Lambda}} \\ &+ \frac{9(1-\alpha(2-\zeta))}{4(1-\alpha(2-\zeta)\tilde{\Lambda})^2} + \frac{4}{1-\frac{2\alpha(2-\zeta)\tilde{\Lambda}}{3-\alpha}} + \frac{12+6\alpha(\zeta-2)}{(3-\alpha)\left(1-\frac{2\alpha(2-\zeta)\tilde{\Lambda}}{3-\alpha}\right)^2} \\ &+ \frac{4}{1-\frac{2(\zeta+2)\tilde{\Lambda}}{3-\alpha}} - \frac{6\zeta}{(3-\alpha)\left(1-\frac{2(\zeta+2)\tilde{\Lambda}}{3-\alpha}\right)^2} - 50\Bigg] + B^L(\tilde{\mu}) \ , \end{aligned} \tag{4.65}$$

$$\begin{aligned} B_2 =& \frac{1}{144\pi}\Bigg[-\frac{30}{1-(2-\zeta)\tilde{\Lambda}} - \frac{5\,(8-3\zeta)}{(1-(2-\zeta)\tilde{\Lambda})^2} + \frac{9}{1-\alpha(2-\zeta)\tilde{\Lambda}} \\ &+ \frac{9(1-\alpha(2-\zeta)}{(1-\alpha(2-\zeta)\tilde{\Lambda})^2} + \frac{6}{1-\frac{2\alpha(2-\zeta)\tilde{\Lambda}}{3-\alpha}} + \frac{12+6\alpha(\zeta-2)}{(3-\alpha)\left(1-\frac{2\alpha(2-\zeta)\tilde{\Lambda}}{3-\alpha}\right)^2} \\ &+ \frac{6}{1-\frac{2(\zeta+2)\tilde{\Lambda}}{3-\alpha}} - \frac{6\zeta}{(3-\alpha)\left(1-\frac{2(\zeta+2)\tilde{\Lambda}}{3-\alpha}\right)^2}\Bigg] \ . \end{aligned} \tag{4.66}$$

The result is still quite general: it depends on the parameter ζ, which allows us to interpolate continuously between the purely metric formulation ($\zeta = 0$) and the purely tetrad formulation ($\zeta = 1$), on the arbitrary gauge parameter α, which allows us to test the gauge dependence of the results, and on the dimensionless parameter $\tilde{\mu} = \mu/k$ that allows us to weigh differently the contribution of the Lorentz ghosts encoded in the terms A_L and B_L (see Appendixes **??** for an explicit expression). Let us now describe the main features of these flows. Both in the metric and in the tetrad formulations, a UV attractive fixed point is found for all values of μ and for α not too large. Its location and the corresponding critical exponents ϑ (which are defined as minus the eigenvalues of the stability matrix) are given in Table 4.1 in the metric ($\zeta = 0$) or tetrad ($\zeta = 1$) formalism, in the gauges $\alpha = 0$, $\alpha = 1$ and with two different values of the dimensionless Lorentz ghost parameter

$\tilde{\mu} = \mu/k$: $\tilde{\mu} = \infty$, and $\tilde{\mu} = 1.2$. The former corresponds to neglecting the Lorentz ghosts entirely and the latter is chosen to ease comparison with [36], who found that this value gives results that are closest to the metric formalism in the gauge and scheme they use. Note that the case $\zeta = 0$, $\alpha = 1$ corresponds to the purely metric flow with type Ib cutoff, which had already been discussed previously in the literature. Indeed the second row in Table 4.1 agrees with the third row in Table II in [18].

Whereas with a type Ia cutoff the fixed point becomes UV repulsive, and a limit cycle develops, for $\tilde{\mu}$ sufficiently large, with the type Ib cutoff it remains UV attractive for arbitrarily large $\tilde{\mu}$. This is a nice feature of this scheme, because it means that the fixed point can also be found if one adopts the perturbative prescription of neglecting the Lorentz ghosts entirely. However, the results in the tetrad formalism match most closely those of the metric formalism when $\tilde{\mu}$ is chosen to be a bit larger than one. As with the type Ia cutoff, for $\tilde{\mu}$ smaller than a critical value $\tilde{\mu}_c$, the critical exponents become real. We find $\tilde{\mu}_c \approx 0.705$ for $\alpha = 0$ and $\tilde{\mu}_c \approx 0.715$ for $\alpha = 1$.

The dependence of the critical exponents at the fixed point on the $\tilde{\mu}$ parameters in both $\alpha = 0$ and $\alpha = 1$ gauge is illustrated in Fig.4.1.

The dependence of the universal quantities on the gauge parameters is illustrated in Fig. 4.2. The slow decrease of the real part of the critical exponent for $0 < \alpha < 2$ is in agreement with earlier calculations in the metric formalism (see e.g. Fig. 9 in [37]). The results of different schemes seem to converge for $\alpha \to 0$ which, we recall, is believed to give the physically most reliable picture. On the other hand, when α is greater than some value of order 2, the fixed point becomes repulsive, reproducing the behavior that had been observed in [36] for large $\tilde{\mu}$. However it should be noted that large values of the gauge parameter are not expected to yield reliable results since a large value of α corresponds to relaxing the gauge condition. It is tempting to conjecture that also in the cutoff scheme Ia used in [36] the fixed point would have the usual properties, even for large $\tilde{\mu}$, if one could choose α closer to zero. The strong $\tilde{\mu}$ dependence that had been observed there may be due to a particularly strong α dependence. Altogether it appears that with a type Ib cutoff, the tetrad formalism leads to results that are qualitatively similar to those of the metric formalism, and that the correspondence is best when $0 < \alpha < 1$ and the Lorentz ghosts are turned on, with a parameter $\tilde{\mu}$ that is a little larger than one.

Scheme	$\tilde{\Lambda}_*$	$\tilde{G}_*$	$\tilde{\Lambda}_*\tilde{G}_*$	ϑ
Ib, $\zeta = 0$, $\alpha = 0$	0.1569	0.9028	0.1416	$2.147 \pm 2.620i$
Ib, $\zeta = 0$, $\alpha = 1$	0.1715	0.7012	0.1203	$1.689 \pm 2.486i$
Ib, $\zeta = 1$, $\tilde{\mu} = \infty$, $\alpha = 0$	0.2288	1.363	0.3119	$2.086 \pm 2.042i$
Ib, $\zeta = 1$, $\tilde{\mu} = \infty$, $\alpha = 1$	0.2478	0.9472	0.2347	$0.595 \pm 3.753i$
Ib, $\zeta = 1$, $\tilde{\mu} = 1.2$, $\alpha = 0$	0.0691	1.518	0.1050	$2.237 \pm 1.248i$
Ib, $\zeta = 1$, $\tilde{\mu} = 1.2$, $\alpha = 1$	0.0798	1.3196	0.1053	$1.892 \pm 1.093i$

Table 4.1: The nontrivial fixed point in the type Ib cutoff in metric ($\zeta = 0$) and tetrad ($\zeta = 1$) formalism, in the gauges $\alpha = 0$ and $\alpha = 1$ and with different weights of the Lorentz ghosts. Recall $Re(\vartheta) > 0$ implies that the fixed point is UV attractive.

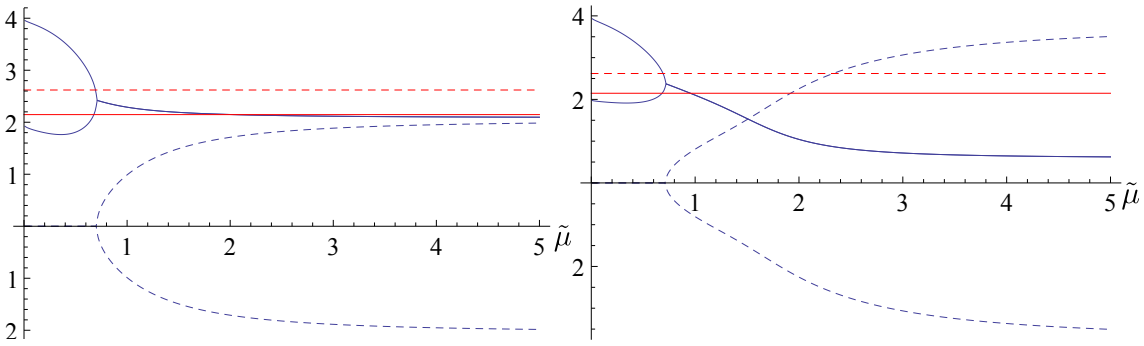

Figure 4.1: Critical Exponents as functions of the $\tilde{\mu}$ parameter for type Ib cutoff. The continuous line is the real part of the critical exponent, the dashed line the imaginary part of the critical exponent. In red the metric case is given for reference. In the left panel the $\alpha = 0$ gauge, in the right panel the $\alpha = 1$ gauge.

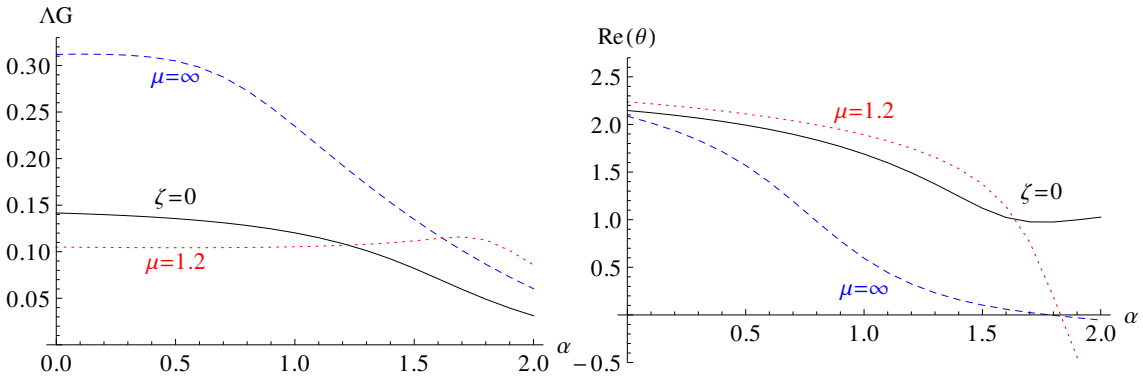

Figure 4.2: Universal quantities as functions of the gauge parameter α for type Ib cutoff. In the left panel the product $\Lambda_* G_*$, and in the right panel the real part of the critical exponent.

4.3.4 Type Ia cutoff

We will summarize here the results for a type Ia cutoff in the $\alpha = \beta = 1$ gauge. The cutoff is a function of the "bare" Laplacian $-D^2$. First we need to compute the Hessian

$$\Gamma_k^{(2)} = \frac{1}{2}\int d^d x h_{\mu\nu}\Big[(\mathbf{1}-\mathbf{P})\left(-D^2-(2-\zeta)\Lambda_k+\left(\tfrac{4-3d+d^2}{d(d-1)}-\tfrac{d-2}{2d}\zeta\right)R\right) \\ -\tfrac{d-2}{2}\mathbf{P}\left(-D^2-2\Lambda_k\left(1+\tfrac{\zeta}{d-2}\right)+\left(\tfrac{d-4+\zeta}{d}\right)R\right)\Big]h_{\rho\sigma} \quad (4.67)$$

The we can compute the coefficient As and Bs as for the type Ib case. Here we just report the result in $d = 4$ and for the cutoff profile (1.35):

$$B_1 = -\frac{(6\Lambda-1)(\Lambda(7\Lambda-5)+1)}{6\pi\left(3\Lambda^2-4\Lambda+1\right)^2}+B_L(\tilde{\mu})\ , \quad (4.68)$$
$$B_2 = -\frac{\Lambda(2\Lambda(63(\Lambda-2)\Lambda+134)-113)+16}{6\pi\left(3\Lambda^2-4\Lambda+1\right)^2}\ .$$

The coefficient B_L is the contribution of the Lorentz ghosts (see Appendixes **??** for an explicit expression).

Fig. 4.3 shows the μ-dependence of the critical exponents at the fixed point (one might expect them to be universal). We notice that, while the very existence of the fixed point is indeed universal, its properties heavily depend on the value of $\tilde{\mu}$. For $\mu \lesssim 0.8$ a UV attractive FP with two real critical exponents can be found, which then turn into a complex conjugated

pair as $\tilde{\mu}$ increases and for a critical value of $\tilde{\mu} \approx 1.35$ the FP changes its character and becomes UV repulsive in both directions and a limit circle around the FP is present.

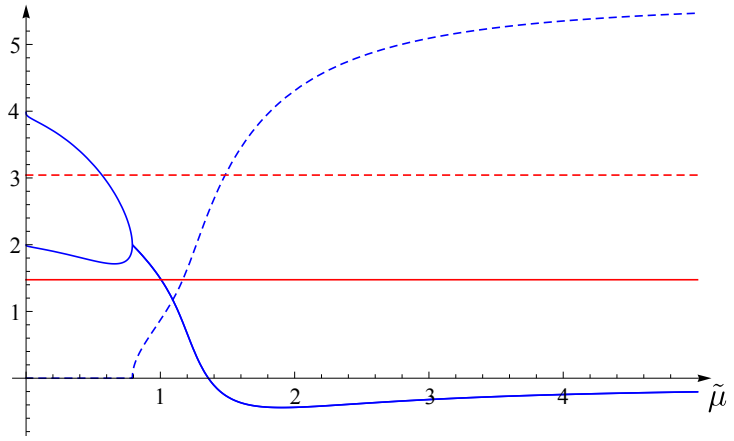

Figure 4.3: Critical Exponents as functions of the $\tilde{\mu}$ parameter for type Ia cutoff. The continuous line is the real part of the critical exponent, the dashed line the imaginary part of the critical exponent. In red the metric case is given for reference. In the left panel the $\alpha = 0$ gauge, in the right panel the $\alpha = 0$ gauge.

4.3.5 Type IIb cutoff

We call type IIb a cutoff imposed separately on each spin component of the graviton, taking as reference operator the Laplace–type operator that appears in the corresponding Hessian, including the curvature terms, but not the term proportional to the cosmological constant. The rationale for excluding the cosmological constant term is that the cosmological constant is a running coupling and if one included it in the reference operator, it would not remain fixed in the course of the flow. Here we choose a reference operator that remains fixed along the flow. [3] As we have already seen in the case of the fermions, the type II cutoffs tend to give somewhat simpler final formulas than the corresponding type I cutoffs, because to leading order one always finds traces of the function $\partial_t R_k / P_k$ and it is not necessary to expand the denominators.

The coefficients A_1, A_2 are the same as with a type Ib cutoff and are given in (4.63) and (4.64). The coefficients B_1 and B_2 for arbitrary dimension and

[3] Cutoffs that depend on the full Hessian, including the terms proportional to the cosmological constant, were called of type III in [18], where they have been applied to the Einstein–Hilbert truncation.

cutoff shape are given in Appendix 4.B. In $d = 4$ and for the cutoff profile (1.35), they become

$$B_1 = \frac{1}{12\pi}\left[-\frac{5(10-3\zeta)}{1-(2-\zeta)\tilde{\Lambda}} + \frac{6(4-3\alpha(2-\zeta))}{1-\alpha(2-\zeta)\tilde{\Lambda}} + \frac{2-\frac{6\zeta}{3-\alpha}}{1-2\frac{2+\zeta}{3-\alpha}\tilde{\Lambda}} + \frac{14-6\frac{4-\alpha\zeta}{3-\alpha}}{1-2\alpha\frac{2-\zeta}{3-\alpha}\tilde{\Lambda}} - 40\right] + B^L \ , \tag{4.69}$$

$$B_2 = \frac{1}{48\pi}\left[-\frac{5(10-3\zeta)}{1-(2-\zeta)\tilde{\Lambda}} - \frac{3(4-3\alpha(2-\zeta)}{1-\alpha(2-\zeta)\tilde{\Lambda}} - \frac{2-\frac{6\zeta}{3-\alpha})}{1-2\frac{2+\zeta}{3-\alpha}\tilde{\Lambda}} - \frac{14-6\frac{4-\alpha\zeta}{3-\alpha}}{1-2\alpha\frac{2-\zeta}{3-\alpha}\tilde{\Lambda}}\right] . \tag{4.70}$$

The coefficient B_L is the contribution of the Lorentz ghosts (see Appendixes **??** for an explicit expression).

Table 4.2 gives the UV–attractive fixed point and the corresponding critical exponents in the metric ($\zeta = 0$) or tetrad ($\zeta = 1$) formalism, in the gauges $\alpha = 0, 1$, and with two different values of the Lorentz ghost parameter, $\tilde{\mu} = \infty$, and $\tilde{\mu} = 1.2$.

Scheme	$\tilde{\Lambda}_*$	$\tilde{G}_*$	$\tilde{\Lambda}_*\tilde{G}_*$	ϑ
IIb, $\zeta = 0$, $\alpha = 0$	0.1052	0.7216	0.0759	$2.562 \pm 1.566i$
IIb, $\zeta = 0$, $\alpha = 1$	0.0924	0.5557	0.0513	$2.424 \pm 1.270i$
IIb, $\zeta = 1$, $\tilde{\mu} = \infty$, $\alpha = 0$	0.1406	1.0176	0.1431	$2.595 \pm 1.131i$
IIb, $\zeta = 1$, $\tilde{\mu} = \infty$, $\alpha = 1$	0.1369	0.8427	0.1154	$2.300 \pm 0.991i$
IIb, $\zeta = 1$, $\tilde{\mu} = 1.2$, $\alpha = 0$	0.0394	1.0008	0.0398	$2.640 \pm 0.730i$
IIb, $\zeta = 1$, $\tilde{\mu} = 1.2$, $\alpha = 1$	0.0361	0.8299	0.0300	$2.547 \pm 0.634i$

Table 4.2: The non-trivial fixed point in the type IIb cutoff in metric ($\zeta = 0$) and tetrad ($\zeta = 1$) formalism, in the gauges $\alpha = 0$ and $\alpha = 1$ and with different weights of the Lorentz ghosts.

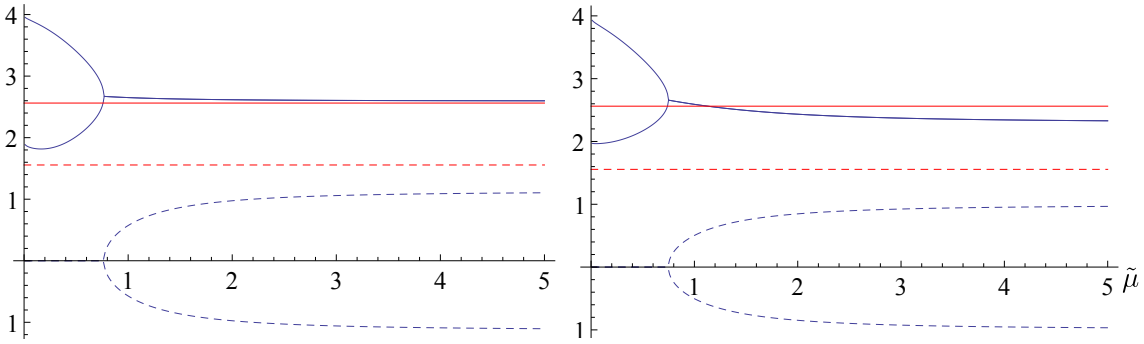

Figure 4.4: Critical Exponents as functions of the $\tilde{\mu}$ parameter for type IIb cutoff. The continuous line is the real part of the critical exponent, the dashed line the imaginary part of the critical exponent. In red the metric case is given for reference. In the left panel the $\alpha = 0$ gauge, in the right panel the $\alpha = 0$ gauge.

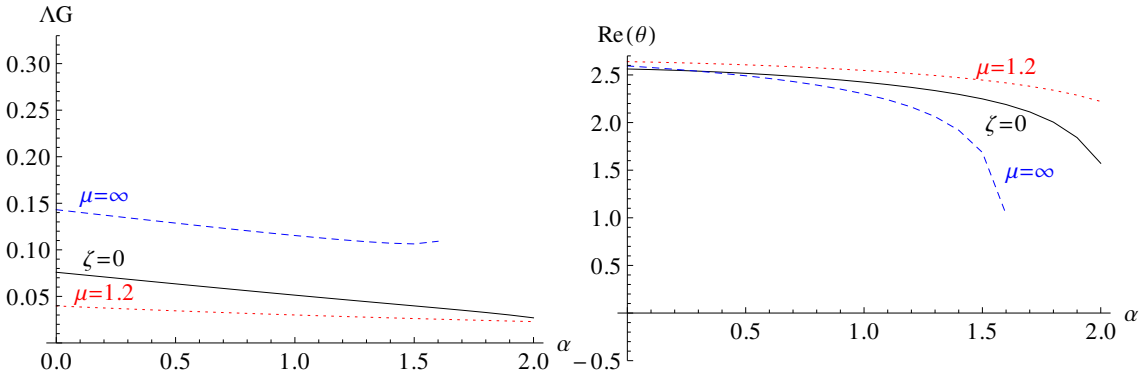

Figure 4.5: Universal quantities as functions of the gauge parameter α for type IIb cutoff. In the left panel the product $\Lambda_* G_*$, and in the right panel the real part of the critical exponent.

The results are qualitatively similar to the ones obtained with the type Ib cutoff. This is in line with all the results obtained previously in the Einstein–Hilbert truncation. The nontrivial FP exists and has complex critical exponents for all values of $\tilde{\mu}$ greater than a critical value $\tilde{\mu}_c$, which is approximately equal to 0.766 for $\alpha = 0$ and 0.748 for $\alpha = 1$. For small $\tilde{\mu}$ the FP moves toward negative values of $\tilde{\Lambda}$. For large $\tilde{\mu}$ the fixed point remains UV attractive, in contrast to the result found in [36] with the type Ia cutoff scheme.

In particular, we find that the FP has properties close to the standard ones of the metric formulation also when the Lorentz ghosts are neglected.

Fig. 4.5 gives the gauge dependence of the universal quantities ΛG and ϑ. Note that the real part of the scaling exponent ϑ is particularly stable in this scheme, for $0 < \alpha < 1$.

The dependence of the critical exponents at the fixed point on the $\tilde{\mu}$ parameters in both $\alpha = 0$ and $\alpha = 1$ gauge is illustrated in Fig.4.4.

4.3.6 Type IIa cutoff

For completeness we mention here also the results for the cutoff of type IIa. In this scheme only the gauge $\alpha = 1$ is easily computable. In this gauge it is enough to split the metric fluctuation into its trace and tracefree parts to write the Hessian of the Einstein–Hilbert action as two minimal Laplace–type operators as explained in Section 3.3.4. The cutoff is then defined as a function of these operators, including the curvature terms but excluding the cosmological constant term. This prescription leads to particularly simple expressions.

The coefficients A_1, A_2 are the same as with the other cutoff types considered here and are given in (4.63,4.64). The coefficients B_1 and B_2 in $d = 4$ and for the cutoff profile (1.35) are simply

$$B_1 = \frac{1}{12\pi}\left[\frac{2-3\zeta}{1-(2+\zeta)\tilde{\Lambda}} - \frac{27(2-\zeta)}{1-(2-\zeta)\tilde{\Lambda}} - 40\right] + B^L \ , \tag{4.71}$$

$$B_2 = \frac{1}{48\pi}\left[\frac{2-3\zeta}{1-(2+\zeta)\tilde{\Lambda}} - \frac{27(2-\zeta)}{1-(2-\zeta)\tilde{\Lambda}}\right] \ . \tag{4.72}$$

The coefficient B_L is the contribution of the Lorentz ghosts (see Appendixes **??** for an explicit expression).

These expressions coincide with the type IIb ones ((4.69) and (4.70) in the gauge $\alpha = 1$ as already noted in Section 3.3.4.

As a consequence, all properties of the flow are the same, and we will not discuss this case further.

It is nevertheless interesting to understand the reason for this coincidence, which is not restricted to $d = 4$ and is also independent of the shape of the function R_k. [4]

For the sake of simplicity we shall discuss here only the case $\zeta = 0$, but the result is general. Since in all cases the trace field h is treated separately, and its contribution is the same for type a and b cutoffs, it is enough to consider the tracefree part of the graviton, namely the components $h^{TT}_{\mu\nu}$, ξ_μ and σ.

[4]The agreement between cutoffs IIa and IIb for $\alpha = 1$ had been noticed before in [38].

In the gauge $\alpha = 1$, the Hessian in the tracefree subsector is a minimal second order operator of the form

$$-\nabla^2 + C_T R - 2\Lambda \ , \tag{4.73}$$

where $C_T = \frac{d(d-3)+4}{d(d-1)}$. When one uses a cutoff of type IIa (no further decomposition) the contribution of this sector to the r.h.s. of the FRGE is

$$\sum_n \frac{\partial_t R(\lambda_n) + \eta R_k(\lambda_n)}{P_k(\lambda_n) - 2\Lambda} \ , \tag{4.74}$$

where λ_n are the eigenvalues of the operator $\mathcal{O} = -\nabla^2 + C_T R$. One can divide these eigenvalues into three classes, depending on the spin of the corresponding eigenfunction. Upon using the TT decomposition (4.52) one finds that the eigenvalues of $\mathcal{O}$ on fields of type $h^{TT}_{\mu\nu}$, $\nabla_\mu \xi_\nu - \nabla_\nu \xi_\mu$ and $\nabla_\mu \nabla_\nu \sigma - \frac{1}{d}\nabla^2 \sigma$ are equal to the eigenvalues of the operators in square brackets in (4.53),(4.54) and (4.55), stripped of the Λ terms. We denote these operators $\mathcal{O}^{TT} = -\nabla^2 + C_T R$, $\mathcal{O}^\xi = -\nabla^2 + C_\xi R$ and $\mathcal{O}^\sigma = -\nabla^2 + C_\sigma R$ and the corresponding eigenvalues λ^{TT}_n, λ^ξ_n and λ^σ_n. So, the trace (4.74) is equal to

$$\sum_n \frac{\partial_t R(\lambda^{TT}_n) + \eta R_k(\lambda^{TT}_n)}{P_k(\lambda^{TT}_n) - 2\Lambda} + \sum_n \frac{\partial_t R(\lambda^{\xi}_n) + \eta R_k(\lambda^{\xi}_n)}{P_k(\lambda^{\xi}_n) - 2\Lambda} + \sum_n \frac{\partial_t R(\lambda^{\sigma}_n) + \eta R_k(\lambda^{\sigma}_n)}{P_k(\lambda^{\sigma}_n) - 2\Lambda} \ . \tag{4.75}$$

Since for $\alpha = 1$ the coefficients of Λ in (4.53),(4.54) and (4.55) are all the same and equal to -2, this is recognized as the contribution of the fields $h^{TT}_{\mu\nu}$, ξ_μ and σ to the r.h.s. of the FRGE when one uses a cutoff of type IIb. By a similar reasoning one also concludes that the ghost contribution is the same in the IIa and IIb schemes.

Things do not work in the same way for type I cutoffs, *i.e.* when the cutoff is a function of $-\nabla^2$. For a type Ia cutoff the contribution of the tracefree sector to the r.h.s. of the FRGE is

$$\sum_n \frac{\partial_t R(\lambda_n) + \eta R_k(\lambda_n)}{P_k(\lambda_n) + C_T R - 2\Lambda} \ , \tag{4.76}$$

where λ_n now denote the eigenvalues of $-\nabla^2$. This can be expanded as

$$\sum_n^{TT} \frac{\partial_t R(\lambda_n) + \eta R_k(\lambda_n)}{P_k(\lambda_n) + C_T R - 2\Lambda} + \sum_n^{\xi} \frac{\partial_t R(\lambda_n) + \eta R_k(\lambda_n)}{P_k(\lambda_n) + C_T R - 2\Lambda} + \sum_n^{\sigma} \frac{\partial_t R(\lambda_n) + \eta R_k(\lambda_n)}{P_k(\lambda_n) + C_T R - 2\Lambda} \ , \tag{4.77}$$

where $\sum^{TT}$, $\sum^{\xi}$ and $\sum^{\sigma}$ denote the sum over eigenvalues of $-\nabla^2$ on $h^{TT}_{\mu\nu}$, $\nabla_\mu\xi_\nu - \nabla_\nu\xi_\mu$ and $\nabla_\mu\nabla_\nu\sigma - \frac{1}{d}\nabla^2\sigma$ respectively. On the other hand for a type Ib cutoff the same contribution is

$$\sum_n^{TT} \frac{\partial_t R(\lambda_n) + \eta R_k(\lambda_n)}{P_k(\lambda_n) + C_T R - 2\Lambda} + \sum_n^{\xi} \frac{\partial_t R(\lambda_n) + \eta R_k(\lambda_n)}{P_k(\lambda_n) + C_\xi R - 2\Lambda} + \sum_n \frac{\partial_t R(\lambda_n) + \eta R_k(\lambda_n)}{P_k(\lambda_n) + C_\sigma R - 2\Lambda} \,. \tag{4.78}$$

One clearly sees that the two traces are different.

4.A Details of type Ib calculation

We report here the detailed computation of the A and B coefficients of (4.59) and (4.60) for a type Ib cutoff. The FRGE is the sum of traces over the irreducible components of the metric fluctuation defined in (4.52). They give:

$$\frac{1}{2}\mathrm{Tr}_{(2)}\frac{\partial_t R_k+\eta R_k}{P_k+\left(\frac{d(d-3)+4}{d(d-1)}-\zeta\frac{d-2}{2d}\right)R-(2-\zeta)\Lambda}= \tag{4.79}$$
$$\frac{1}{2}\frac{1}{(4\pi)^{d/2}}\int dx\sqrt{g}\Bigg[\frac{(d-2)(d+1)}{2}Q_{\frac{d}{2}}\left(\frac{\partial_t R_k+\eta R_k}{P_k-(2-\zeta)\Lambda}\right)$$
$$+\frac{(d-5)(d+1)(d+2)}{12(d-1)}Q_{\frac{d}{2}-1}\left(\frac{\partial_t R_k+\eta R_k}{P_k-(2-\zeta)\Lambda}\right)R$$
$$-\left(\frac{d\,(d-3)+4}{d\,(d-1)}-\zeta\frac{d-2}{2d}\right)\frac{(d-2)(d+1)}{2}Q_{\frac{d}{2}}\left(\frac{\partial_t R_k+\eta R_k}{\left(P_k-(2-\zeta)\Lambda\right)^2}\right)R\Bigg]$$

$$\frac{1}{2}\mathrm{Tr}'_{(1)}\frac{\partial_t R_k+\eta R_k}{P_k+\left(\frac{\alpha(d-2)-1}{d}-\zeta\alpha\frac{d-2}{2d}\right)R-\alpha\,(2-\zeta)\,\Lambda}= \tag{4.80}$$
$$\frac{1}{2}\frac{1}{(4\pi)^{d/2}}\int dx\sqrt{g}\Bigg[(d-1)Q_{\frac{d}{2}}\left(\frac{\partial_t R_k+\eta R_k}{P_k-\alpha\,(2-\zeta)\,\Lambda}\right)$$
$$+\frac{(d-3)(d+2)}{6d}Q_{\frac{d}{2}-1}\left(\frac{\partial_t R_k+\eta R_k}{P_k-\alpha\,(2-\zeta)\,\Lambda}\right)R$$
$$-\left(\frac{\alpha\,(d-2)-1}{d}-\zeta\alpha\frac{d-2}{2d}\right)(d-1)Q_{\frac{d}{2}}\left(\frac{\partial_t R_k+\eta R_k}{\left(P_k-\alpha\,(2-\zeta)\,\Lambda\right)^2}\right)R\Bigg]$$

$$\frac{1}{2}\mathrm{Tr}''_{(0)}\frac{\partial_t R_k+\eta R_k}{P_k+\frac{\alpha(d-2)(2-\zeta)-4}{2(d-1)-\alpha(d-2)}R-\frac{\alpha d(2-\zeta)}{2(d-1)-\alpha(d-2)}\Lambda}= \tag{4.81}$$
$$\frac{1}{2}\frac{1}{(4\pi)^{d/2}}\int dx\sqrt{g}\Bigg[Q_{\frac{d}{2}}\left(\frac{\partial_t R_k+\eta R_k}{P_k-\frac{\alpha d(2-\zeta)}{2(d-1)-\alpha(d-2)}\Lambda}\right)$$
$$+\frac{1}{6}Q_{\frac{d}{2}-1}\left(\frac{\partial_t R_k+\eta R_k}{P_k-\frac{\alpha d(2-\zeta)}{2(d-1)-\alpha(d-2)}\Lambda}\right)R$$
$$-\frac{\alpha(d-2)(2-\zeta)-4}{2(d-1)-\alpha(d-2)}Q_{\frac{d}{2}}\left(\frac{\partial_t R_k+\eta R_k}{\left(P_k-\frac{\alpha d(2-\zeta)}{2(d-1)-\alpha(d-2)}\Lambda\right)^2}\right)R\Bigg]$$

$$\frac{1}{2}\mathrm{Tr}_{(0)}\frac{\partial_t R_k+\eta R_k}{P_k+\frac{d-4+\zeta}{2(d-1)-\alpha(d-2)}R-\frac{2d\left(1+\frac{\zeta}{d-2}\right)}{2(d-1)-\alpha(d-2)}\Lambda}= \tag{4.82}$$

$$\begin{aligned}\frac{1}{2}\frac{1}{(4\pi)^{d/2}}\int dx\sqrt{g}\Bigg[&Q_{\frac{d}{2}}\left(\frac{\partial_t R_k+\eta R_k}{P_k-\frac{2d\left(1+\frac{\zeta}{d-2}\right)}{2(d-1)-\alpha(d-2)}\Lambda}\right)\\&+\frac{1}{6}Q_{\frac{d}{2}-1}\left(\frac{\partial_t R_k+\eta R_k}{P_k-\frac{2d\left(1+\frac{\zeta}{d-2}\right)}{2(d-1)-\alpha(d-2)}\Lambda}\right)R\\&-\frac{d-4+\zeta}{2(d-1)-\alpha(d-2)}Q_{\frac{d}{2}}\left(\frac{\partial_t R_k+\eta R_k}{\left(P_k-\frac{2d\left(1+\frac{\zeta}{d-2}\right)}{2(d-1)-\alpha(d-2)}\Lambda\right)^2}\right)R\Bigg]\end{aligned}$$

Here a prime or a double prime indicate that the first or the first and the second eigenvalues have to be omitted from the trace (because ξ_μ and σ obey some differential constraints, for more details see Appendix 3.B). The contribution of the transverse and longitudinal parts of the diffeomorphism ghosts are

$$\begin{aligned}-\mathrm{Tr}_{(1)}\frac{\partial_t R_k}{P_k-\frac{R}{d}}=&-\frac{1}{(4\pi)^{d/2}}\int dx\sqrt{g}\Bigg[(d-1)Q_{\frac{d}{2}}\left(\frac{\partial_t R_k}{P_k}\right)-\frac{d-1}{d}Q_{\frac{d}{2}}\left(\frac{\partial_t R_k}{P_k^2}\right)R\\&+\frac{(d+2)(d-3)}{6d}Q_{\frac{d}{2}-1}\left(\frac{\partial_t R_k}{P_k}\right)R\Bigg];\end{aligned} \tag{4.83}$$

$$-\mathrm{Tr}_{(0)}\frac{\partial_t R_k}{P_k-\frac{2R}{d}}=-\frac{1}{(4\pi)^{d/2}}\int dx\sqrt{g}\left[Q_{\frac{d}{2}}\left(\frac{\partial_t R_k}{P_k}\right)-\frac{2}{d}Q_{\frac{d}{2}}\left(\frac{\partial_t R_k}{P_k^2}\right)R+\frac{1}{6}Q_{\frac{d}{2}-1}\left(\frac{\partial_t R_k}{P_k}\right)R\right]. \tag{4.84}$$

Collecting the coefficients of $\int\sqrt{g}$ and $-\int\sqrt{g}R$ we extract the A and B coefficients:

$$\begin{aligned}A_1=\frac{1}{2}\frac{16\pi}{(4\pi)^{d/2}}\Bigg[&\frac{(d-2)(d+1)}{2}\tilde{Q}_{\frac{d}{2}}\left(\frac{\partial_t R_k}{P_k-(2-\zeta)\Lambda}\right)+(d-1)\tilde{Q}_{\frac{d}{2}}\left(\frac{\partial_t R_k}{P_k-\alpha(2-\zeta)\Lambda}\right)\\&+\tilde{Q}_{\frac{d}{2}}\left(\frac{\partial_t R_k}{P_k-\frac{\alpha d(2-\zeta)}{2(d-1)-\alpha(d-2)}\Lambda}\right)+\tilde{Q}_{\frac{d}{2}}\left(\frac{\partial_t R_k}{P_k-\frac{2d\left(1+\frac{\zeta}{d-2}\right)}{2(d-1)-\alpha(d-2)}\Lambda}\right)-2d\tilde{Q}_{\frac{d}{2}}\left(\frac{\partial_t R_k}{P_k}\right)\Bigg]\end{aligned} \tag{4.85}$$

$$A_2 = \frac{1}{2}\frac{16\pi}{(4\pi)^{d/2}}\left[\frac{(d-2)(d+1)}{2}\tilde{Q}_{\frac{d}{2}}\left(\frac{R_k}{P_k-(2-\zeta)\Lambda}\right)+(d-1)\tilde{Q}_{\frac{d}{2}}\left(\frac{R_k}{P_k-\alpha(2-\zeta)\Lambda}\right)\right.$$
$$\left.+\tilde{Q}_{\frac{d}{2}}\left(\frac{R_k}{P_k-\frac{\alpha d(2-\zeta)}{2(d-1)-\alpha(d-2)}\Lambda}\right)+\tilde{Q}_{\frac{d}{2}}\left(\frac{R_k}{P_k-\frac{2d\left(1+\frac{\zeta}{d-2}\right)}{2(d-1)-\alpha(d-2)}\Lambda}\right)\right] \tag{4.86}$$

$$B_1 = \frac{1}{2}\frac{16\pi}{(4\pi)^{d/2}}\left[\frac{(d-5)(d+1)(d+2)}{12(d-1)}\tilde{Q}_{\frac{d}{2}-1}\left(\frac{\partial_t R_k}{P_k-(2-\zeta)\Lambda}\right)\right.$$
$$-\left(\frac{d\,(d-3)+4}{d\,(d-1)}-\zeta\frac{d-2}{2d}\right)\frac{(d-2)(d+1)}{2}\tilde{Q}_{\frac{d}{2}}\left(\frac{\partial_t R_k}{\left(P_k-(2-\zeta)\Lambda\right)^2}\right)$$
$$+\frac{(d-3)(d+2)}{6d}\tilde{Q}_{\frac{d}{2}-1}\left(\frac{\partial_t R_k}{P_k-\alpha(2-\zeta)\Lambda}\right)$$
$$-\left(\frac{\alpha\,(d-2)-1}{d}-\zeta\alpha\frac{d-2}{2d}\right)(d-1)\tilde{Q}_{\frac{d}{2}}\left(\frac{\partial_t R_k}{\left(P_k-\alpha(2-\zeta)\Lambda\right)^2}\right)$$
$$+\frac{1}{6}\tilde{Q}_{\frac{d}{2}-1}\left(\frac{\partial_t R_k}{P_k-\frac{\alpha d(2-\zeta)}{2(d-1)-\alpha(d-2)}\Lambda}\right)-\frac{\alpha(d-2)(2-\zeta)-4}{2(d-1)-\alpha(d-2)}\tilde{Q}_{\frac{d}{2}}\left(\frac{\partial_t R_k}{\left(P_k-\frac{\alpha d(2-\zeta)}{2(d-1)-\alpha(d-2)}\Lambda\right)^2}\right)$$
$$+\frac{1}{6}\tilde{Q}_{\frac{d}{2}-1}\left(\frac{\partial_t R_k}{P_k-\frac{2d\left(1+\frac{\zeta}{d-2}\right)}{2(d-1)-\alpha(d-2)}\Lambda}\right)-\frac{d-4+\zeta}{2(d-1)-\alpha(d-2)}\tilde{Q}_{\frac{d}{2}}\left(\frac{\partial_t R_k}{\left(P_k-\frac{2d\left(1+\frac{\zeta}{d-2}\right)}{2(d-1)-\alpha(d-2)}\Lambda\right)^2}\right)$$
$$\left.-\frac{d^2-6}{3d}\tilde{Q}_{\frac{d}{2}-1}\left(\frac{\partial_t R_k}{P_k}\right)-2\frac{d+1}{d}\tilde{Q}_{\frac{d}{2}}\left(\frac{\partial_t R_k}{P_k^2}\right)\right] \tag{4.87}$$

$$
\begin{aligned}
B_2 = \frac{1}{2}\frac{16\pi}{(4\pi)^{d/2}}\Bigg[& \frac{(d-5)(d+1)(d+2)}{12(d-1)}\tilde{Q}_{\frac{d}{2}-1}\left(\frac{R_k}{P_k-(2-\zeta)\Lambda}\right) \\
& -\left(\frac{d\,(d-3)+4}{d\,(d-1)}-\zeta\frac{d-2}{2d}\right)\frac{(d-2)(d+1)}{2}\tilde{Q}_{\frac{d}{2}}\left(\frac{R_k}{\left(P_k-(2-\zeta)\Lambda\right)^2}\right) \\
& +\frac{(d-3)(d+2)}{6d}\tilde{Q}_{\frac{d}{2}-1}\left(\frac{R_k}{P_k-\alpha(2-\zeta)\Lambda}\right) \\
& -\left(\frac{\alpha\,(d-2)-1}{d}-\zeta\alpha\frac{d-2}{2d}\right)(d-1)\tilde{Q}_{\frac{d}{2}}\left(\frac{R_k}{\left(P_k-\alpha(2-\zeta)\Lambda\right)^2}\right) \\
& +\frac{1}{6}\tilde{Q}_{\frac{d}{2}-1}\left(\frac{R_k}{P_k-\frac{\alpha d(2-\zeta)}{2(d-1)-\alpha(d-2)}\Lambda}\right)-\frac{\alpha(d-2)(2-\zeta)-4}{2(d-1)-\alpha(d-2)}\tilde{Q}_{\frac{d}{2}}\left(\frac{R_k}{\left(P_k-\frac{\alpha d(2-\zeta)}{2(d-1)-\alpha(d-2)}\Lambda\right)^2}\right) \\
& +\frac{1}{6}\tilde{Q}_{\frac{d}{2}-1}\left(\frac{R_k}{P_k-\frac{2d\left(1+\frac{\zeta}{d-2}\right)}{2(d-1)-\alpha(d-2)}\Lambda}\right)-\frac{d-4+\zeta}{2(d-1)-\alpha(d-2)}\tilde{Q}_{\frac{d}{2}}\left(\frac{R_k}{\left(P_k-\frac{2d\left(1+\frac{\zeta}{d-2}\right)}{2(d-1)-\alpha(d-2)}\Lambda\right)^2}\right)\Bigg]
\end{aligned}
\tag{4.88}
$$

Here we have defined the dimensionless versions of the Q functionals: $\tilde{Q}_{\frac{d}{2}} = k^{-d}Q_{\frac{d}{2}}$ and $\tilde{Q}_{\frac{d}{2}-1} = k^{2-d}Q_{\frac{d}{2}-1}$.

Finally let us consider the contribution of Lorentz ghosts. They do not propagate and therefore are usually neglected in the evaluation of the effective action in perturbation theory. Nevertheless if, following [36], we impose a cutoff on their determinant, they contribute to the r.h.s. of the FRGE an amount

$$
-\mathrm{Tr}\frac{\partial_t R_k}{R_k+\frac{2\mu^2}{\sqrt{\zeta}}} = -\frac{1}{(4\pi)^{d/2}}\frac{d(d-1)}{2}\int dx\sqrt{g}\,\left[Q_{\frac{d}{2}}\left(\frac{\partial_t R_k}{R_k+\frac{2\mu^2}{\sqrt{\zeta}}}\right)+\frac{1}{6}Q_{\frac{d}{2}-1}\left(\frac{\partial_t R_k}{R_k+\frac{2\mu^2}{\sqrt{\zeta}}}\right)R\right]
\tag{4.89}
$$

Here we have introduced the arbitrary mass parameter μ (denoted $\bar{\mu}$ in [36]). In particular note that in the limit $\mu\to\infty$ the ghost contribution vanishes and one recovers the standard perturbative result where the Lorentz ghosts are neglected. Let A^L and B^L be the contribution of the Lorentz ghosts to the coefficients A_1 and B_1, defined in (4.59) and (4.60). From the above we read off

$$
A^L = -\frac{16\pi}{(4\pi)^{d/2}}\frac{d(d-1)}{2}\tilde{Q}_{\frac{d}{2}}\left(\frac{\partial_t R_k}{R_k+\frac{2\mu^2}{\sqrt{\zeta}}}\right)\;; \tag{4.90}
$$

$$
B^L = -\frac{16\pi}{(4\pi)^{d/2}}\frac{d(d-1)}{12}\tilde{Q}_{\frac{d}{2}-1}\left(\frac{\partial_t R_k}{R_k+\frac{2\mu^2}{\sqrt{\zeta}}}\right)\;. \tag{4.91}
$$

Note the appearance of R_k instead of P_k in the denominators. In general the Q functionals $Q_n\left(\frac{\partial_t R_k}{R_k+2\mu^2/\sqrt{\zeta}}\right)$ can be computed explicitly, with cutoff (1.35), in terms of hypergeometric functions. For the calculations in four dimensions we only need the following

$$\tilde{Q}_1\left(\frac{\partial_t R_k}{R_k+\frac{2\mu^2}{\sqrt{\zeta}}}\right) = \mathrm{Log}\left(1+\frac{\sqrt{\zeta}}{2\tilde{\mu}^2}\right) \ ; \tag{4.92}$$

$$\tilde{Q}_2\left(\frac{\partial_t R_k}{R_k+\frac{2\mu^2}{\sqrt{\zeta}}}\right) = -1+\left(1+\frac{2\tilde{\mu}^2}{\sqrt{\zeta}}\right)\mathrm{Log}\left(1+\frac{\sqrt{\zeta}}{2\tilde{\mu}^2}\right) \ . \tag{4.93}$$

4.B Details of type IIb calculation

We report here the A and B coefficients of (4.59) and (4.60) for a type IIb cutoff. The contributions of the irreducible components of the metric fluctuation to the r.h.s. of the FRGE are

$$\frac{1}{2}\mathrm{Tr}_{(2)}\frac{\partial_t R_k+\eta R_k}{P_k-(2-\zeta)\Lambda}= \tag{4.94}$$
$$\frac{1}{2}\frac{1}{(4\pi)^{d/2}}\int dx\sqrt{g}\left[\frac{(d-2)(d+1)}{2}Q_{\frac{d}{2}}\left(\frac{\partial_t R_k+\eta R_k}{P_k-(2-\zeta)\Lambda}\right)\right.$$
$$\left.-\frac{(d+1)}{12d}\left(5d^2-22d+48-3\zeta\,(d-2)^{\,2}\right)\;Q_{\frac{d}{2}-1}\left(\frac{\partial_t R_k+\eta R_k}{P_k-(2-\zeta)\Lambda}\right)R\right]$$

$$\frac{1}{2}\mathrm{Tr}'_{(1)}\frac{\partial_t R_k+\eta R_k}{P_k-\alpha\,(2-\zeta)\,\Lambda}= \tag{4.95}$$
$$\frac{1}{2}\frac{1}{(4\pi)^{d/2}}\int dx\sqrt{g}\left[(d-1)Q_{\frac{d}{2}}\left(\frac{\partial_t R_k+\eta R_k}{P_k-\alpha\,(2-\zeta)\,\Lambda}\right)\right.$$
$$\left.-\frac{\left(d^2+5d-12+3\alpha(\zeta-2)\,(d-1)\,(d-2)\right)}{6d}\;Q_{\frac{d}{2}-1}\left(\frac{\partial_t R_k+\eta R_k}{P_k-\alpha\,(2-\zeta)\,\Lambda}\right)R\right]$$

$$\frac{1}{2}\mathrm{Tr}''_{(0)}\frac{\partial_t R_k+\eta R_k}{P_k-\frac{\alpha d(2-\zeta)}{2(d-1)-\alpha(d-2)}\Lambda}= \tag{4.96}$$
$$\frac{1}{2}\frac{1}{(4\pi)^{d/2}}\int dx\sqrt{g}\left[Q_{\frac{d}{2}}\left(\frac{\partial_t R_k+\eta R_k}{P_k-\frac{\alpha d(2-\zeta)}{2(d-1)-\alpha(d-2)}\Lambda}\right)\right.$$
$$\left.+\frac{14+(2-7\alpha-3\zeta\alpha)(d-2)}{6(2(d-1)-\alpha(d-2))}Q_{\frac{d}{2}-1}\left(\frac{\partial_t R_k+\eta R_k}{P_k-\frac{\alpha d(2-\zeta)}{2(d-1)-\alpha(d-2)}\Lambda}\right)R\right]$$

$$\frac{1}{2}\mathrm{Tr}_{(0)}\frac{\partial_t R_k+\eta R_k}{P_k-\frac{2d\left(1+\frac{\zeta}{d-2}\right)}{2(d-1)-\alpha(d-2)}\Lambda}= \tag{4.97}$$
$$\frac{1}{2}\frac{1}{(4\pi)^{d/2}}\int dx\sqrt{g}\left[Q_{\frac{d}{2}}\left(\frac{\partial_t R_k+\eta R_k}{P_k-\frac{2d\left(1+\frac{\zeta}{d-2}\right)}{2(d-1)-\alpha(d-2)}\Lambda}\right)\right.$$
$$\left.+\frac{22-4d+(2-d)\alpha-6\zeta}{6(2(d-1)-\alpha(d-2))}Q_{\frac{d}{2}-1}\left(\frac{\partial_t R_k+\eta R_k}{P_k-\frac{2d\left(1+\frac{\zeta}{d-2}\right)}{2(d-1)-\alpha(d-2)}\Lambda}\right)R\right]$$

The contribution of the diffeomorphism ghosts is

$$-\mathrm{Tr}_{(1)}\frac{\partial_t R_k}{P_k} = -\frac{1}{(4\pi)^{d/2}}\int dx\sqrt{g}\left[(d-1)Q_{\frac{d}{2}}\left(\frac{\partial_t R_k}{P_k}\right)+\frac{d^2+5d-12}{6d}R\,Q_{\frac{d}{2}-1}\left(\frac{\partial_t R_k}{P_k}\right)\right] \tag{4.98}$$

$$-\mathrm{Tr}_{(0)}\frac{\partial_t R_k}{P_k} = -\frac{1}{(4\pi)^{d/2}}\int dx\sqrt{g}\left[Q_{\frac{d}{2}}\left(\frac{\partial_t R_k}{P_k}\right)+\frac{d+12}{6d}R\,Q_{\frac{d}{2}-1}\left(\frac{\partial_t R_k}{P_k}\right)\right]\ . \tag{4.99}$$

The contribution of Lorentz ghosts is the same as in the type Ib case. The coefficients A_1 and A_2 are the same as in Eqs. (4.85) and (4.86), whereas

$$\begin{aligned}B_1 = \frac{1}{2}\frac{16\pi}{(4\pi)^{d/2}}\Bigg[&-\frac{(d+1)}{12d}\left(5d^2-22d+48-3\zeta\,(d-2)^{\,2}\right)\tilde{Q}_{\frac{d}{2}-1}\left(\frac{\partial_t R_k}{P_k-(2-\zeta)\Lambda}\right) \\ &+\frac{d^2+5d-12+3\alpha(\zeta-2)(d-1)(d-2)}{6d}\tilde{Q}_{\frac{d}{2}-1}\left(\frac{\partial_t R_k}{P_k-\alpha\,(2-\zeta)\,\Lambda}\right) \\ &+\frac{22-4d+(2-d)\alpha-6\zeta}{6(2(d-1)-\alpha(d-2))}\tilde{Q}_{\frac{d}{2}-1}\left(\frac{\partial_t R_k}{P_k-\frac{2d\left(1+\frac{\zeta}{d-2}\right)}{2(d-1)-\alpha(d-2)}\Lambda}\right) \\ &+\frac{14+(2-7\alpha-3\zeta\alpha)(d-2)}{6(2(d-1)-\alpha(d-2))}\tilde{Q}_{\frac{d}{2}-1}\left(\frac{\partial_t R_k}{P_k-\frac{\alpha d(2-\zeta)}{2(d-1)-\alpha(d-2)}\Lambda}\right)-\frac{d+6}{3}\,\tilde{Q}_{\frac{d}{2}-1}\left(\frac{\partial_t R_k}{P_k}\right)\Bigg]\end{aligned} \tag{4.100}$$

$$\begin{aligned}B_2 = \frac{1}{2}\frac{16\pi}{(4\pi)^{d/2}}\Bigg[&-\frac{(d+1)}{12d}\left(5d^2-22d+48-3\zeta\,(d-2)^{\,2}\right)\tilde{Q}_{\frac{d}{2}-1}\left(\frac{R_k}{P_k-(2-\zeta)\Lambda}\right) \\ &+\frac{d^2+5d-12+3\alpha(\zeta-2)(d-1)(d-2)}{6d}\tilde{Q}_{\frac{d}{2}-1}\left(\frac{R_k}{P_k-\alpha\,(2-\zeta)\,\Lambda}\right) \\ &+\frac{22-4d+(2-d)\alpha-6\zeta}{6(2(d-1)-\alpha(d-2))}\tilde{Q}_{\frac{d}{2}-1}\left(\frac{R_k}{P_k-\frac{2d\left(1+\frac{\zeta}{d-2}\right)}{2(d-1)-\alpha(d-2)}\Lambda}\right) \\ &+\frac{14+(2-7\alpha-3\zeta\alpha)(d-2)}{6(2(d-1)-\alpha(d-2))}\,\tilde{Q}_{\frac{d}{2}-1}\left(\frac{R_k}{P_k-\frac{\alpha d(2-\zeta)}{2(d-1)-\alpha(d-2)}\Lambda}\right)\Bigg]\end{aligned} \tag{4.101}$$

4.C The running of μ

We report here the computation of the beta function for the μ parameter. To do that it is sufficient to compute the FRGE for the $O(d)$ ghost two point function. Since the part of the action quadratic in Σ is

$$2\mu^2 \bar{\Sigma}^{\mu\nu}\Sigma_{\mu\nu} \tag{4.102}$$

it is immediate to find

$$\left(\frac{d}{dt}\mu^2\right) 1_{\mu\nu\rho\sigma} = \frac{1}{2}\frac{\delta^2\partial_t\Gamma_k}{\delta\Sigma^{\mu\nu}\delta\Sigma^{\rho\sigma}} \tag{4.103}$$

We can use the computation we already done at the end of Section 1.3.2 in particular (1.51) where the generic field ϕ can be any component of the graviton (h^{TT}, ξ, σ or h), $\bar{c}_\mu$, c_μ, $\bar{\Sigma}_{\mu\nu}$ or $\Sigma_{\mu\nu}$.

It's easy to compute all the 3 and 4 field vertices involving the field $\Sigma_{\mu\nu}$ since the only non vanishing one is $\delta^3\Gamma_k/\delta h_{\mu\nu}\delta c_\rho\delta\bar{\Sigma}_{\alpha\beta}$ where by $h_{\mu\nu}$ we intend any of the graviton component, in particular any vertex with a Σ leg is zero. This translate into the impossibility of building a diagram with a Σ and a $\bar{\Sigma}$ external leg, thus the beta function of μ is zero.

With the definition of μ given in the text, this implies that $\tilde{\mu}$ runs like $1/k$. For $k \to 0$, which corresponds to the domain where the perturbative effective field theory of gravity holds, one finds that the contribution of the Lorentz ghosts becomes negligible.

Chapter 5

Matter fields coupled to gravity

A quantum theory of gravity that is a viable description of the microscopic dynamics of our universe must include dynamical matter degrees of freedom.

Nevertheless, matter is often ignored in quantum gravity, or not included in a fully dynamical way. While this could result in a self-consistent quantum theory of gravity, it is not clear whether it can yield a model of quantum gravity applicable to our universe.

As in other settings, where the addition of further degrees of freedom can fundamentally alter the character of the theory, dynamical matter might not be easily incorporated into a consistent microscopic description of gravity. As an example, consider Yang-Mills theory, which is ultraviolet (UV) complete due to asymptotic freedom. If too many fermions are present, asymptotic freedom is destroyed. A similar effect could occur in gravity, where too many matter degrees of freedom could preclude a particular scenario for a UV completion.

An important technical advantage of the asymptotic safety framework lies in its formulation as a local continuum quantum field theory. Many powerful tools, which have been successfully used to describe the other interactions, are available in this setting. In particular the inclusion of matter is in principle straightforward, and there is no difficulty in considering, e.g., chiral fermions [35, 39, 40], in contrast to several other approaches to quantum gravity.

A complete study may seem to be hopelessly complicated, but there are several arguments for pursuing it even at this early stage. One is the general philosophy, which is widely held in the particle physics community, that a consistent theory of gravity requires the inclusion of matter. We will see that the available evidence for asymptotic safety is not particularly supportive of this point of view, in the sense that a fixed point seems to exist also for pure gravity, but it is still too early to tell.

Then, even assuming that a pure gravity fixed point existed, its appli-

cability to the real world would require that matter becomes noninteracting in the ultraviolet, and quantum fluctuations of matter do not change the microscopic dynamics of gravity.

Within a path-integral approach to quantum gravity, it seems more likely that quantum fluctuations of all fields determine the microscopic dynamics and drive the Renormalization Group flow. This view is supported by the result that quantum gravity fluctuations, parametrized as metric or vielbein fluctuations in a continuum setting, generate matter interactions even in a free theory [35, 39, 41, 42].

Other arguments are of a negative character. It is not likely that a firm proof of (non-)existence of a gravitational fixed point can be reached. By widening the scope of the exploration one also enhances the chances of disproving this scenario. For example, if standard model matter turned out to be incompatible with a fixed point within the presently available approximations, the case for asymptotic safety would be correspondingly weakened.

On the experimental side, barring possible surprises, it does not seem very likely that we will see signatures of Planck scale physics within the foreseeable future. On the other hand, much more data is expected to become available in particle physics, and it is possible that some signs in favor of, or against, asymptotic safety can be found in them. A striking example is the relatively successful prediction of the Higgs mass by Shaposhnikov and Wetterich [43]. Putting that prediction on a firm theoretical basis will require much work on the mutual influence of gravity and matter at high energy.

In the following we will investigate the consistency of the interacting fixed point in gravity with the existence of minimally coupled matter. While neglecting matter self-interactions may not be a realistic assumption, it is enough to give at least some hint of the effect that matter can have. We find that within our approximations there are strong restrictions on the total number of matter fields. While the standard model seems to be compatible with asymptotic safety of gravity, many popular scenarios of BSM physics are not within the analysis we perform here.

5.1 Computation of the Anomalous Dimensions

In this section we want to compute the effect of minimally coupled matter on the running of the Newton constant and the Cosmological constant. The truncation we want to study divides into a gravitational part and a matter part. For the gravitational part we will use the standard Einstein–Hilbert

truncation (3.13) that we studied extensively in the previous chapters. As anticipated we will lift the approximation that consist on identifying the graviton anomalous dimension with the "background" anomalous dimension $-\partial_t \log G$ to provide a consistent closure of the flow equation from which we will extract the β functions of the background field G and Λ. In this chapter if not specified we will always use an optimized cutoff shape (1.35).

5.1.1 The gravitational sector

The anomalous dimension of the graviton field η_h is extracted from the running of two point function of the graviton field. Furthermore we can separate the contribution to η_h due to the matter fields from the one due to the graviton itself and the diffeomorphism ghosts.

$$\eta_h = \eta_h\big|_{\text{gravity}} + \eta_h\big|_{\text{matter}} \ .$$

The computation of $\eta_h\big|_{\text{gravity}}$ was first done in [44] here we basically reproduce their computation with some technical differences. Following the diagrammatic notation we introduced in Section 1.3.2 we can compute $\delta^2\Gamma_k/\delta h_{\alpha\beta}\delta h_{\rho\sigma}$

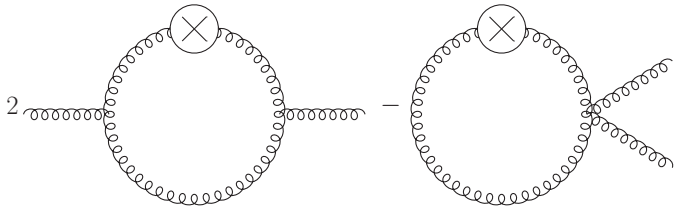

Figure 5.1: Graviton contribution to the graviton two point function.

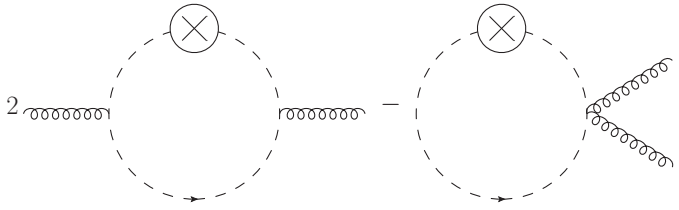

Figure 5.2: Ghost contribution to the graviton two point function, springy lines corresponds to the graviton, dashed lines to the ghost

Notice the factor 2 in front of each of the first diagrams, it comes from the sum of two equivalent diagrams.

To evaluate the anomalous dimensions η_h we proceed as in [35, 45], expanding around flat space and extracting from the r.h.s. of the flow equation terms quadratic in momentum and in the fluctuation field h. The main difference between the computation we present here and the one in [44] consist in subtle point, to simplify the computation we contract $\delta^2\Gamma_k/\delta h_{\alpha\beta}\delta h_{\rho\sigma}$ with

$$K_{\alpha\beta\rho\sigma} = \frac{1}{2}\left(\delta_{\alpha\rho}\delta_{\beta\sigma} + \delta_{\alpha\sigma}\delta_{\beta\rho} - \delta_{\alpha\beta}\delta_{\rho\sigma}\right) \ , \tag{5.1}$$

while they use the projector on the spin-2 part of the graviton. Even if this difference seems innocuous, it leads to different results. We believe that this difference comes from the fact that each spin component of the graviton have an independent anomalous dimension and contracting diagrams 5.1 and 5.2 with any tensor select a certain linear combination of them. We opted for the conservative choice of $K_{\alpha\beta\rho\sigma}$ which is the structure of the graviton propagator in the $\alpha = 1$ gauge that we are using here.

With the same strategy we also computed the anomalous dimension of the diffeo ghost field η_c.

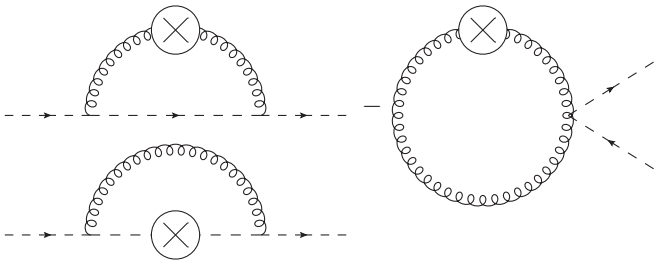

Figure 5.3: Graviton and ghost contribution to the ghost two point function, curly lines corresponds to the graviton, dashed lines to the ghost

The gravitational contribution to the graviton anomalous dimension can be written in the form

$$\eta_h\Big|_{\text{gravity}} = \left[a(\tilde{\Lambda}_k) + c(\tilde{\Lambda}_k)\eta_h + e(\tilde{\Lambda}_k)\eta_c\right]\tilde{G}_k \ . \tag{5.2}$$

Notice that the η_h that appears in the r.h.s. is the full graviton anomalous dimension and comes from the computation of diagrams in Figure 5.1, while η_c comes from the computation of diagrams in Figure 5.2. We have checked the results of [44] when η_h is defined by projecting on the spin two propagator. With our definition of η_h, which involves projection on the tensor K the

coefficients turn out to be:

$$
\begin{aligned}
a(\tilde{\Lambda}) &= \frac{a_0 + a_1\tilde{\Lambda} + a_2\tilde{\Lambda}^2 + a_3\tilde{\Lambda}^3 + a_4\tilde{\Lambda}^4}{(4\pi)^{d/2}\Gamma(d/2)d^2(d^2-4)(3d-2)(1-2\tilde{\Lambda})^4} \ , \qquad (5.3)\\
a_0 &= -4\pi\,(d-2)\,(-896 + 264\,d + 1076\,d^2 - 434\,d^3 + 21\,d^4 + d^5) \ ,\\
a_1 &= 16\pi\,(d-2)\,(-2048 + 2552\,d - 318\,d^2 - 125\,d^3 + 2\,d^4 + d^5) \ ,\\
a_2 &= -16\pi(12544 - 25760\,d + 16968\,d^2 - 4228\,d^3 + 354\,d^4 - 17\,d^5 + d^6) \ ,\\
a_3 &= 4096\pi(d-2)(-32 + 50\,d - 19\,d^2 + 2\,d^3) \ ,\\
a_4 &= -2048\pi(d-2)(-32 + 50\,d - 19\,d^2 + 2\,d^3) \ ;\\
c(\tilde{\Lambda}) &= \frac{8\pi(d-1)\left[128 + 720\,d - 350\,d^2 + 29\,d^3 + 32(d-2)(d+4)\tilde{\Lambda}\right]}{(4\pi)^{d/2}\Gamma(d/2)\,d^2(d+2)(d+4)(3d-2)(1-2\tilde{\Lambda})^3} \qquad (5.4)\\
e(\tilde{\Lambda}) &= -\frac{128\pi\,(32 - 50\,d + 23\,d^2)}{(4\pi)^{d/2}\Gamma(d/2)d^2(d+2)(d+4)(3\,d-2)} \ . \qquad (5.5)
\end{aligned}
$$

The ghost anomalous dimension is computed directly from diagrams in Figure 5.3

$$\eta_c = \left[b(\tilde{\Lambda}_k) + d(\tilde{\Lambda}_k)\eta_h + f(\tilde{\Lambda}_k)\eta_c\right]\tilde{G}_k \ . \qquad (5.6)$$

with

$$
\begin{aligned}
b(\tilde{\Lambda}) &= \frac{64\pi\left[-8 + 4\,d + 18\,d^2 - 7\,d^3 + 2(4 - 9\,d^2 + 3\,d^3)\tilde{\Lambda}\right]}{(4\pi)^{d/2}\Gamma(d/2)d^2(d^2-4)(d+4)(1-2\tilde{\Lambda})^2} \qquad (5.7)\\
d(\tilde{\Lambda}) &= \frac{-64\pi(4 - 4\,d - 9\,d^2 + 4\,d^3)}{(4\pi)^{d/2}\Gamma(d/2)d^2(d^2-4)(d+4)(1-2\tilde{\Lambda})^2} \qquad (5.8)\\
f(\tilde{\Lambda}) &= \frac{-64\pi(4 - 9\,d^2 + 3\,d^3)}{(4\pi)^{d/2}\Gamma(d/2)d^2(d^2-4)(d+4)(1-2\tilde{\Lambda})^2} \ . \qquad (5.9)
\end{aligned}
$$

5.1.2 The matter sector

The matter part of the action is given by

$$\begin{aligned}
\Gamma_{\text{matter}} &= S_S + S_D + S_V \\
S_S &= \frac{Z_S}{2}\int d^dx\sqrt{g}\, g^{\mu\nu}\sum_{i=1}^{N_S}\partial_\mu\phi^i\partial_\nu\phi^i \qquad (5.10)\\
S_D &= iZ_D\int d^dx\sqrt{g}\sum_{i=1}^{N_D}\bar{\psi}^i\not{\nabla}\psi^i, \qquad (5.11)\\
S_V &= \frac{Z_V}{4}\int d^dx\sqrt{g}\sum_{i=1}^{N_V} g^{\mu\nu}g^{\kappa\lambda}F^i_{\mu\kappa}F^i_{\nu\lambda} \qquad (5.12)\\
&\quad +\frac{Z_V}{2\xi}\int d^dx\sqrt{\bar{g}}\sum_{i=1}^{N_V}\left(\bar{g}^{\mu\nu}\bar{D}_\mu A^i_\nu\right)^2\\
&\quad +\frac{1}{2}\int d^dx\sqrt{\bar{g}}\sum_{i=1}^{N_V}\bar{C}_i(-\bar{D}^2)C_i\ .
\end{aligned}$$

In each case, i is a summation index over matter species (not to be confused with the representation index of some non-Abelian gauge group). Similar actions, but without the factors Z_Ψ ($\Psi = S,\ D,\ V$), have been considered before in [19, 28, 29]. Fermions in asymptotically gravity have been further discussed in [20, 33, 35, 36, 39, 40]. The details of the minimal coupling of fermion fields have been investigated in the previous chapter, we adopt a symmetric gauge-fixing of $O(d)$, such that vielbein fluctuations can be re-expressed completely in terms of the metric fluctuations [40, 46, 47]. We will therefore not rewrite the gravitational part of the action in terms of vierbeins, and consistently with the previous chapter we disregard the $O(d)$ ghosts.

There are no gauge interactions, so the fermions (as well as the scalars) are uncharged and there are no gauge covariant derivatives.

In the Abelian gauge field action the second term is a gauge fixing term with gauge-fixing parameter ξ and the third term represents the Abelian ghosts.

The ghosts are decoupled from the metric and gauge field fluctuations and therefore do not contribute to the running of Z_h and Z_V, however they are coupled to the gravitational background and therefore contribute to the beta functions of G and Λ.

Concerning the question of the mixing between Abelian and diffeomorphism ghosts as addressed in [48], it turns out that there is no contribution to the running of Z_V, if a regulator is chosen that is diagonal in the ghost

fieds. We do not introduce a wave function renormalization for the abelian ghosts in this work.

In the following we compute the FRGE for matter fields with type II cutoff and optimize shape (1.35). The inclusion of scalar fields is trivial. For each minimally coupled field scalar field (5.10) we will have a contribution

$$\begin{aligned}\partial_t \Gamma_k|_{\text{scalar}} &= \frac{1}{2}\mathrm{Tr}\frac{\partial_t R_k(\Delta_S) - \eta_S R_k(\Delta_S)}{P_k(\Delta_S)} = \\ &\frac{N_S}{\Gamma\left(\frac{d}{2}+1\right)(4\pi)^{d/2}}\int d^dx\,\sqrt{g}\left[k^d\left(1+\frac{\eta_S}{d+2}\right)+\frac{1}{3}k^{d-2}R\left(1+\frac{\eta_S}{d}\right)\right]\,.\end{aligned} \tag{5.13}$$

where $\Delta_S = -D^2$.

We extensively discussed the contribution to FRGE of fermion fields (5.11) in Section 4.2.2 and we found (4.30)

$$\begin{aligned}\frac{d\Gamma_k}{dt} &= -\frac{1}{2}\mathrm{Tr}\frac{\partial_t R_k(\Delta_D) - \eta_D R_k(\Delta_D)}{P_k(\Delta_D)} = \\ &-\frac{N_D 2^{[d/2]}}{\Gamma\left(\frac{d}{2}+1\right)(4\pi)^{d/2}}\int d^dx\,\sqrt{g}\left[k^d\left(1+\frac{\eta_D}{d+2}\right)-\frac{d}{24}k^{d-2}R\left(1+\frac{\eta_D}{d}\right)\right]\,.\end{aligned} \tag{5.14}$$

where $\Delta_D = -D^2 + \frac{R}{4}$.

We now consider minimally coupled $U(1)$ abelian gauge fields (5.12) their contribution is the sum of two contributions

$$\begin{aligned}\frac{d\Gamma_k}{dt} &= \frac{1}{2}\mathrm{Tr}\frac{\partial_t R_k(\Delta_V) - \eta_V R_k(\Delta_V)}{P_k(\Delta_V)} - \mathrm{Tr}\frac{\partial_t R_k(\Delta_{gh})}{P_k(\Delta_{gh})} = \\ &\frac{N_V}{\Gamma\left(\frac{d}{2}+1\right)(4\pi)^{d/2}}\int d^dx\,\sqrt{g}\left[k^d\left(d-2+d\frac{\eta_V}{d+2}\right)+\frac{1}{3}k^{d-2}R\left(d-8+(d-6)\frac{\eta_V}{d}\right)\right]\,.\end{aligned} \tag{5.15}$$

where $\Delta_V = -D^2 + \text{Ricci}$ and $\Delta_{gh} = -D^2$. Here "Ricci" stands for the Ricci tensor regarded as a linear operator acting on vectors: $Ricci(v)_\mu = R_\mu{}^\nu v_\nu$.

Finally to compute the contribution of the various matter species to β functions of the background field G and Λ from the FRGE we can use (3.14).

The calculation of the matter anomalous dimensions and the matter contribution to the graviton anomalous dimension then proceeds as follows. We choose regulators of type II as defined in Section 3.3.1. Following the computation for $\eta_h|_{\text{gravity}}$ we can compute for each type of matter field its contribution to the graviton two point functional.

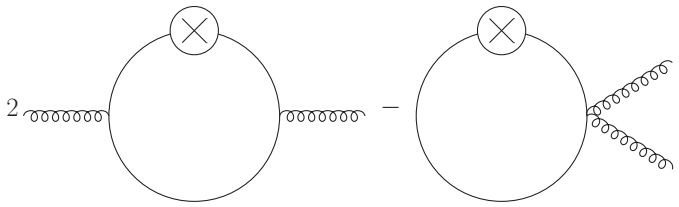

Figure 5.4: The contribution of a scalar field to the graviton two point function, curly lines corresponds to the graviton, continuous lines to a scalar field. Similar diagrams are present also for a fermion and vector field.

Then the matter contribution is

$$\begin{aligned}\eta_h\Big|_{\text{matter}} &= -N_S\,\frac{32\pi\tilde{G}}{(4\pi)^{d/2}\Gamma(d/2)}\,\frac{1}{d^2(d+2)(3d-2)}\left[(d-2)^3+2\frac{8-10\,d+d^2}{d+4}\,\eta_S\right]\\ &\quad +N_D\,2^{[d/2]}\frac{16\pi\tilde{G}}{(4\pi)^{d/2}\Gamma(d/2)}\,\frac{(d-1)(d-2)}{d^3(3d-2)}\left[2+\frac{d-2}{d+1}\,\eta_D\right] \qquad (5.16)\\ &\quad -N_V\,\frac{32\pi\tilde{G}}{(4\pi)^{d/2}\Gamma(d/2)}\,\frac{(d-1)(d-2)}{d^2(d+2)(3d-2)}\left[d^2-12\,d+8-2\frac{16-d}{d+4}\eta_V\right]\,.\end{aligned}$$

The anomalous dimensions of the matter fields are computed from the following diagrams

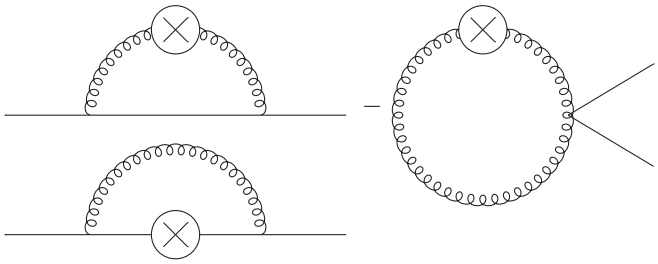

Figure 5.5: The computation of the scalar field two point function, curly lines corresponds to the graviton, continuous lines to a scalar field. Similar diagrams are there also for a fermion and vector field.

$$
\begin{aligned}
\eta_S &= -\frac{32\pi\tilde{G}}{(4\pi)^{d/2}\Gamma(d/2)}\left[\frac{2}{d+2}\frac{1}{(1-2\tilde{\Lambda})^2}\left(1-\frac{\eta_h}{d+4}\right)\right. \\
&\qquad +\frac{2}{d+2}\frac{1}{1-2\tilde{\Lambda}}\left(1-\frac{\eta_S}{d+4}\right) \\
&\qquad \left.+\frac{(d+1)(d-4)}{2d(1-2\tilde{\Lambda})^2}\left(1-\frac{\eta_h}{d+2}\right)\right], \qquad (5.17) \\
\eta_D &= \frac{32\pi\tilde{G}}{(4\pi)^{d/2}\Gamma(d/2)}\left[\frac{(d-1)(d^2+9\,d-8)}{8d\,(d-2)(d+1)(1-2\tilde{\Lambda})^2}\left(1-\frac{\eta_h}{d+3}\right)\right. \\
&\qquad +\frac{(d-1)^2}{2d(d+1)(d-2)}\frac{1}{1-2\tilde{\Lambda}}\left(1-\frac{\eta_D}{d+2}\right) \\
&\qquad \left.-\frac{(d-1)(2d^2-3d-4)}{4d(d-2)(1-2\tilde{\Lambda})^2}\left(1-\frac{\eta_h}{d+2}\right)\right] \qquad (5.18) \\
\eta_V &= -\frac{32\pi\tilde{G}}{(4\pi)^{d/2}\Gamma(d/2)}\left[\frac{(d-1)(16+10\,d-9\,d^2+d^3)}{2d^2(d-2)(1-2\tilde{\Lambda})^2}\left(1-\frac{\eta_h}{d+2}\right)\right. \\
&\qquad +\frac{4(d-1)(2d-5)}{d(d^2-4)(1-2\tilde{\Lambda})}\left(1-\frac{\eta_V}{d+4}\right) \\
&\qquad \left.+\frac{4(d-1)(2d-5)}{d(d^2-4)(1-2\tilde{\Lambda})^2}\left(1-\frac{\eta_h}{d+4}\right)\right]. \qquad (5.19)
\end{aligned}
$$

5.2 Beta functions

The beta functions for $\tilde{G}$ and $\tilde{\Lambda}$ have the following form:

$$\begin{aligned}\frac{d\tilde{\Lambda}}{dt} =& -2\tilde{\Lambda} + \frac{8\pi\tilde{G}}{(4\pi)^{d/2}d(d+2)\Gamma[d/2]}\left[\frac{d(d+1)(d+2-\eta_h)}{1-2\tilde{\Lambda}} - 4d(d+2-\eta_c)\right.\\ &\left. +2N_S(2+d-\eta_S) - 2N_D 2^{[d/2]}(2+d-\eta_D) + 2N_V(d^2-4-d\,\eta_V)\right]\\ &-\frac{4\pi\tilde{G}\tilde{\Lambda}}{3d(4\pi)^{d/2}\Gamma[d/2]}\left[\frac{d(5d-7)(d-\eta_h)}{1-2\tilde{\Lambda}} + 4(d+6)(d-\eta_c)\right.\\ &\left. -2N_S(d-\eta_S) - N_D 2^{[d/2]}(d-\eta_D) + 2N_V(d\,(8-d) - (6-d)\eta_V)\right]\end{aligned} \tag{5.20}$$

$$\begin{aligned}\frac{d\tilde{G}}{dt} =& (d-2)\tilde{G} - \frac{4\pi\tilde{G}^2}{3d(4\pi)^{d/2}\Gamma(d/2)}\left[\frac{d(5d-7)(d-\eta_h)}{1-2\tilde{\Lambda}} + 4(d+6)(d-\eta_c)\right.\\ &\left. -2N_S(d-\eta_S) - N_D 2^{[d/2]}(d-\eta_D) + 2N_V(d(8-d) - (6-d)\eta_V)\right] .\end{aligned} \tag{5.21}$$

5.3 Results

5.3.1 Perturbative approximation

In order to get a rough idea of the effect of matter on the RG flow, in a context where solutions can be found analytically rather than numerically, it is useful to consider first the perturbative approximation, which consists of neglecting all anomalous dimensions and expanding the beta functions to second order in $\tilde{\Lambda}$ and $\tilde{G}$. This is justified in some neighborhood of the Gaussian fixed point. In $d = 4$ the beta functions become

$$\beta_{\tilde{G}} = 2\tilde{G} + \frac{\tilde{G}^2}{6\pi}\left(N_S + 2N_D - 4N_V - 46\right) , \tag{5.22}$$

$$\begin{aligned}\beta_{\tilde{\Lambda}} =& -2\tilde{\Lambda} + \frac{\tilde{G}}{4\pi}\left(N_S - 4N_D + 2N_V + 2\right)\\ &+\frac{\tilde{G}\tilde{\Lambda}}{6\pi}\left(N_S + 2N_D - 4N_V - 16\right) .\end{aligned} \tag{5.23}$$

The numbers 46, 2 and 16 represent the contributions of gravitons and ghosts to the beta functions. These contributions are such that the RG flow admits a nontrivial fixed point when matter is absent. Let us see what effect matter

has, in this approximation. The beta function have a nontrivial fixed point at

$$\tilde{\Lambda}_* = -\frac{3}{4}\frac{N_S - 4N_D + 2N_V + 2}{N_S + 2N_D - 4N_V - 31} , \tag{5.24}$$

$$\tilde{G}_* = -\frac{12\pi}{N_S + 2N_D - 4N_V - 46} . \tag{5.25}$$

Since the beta functions vanish for $\tilde{G} = 0$, flow lines cannot cross from negative to positive $\tilde{G}$. Since the low energy Newton's coupling is experimentally bound to be positive, we require that also the fixed point occurs at positive $\tilde{G}$. This puts a bound on the matter content. In the following we shall find it convenient to present the results in the N_S-N_D-plane, treating the number of gauge fields as a fixed parameter. Positivity of $\tilde{G}_*$ demands that

$$N_D < 23 + 2N_V - \frac{1}{2}N_S . \tag{5.26}$$

Notice that gauge fields contribute with the same sign as gravity, so they facilitate the existence of the fixed point, whereas scalars and fermions tend to destroy it. When their number increases, the fixed-point value of $\tilde{G}_*$ increases and reaches a singularity on the line $N_D = 11 + 2N_V - \frac{1}{2}N_S$. On the other side of the singularity $\tilde{G}_*$ is negative. Fig. 5.6 shows the existence region of a positive fixed point for $\tilde{G}_*$ for no gauge fields or 12, 24, 45 gauge fields. (The significance of these numbers will be discussed later.) We see that the existence region grows with the number of gauge fields, but most importantly, for a given number of gauge fields, only a finite number of combinations of scalar and Dirac fields is allowed.

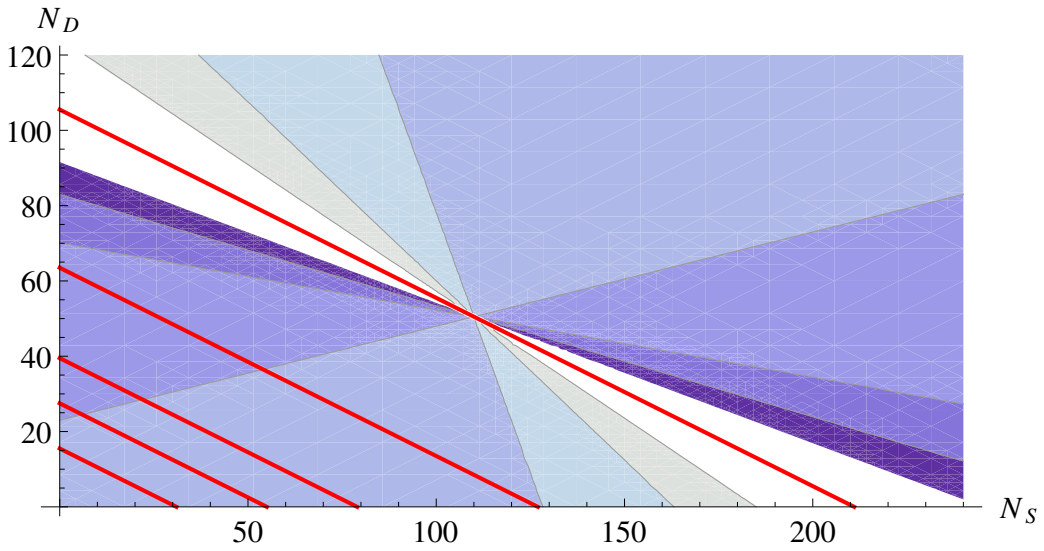

Figure 5.6: The thick red lines are the areas in the N_S-N_D plane compatible with a gravitational fixed point for $N_V = 0$ (in bottom left corner), $N_V = 6, 12, 24, 45$ (from bottom to top). The colored triangles are the contours of the function $\tilde{\Lambda}^*$ for $N_V = 45$.

The cosmological constant has a singularity on the line

$$N_D = \frac{31}{2} + 2N_V - \frac{1}{2}N_S \ . \tag{5.27}$$

This singularity in $\tilde{\Lambda}_*$ is parallel to the singularity in $\tilde{G}_*$ and is shifted downwards by $N_D = 7.5$. There are fixed points in the intermediate region between these singularities, but they are disconnected from the one in the origin (*i.e.*, with no matter), so we regard them as physically very untrustworthy. For "phenomenological" applications we will restrict our attention to points that are below the singularity in the cosmological constant. The allowed region is therefore somewhat smaller than the one shown in fig. 5.6. In the absence of gauge fields this leaves only the area $N_D < \frac{31}{2} - \frac{1}{2}N_S$, which means that at most 31 Weyl spinors or 31 scalars, or a combinations thereof, are admissible.

When we restrict ourselves to the allowed region, the sign of the cosmological constant at the fixed point is determined by the numerator in (5.24): above (or left) of the line

$$N_D = \frac{2 + 2N_V + N_S}{4} \ , \tag{5.28}$$

the cosmological constant is negative, whereas below (or right) of this line it is positive. Note that in the beta function for $\tilde{\Lambda}$ the contribution of each

field is weighed with the number of degrees of freedom it carries, with a plus sign for bosons and a minus sign for fermions. The line (5.28) is where any supersymmetric theory would lie. The contours of constant $\tilde{\Lambda}_*$ are straight lines passing through the point $(2N_V + 20, N_V + 11/2)$, where (5.27) and (5.28) intersect. The singularity of the cosmological constant on (5.27) is negative left of this point and positive right of it.

The stability matrix

$$M = \begin{pmatrix} \frac{\partial \beta_{\tilde{\Lambda}}}{\partial \tilde{\Lambda}} & \frac{\partial \beta_{\tilde{\Lambda}}}{\partial \tilde{G}} \\ \frac{\partial \beta_{\tilde{G}}}{\partial \tilde{\Lambda}} & \frac{\partial \beta_{\tilde{G}}}{\partial \tilde{G}} \end{pmatrix} , \tag{5.29}$$

has eigenvalues -2 and $-4\frac{N_S+2N_D-4N_V-31}{N_S+2N_D-4N_V-46}$. Below the singularites of $\tilde{\Lambda}_*$ and $\tilde{G}_*$, the numerator and denominator of this ratio are positive, so both eigenvalues are negative. In the region between the singularities the second eigenvalue would be positive.

In this perturbative approximation one can examine effect of matter on higher gravitational couplings. If we parametrize the curvature squared terms, up to total derivatives, as

$$\int d^4x \sqrt{g} \left[\frac{1}{2\lambda} C^2 + \frac{1}{\xi} R^2 \right] , , \tag{5.30}$$

where C is the Weyl tensor, the beta functions of the couplings are

$$\begin{aligned} \beta_\lambda &= -\frac{1}{(4\pi)^2} \frac{133}{10} \lambda^2 - 2\lambda^2 a_\lambda^{(4)} , \\ \beta_\xi &= -\frac{1}{(4\pi)^2} \left(10\lambda^2 - 5\lambda\xi + \frac{5}{36}\xi^2 \right) - \xi^2 a_\xi^{(4)} , \end{aligned}$$

where

$$a_\lambda^{(4)} = \frac{1}{2880\pi^2} \left(\frac{3}{2} N_S + 9N_D + 18N_V \right) , \tag{5.31}$$

$$a_\xi^{(4)} = \frac{1}{2880\pi^2} \frac{5}{2} N_S . \tag{5.32}$$

It is remarkable that all types of matter contribute with the same sign to the running of these couplings, which are always asymptotically free.

In the perturbative approximation it is easy to compute the beta functions also with other definitions of the cutoff. If we choose the type Ia cutoff on

gravitons (see Section 3.3.1) the one loop beta functions are given by

$$\beta_{\tilde{G}} = 2\tilde{G} + \frac{\tilde{G}^2}{6\pi}\left(N_S + 2N_D - 4N_V - 22\right) , \tag{5.33}$$

$$\beta_{\tilde{\Lambda}} = -2\tilde{\Lambda} + \frac{\tilde{G}}{4\pi}\left(N_S - 4N_D + 2N_V + 2\right) + \frac{\tilde{G}\tilde{\Lambda}}{6\pi}\left(N_S + 2N_D - 4N_V + 8\right) . \tag{5.34}$$

Notice that the matter contribution has not changed: for massless scalars the two types of cutoff are the same, for fermions we must always use the type II cutoff and for simplicity we have maintained this cutoff also for gauge fields. The only difference is therefore in the gravitational contribution. One can repeat the preceding discussion with little changes. The main effect is that the permitted region is smaller, with the singularities shifted downwards: 23 is replaced by 11 in (5.26) and 31/2 is replaced by 7/2 in (5.27). We can view these shifts as a measure of the typical theoretical uncertainties in this approximation.

The coefficients (5.31) are universal and, as noticed in [32], with type II cutoff and with the shape function (1.35) the contribution of matter to the running of all couplings multiplying terms with six or more derivatives is identically zero.

5.3.2 The full system

Anomalous dimensions and RG improvement

Next we want to analyze the fixed point of the full nonlinear system of beta functions (5.20,5.21), including the anomalous dimensions. The formulas (**??**) do not directly give the anomalous dimensions, rather they give a set of linear equations for the anomalous dimensions. The appearance of the anomalous dimensions on the r.h.s. of these equations is due to the fact that couplings that enter the regulator function (in this case, the wave function renormalizations Z_Ψ) have to be treated as running parameters. If we denote $\vec{\eta} = (\eta_h, \eta_c, \eta_S, \eta_D, \eta_V)$, these equations can be written in the form

$$\vec{\eta} = \vec{\eta}_1(\tilde{\Lambda}, \tilde{G}) + A(\tilde{\Lambda}, \tilde{G})\vec{\eta} \, . \tag{5.35}$$

where $\vec{\eta}_1$ is the leading one loop term and A is a matrix of coefficients.

The reason for calling η_1 the one loop anomalous dimension is that in the functional RG the one loop approximation consists precisely of neglecting the running of the couplings in the r.h.s. of the Wetterich equation. To avoid

misunderstandings, let us also comment that in a single-field truncation, where one neglects the terms of order h in (3.13), the anomalous dimension is identified with

$$-k\frac{d}{dk}\log\left(G_k\right) \ . \tag{5.36}$$

This is the origin of the usual statement that the one loop approximation consists of neglecting the anomalous dimensions. In a two-field truncation, with independent wave function renormalization for the fluctuation field, this statement is not true and one can have anomalous dimensions at one loop.

In order to write the anomalous dimensions as functions of $\tilde{G}$ and $\tilde{\Lambda}$ one has to solve the system of equations (5.2) (5.6). We refer to this as "the RG improvement". The resulting expressions are considerably more complicated than the ones appearing in eq. (5.2-5.19). In particular they are rational functions in $\tilde{\Lambda}$ and $\tilde{G}$ whose numerators and denominators are polynomials of higher order than the ones appearing in the leading one loop terms. Since the full equations contain polynomials of higher order than the leading ones, they will also have more solutions. In general we consider to be reliable those features of the system that can be seen already in simple approximations and that persist when more complicated features are taken into account. This implies that all the additional solutions of the full system that are not present in the one loop system are suspected to be spurious.

Furthermore, in situations where the anomalous dimensions become large, the improvement terms can become numerically dominant relative to the leading one loop terms, in which case also the true solutions may exhibit features that are non-physical. Clearly this means that the "RG improved" results have to be taken with great care when the anomalous dimensions become large. In order to avoid potential pitfalls due to these facts, unless otherwise stated in what follows we shall present the results taking only the leading terms of the anomalous dimensions into account. We will discuss explicitly some cases when the full nonlinear system can be studied and gives reliable results.

Selection criteria

Even the leading one loop flow equations are very nonlinear, and for any given triple (N_D, N_S, N_V), there may be several fixed points. How do we know whether a fixed point is physically significant or just an artifact of the truncation? Since the nontrivial fixed point in the absence of matter is relatively well understood, we try to select among all possible fixed points in the presence of matter the one that derives from a continuous deformation of the fixed point without matter.

We discard those fixed points for which $\tilde{G}_* < 0$. As already remarked, although the fixed-point value of $\tilde{G}$ is not restricted by observations, its low-energy value is. Thus a realistic model of gravity must show an RG flow towards the IR, such that $\tilde{G}(k_{\rm IR}) > 0$. To the best of our knowledge, no truncation exists in which $\tilde{G}$ changes sign under the RG flow, thus ruling out $\tilde{G}_* < 0$.

We discard fixed points which have less than two relevant directions. While in principle the low-energy value of the Newton coupling or the cosmological constant could be a prediction of the theory, both correspond to free parameters of the pure-gravity theory. We expect that for a small number of matter degrees of freedom, the number of critical exponents should not change, otherwise the truncation would be insufficient. This does not rule out the possibility that a very large number of matter degrees of freedom leads to substantial changes in the properties of the theory and a viable fixed point has only one relevant direction, but we do not consider this possibility in the following.

Following this procedure, we find severe restrictions on the number of matter and gauge fields compatible with asymptotically safe gravity. Note that some of the fixed points found in this way can have rather large critical exponents. Such large values indicate a huge departure from canonical scaling and imply that quantum fluctuations have a very big effect. Thus our truncation is presumably insufficient to capture the relevant physics in this case, and yields unreliable results.

Anomalous dimensions and predictivity

A connection exists between the anomalous dimension of the fields and the critical exponents at an interacting fixed point, so that we can deduce a bound on the anomalous dimension by requiring predictivity of the theory: Let us consider an operator $\mathcal{O} = \Phi^n$, where Φ stands for any of the fluctuation fields of the theory, e.g., the graviton. The dimensionality of the corresponding coupling $g_{\mathcal{O}}$ is then given by $d_g = d - n\, d_\Phi$, where d_Φ is the dimensionality of the field. Accordingly, the dimensionless coupling $\tilde{g}_{\mathcal{O}}$ is given by

$$\tilde{g}_{\mathcal{O}} = g_{\mathcal{O}} \frac{k^{-d+nd_\Phi}}{Z_\Phi^{\frac{n}{2}}}. \tag{5.37}$$

The β function for the coupling $\tilde{g}_{\mathcal{O}}$ will thus have the following structure

$$\beta_{\tilde{g}_{\mathcal{O}}} = \left(-d + nd_\Phi + \frac{n}{2}\eta_\Phi\right) \tilde{g}_{\mathcal{O}} + \dots \,, \tag{5.38}$$

where we have introduced the anomalous dimension $\eta_\Phi = -\partial_t \ln Z_\Phi$. The additional terms in the β function depend on the particular operator that

we consider, and are nonzero at an interacting fixed point. Neglecting operator mixing, they will result in a shift of the critical exponent $\theta_{\mathcal{O}}$ from the canonical value (which it has at a noninteracting fixed point) to

$$\theta_{\mathcal{O}} = -\frac{\partial \beta_{\tilde{g}_{\mathcal{O}}}}{\partial \tilde{g}_{\mathcal{O}}}|_{\tilde{g}_{\mathcal{O}}=\tilde{g}_{\mathcal{O}*}} = d - n d_\Phi - \frac{n}{2}\eta_\Phi + \dots \ . \tag{5.39}$$

The sign of the critical exponent cannot be determined from general arguments, but must be fixed by an explicit calculation. At an interacting fixed point, the anomalous dimension constitutes a further departure from canonical scaling, that scales with n. Predictivity demands that at most a finite number of operators should be shifted into relevance at an interacting fixed point. This implies that

$$\eta_\Phi > -2d_\Phi + \frac{2d}{n} \xrightarrow{n\to\infty} -2d_\Phi. \tag{5.40}$$

In the case of the graviton, $d_h = \frac{d-2}{2}$, therefore

$$\eta_h > -d + 2. \tag{5.41}$$

Considering operators $\mathcal{O}$ that contain derivatives will generally give a weaker bound; here we will consider the strongest possible bound. We will use this as a fourth criterion to bound the number of matter fields compatible with asymptotic safety. We will not take into account similar bounds on the matter anomalous dimension, as we have neglected all matter self-interaction. We thus assume that our values for the matter anomalous dimensions will change in a more complete truncation.

In the following, we apply the criteria specified above and discuss the compatibility of scalars, Dirac fermions and vectors with a viable fixed point for gravity. All the fixed points we find satisfy also this additional condition.

5.3.3 Fixed points

No matter

The anomalous dimensions of the ghosts had been calculated previously in [45], [49]. The running of the graviton two point-function had been calculated also in [50], [51], [52] where it was interpreted as running of the cosmological and Newton couplings.

At this stage, we ignore the difference between the running of the background cosmological constant and the "mass" term in the graviton propagator.

Our derivation differs from previous ones in the definition of the cutoff and of the anomalous dimension. We use a type II cutoff, in part for coherence with the cutoff in the fermionic sector, but also because it leads to beta functions containing polynomials of lower order and hence with fewer spurious solutions.

Furthermore, in the definition of the anomalous dimension η we have projected the two-point function on the tensor K, which is the structure it has in the internal lines.

This also has the computational advantage of depending only on the metric and not on the external momenta. We list the results in the following table.

	1L-II	full-II	full-Ia	Ref. [44]
$\tilde{\Lambda}_*$	0.010	0.009	-0.049	-0.008
$\tilde{G}_*$	0.772	0.776	1.579	1.446
θ_1	3.298	3.317	3.991	3.323
θ_2	1.954	1.925	1.920	1.954
η_h	0.269	0.299	0.540	0.072
η_c	-0.806	-0.814	-1.390	-1.503

Table 5.1

The first two columns give the results of the "one loop" approximation, as defined in Subsection 3.3, and the "RG improved" equations, both with the type II cutoff. The difference is very small, in accordance with the fact that the anomalous dimension of the graviton is small. The third column gives the result we obtain using a cutoff of type Ia instead of II. The difference with the first column is not very small quantitatively, in line with previous discussions of the scheme-dependence in this approach [53, 54]. A higher order truncation would be needed to improve this aspect. The last column gives the results of reference [44], who also used a cutoff of type Ia. The differences that are seen between the last two columns can thus all be attributed to our different definition of the anomalous dimensions. The main difference between these results and the earlier literature lies in the real critical exponents, which are seen to be only weakly dependent on the technical details. We anticipate that this is mainly due to our identification of the "graviton mass" (the term quadratic in h and without derivatives in (5.63)) with the background cosmological constant. When the graviton mass is allowed to run independently the flow in the $\tilde{\Lambda}$-$\tilde{G}$ plane has again complex critical exponents, while the flow in the mass-$\tilde{G}$ plane looks like the one discussed here. A paper with an improved truncation where mass and higher

order are included is in preparation.

Scalar matter

Even though physically N_S must be an integer, mathematically one can study the dependence treating N_S as a continuous parameter. For $N_S \leq 12$ the effect of scalars is to push $\tilde{\Lambda}_*$ towards larger values, while $\tilde{G}_*$ is almost stable. The product $\tilde{\Lambda}_*\tilde{G}_*$, which is generally known to be quite independent of technical details such as gauge and cutoff choice, increases slowly, see fig. 5.7. In this regime the critical exponents change little while the anomalous dimensions increase in absolute value, maintaining the same sign ($\eta_h > 0$, $\eta_c < 0$ and $\eta_S < 0$). There is a sharp change of behavior of $\tilde{\Lambda}_*$ for $N_S \geq 12$. Beyond this value, the cosmological constant stops growing with N_S, while $\tilde{G}_*$ begins to grow and also the critical exponents become very large ($O(10^3)$).

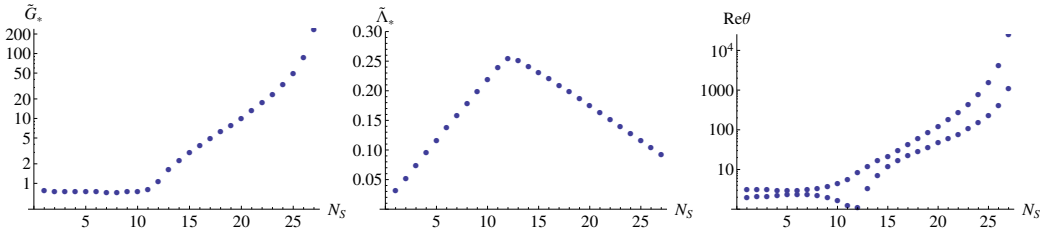

Figure 5.7: Left and middle: Position of the fixed point as a function of the number of scalar fields. Right: critical exponents. Note the logarithmic scales. All with type II cutoff and one loop anomalous dimensions.

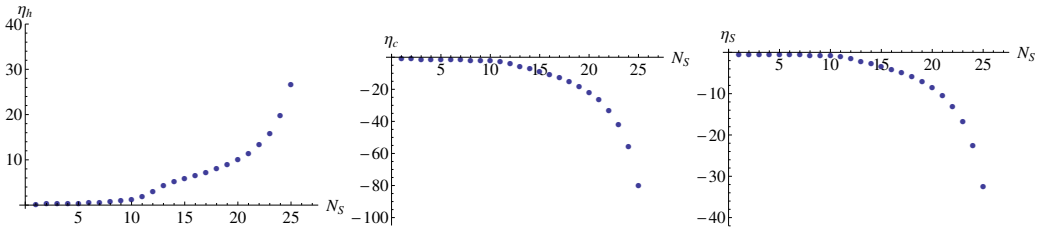

Figure 5.8: The graviton (left), ghost (middle) and scalar (right) anomalous dimensions as functions of the number of scalar fields.

As far as we could see, the change of behavior occurs smoothly over the whole range, so one has a continuous deformation of the pure gravity fixed point up to $N_S \approx 27.7$ where $\tilde{G}_*$ diverges. As in the perturbative approximation, there is therefore a maximal number of scalar fields that is compatible with the existence of a viable fixed point. This is in contrast

to [28, 29], where the fixed point seemed to exist for any number of scalars. We believe that fixed point to be an artifact of the identification of η_h with (5.36) in the single field truncation.

The effect of scalar fields on the position of the fixed point, on the critical exponents and on the anomalous dimensions is shown in figs. 5.7,5.8, at one loop and with type II cutoff. Including the RG improvement results in more complicated behaviour. While the fixed-point value for the Newton coupling is nearly constant up to $N_S = 11$, it rises sharply thereafter. At the same time, $\tilde{\Lambda}_* \approx 0.25$ becomes nearly independent of N_S. The critical exponents are complex for $12 \leq N_S \leq 50$ and their real part is negative for $15 \leq N_S \leq 20$. The singularity is deferred to $N_S \approx 85$.

With a type Ia cutoff the anomalous dimensions remain smaller and the fixed point becomes complex at $N_S \approx 17$. This lower limit is in line with the result of the perturbative approximation. We thus observe a significant scheme-dependence for $N_S > 12$. This, together with the fact that the anomalous dimensions become rather large in that range, makes the full RG improved equations unreliable. This suggests, that the fixed point beyond $N_S = 17$ could be a truncation artifact.

In the future we may understand better which truncation gives physically reliable results but for the time being the scheme dependence has to be taken as a measure of the theoretical uncertainties. For now we can say with good confidence that the fixed point ceases to exist when the number of scalars becomes of the order of 22 ± 5. To sharpen this number, one should study the behavior of higher background curvature terms, for example repeating the analysis in [55] under the inclusion of scalars. On the other hand, in order to understand whether the large negative scalar anomalous dimension could lead to an increase in the number of relevant directions, one should study this question in the presence of scalar self-interactions [41].

Fermionic matter

As already observed in [28], the effect of fermions is to push $\tilde{G}_*$ to larger values and $\tilde{\Lambda}_*$ to more negative values, cf. fig. 5.9.

At a critical number of fermions $N_D \approx 10.1$, $\tilde{G}_*$ goes to $+\infty$ and $\tilde{\Lambda}_*$ goes to $-\infty$. This is similar to the behavior seen in the perturbative analysis. Accordingly fermions have a destabilizing effect on asymptotic safety in gravity, reminiscent of a similar effect of fermions on asymptotic freedom in gauge theories.

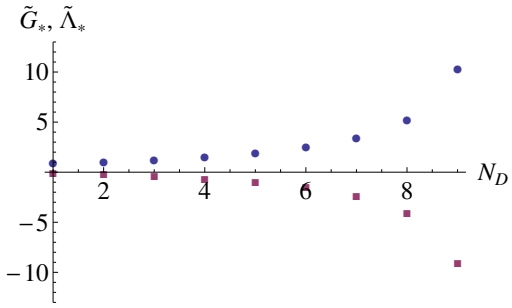

Figure 5.9: The values of $\tilde{G}_*$ (dots) and $\tilde{\Lambda}_*$ (squares) as functions of the number of Dirac fields, at one loop with type II cutoff.

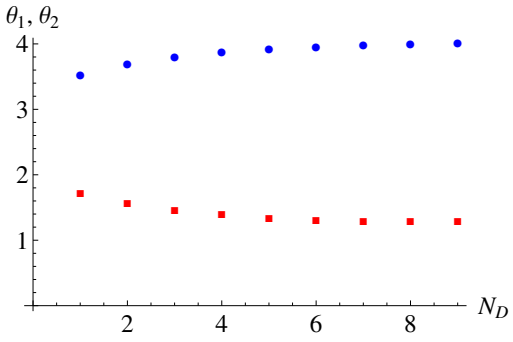

Figure 5.10: The critical exponents $\theta_{1,2}$ as functions of the number of Dirac fields.

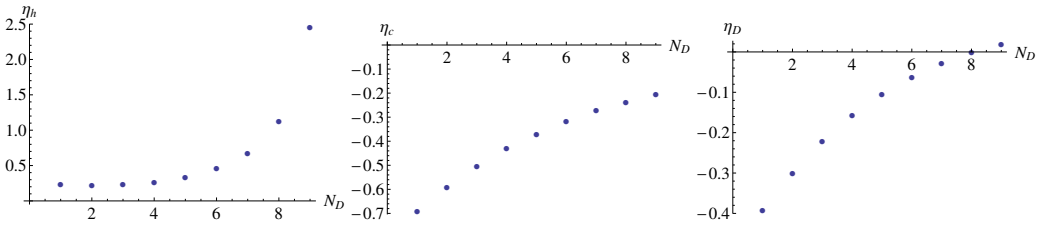

Figure 5.11: The graviton (left), ghost (middle) and fermion (right) anomalous dimensions as functions of the number of fermion fields, all at one loop and with type II cutoff.

Below the critical number the solution to the microscopic equation of motions at the fixed point – within our truncation – is the Euclidean version of anti deSitter space. Thus, AdS/CFT-type dualities might be of use to understand the microscopic gravitational action.

Fermionic fluctuations have only a small effect on the values of the critical exponents, cf. fig. 5.10. This suggests that fermionic matter does not change the number of relevant directions of background operators. In contrast, the graviton anomalous dimension grows, cf. fig. 5.11. These results show only a very weak scheme-dependence. The main difference in the RG improved case lies in the fact that the fermionic anomalous dimension remains negative up to the critical value of N_D.

The main result of our analysis up to this point lies in the existence of a maximum number of fermions and scalars compatible with the gravitational fixed point within our truncation. This is true also for combinations of scalars and fermions, as seen in fig. 5.12, which shows the existence region of the fixed

point in the N_S-N_D-plane for $N_V = 0$. Note the qualitative agreement with the analysis of the perturbative approximation in section IV.A. We conclude that the inclusion of dynamical matter can fundamentally change a quantum theory of gravity, or even make it inconsistent. It is thus crucial to include realistic matter degrees of freedom in the investigation of the asymptotic-safety scenario for quantum gravity.

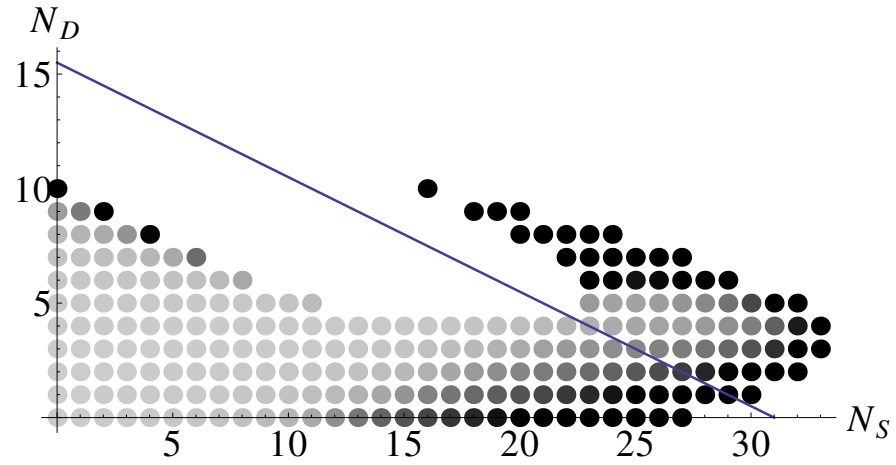

Figure 5.12: The points in the N_S-N_D plane compatible with a gravitational fixed point with two relevant directions for $N_V = 0$. The line represents the perturbative bound (5.27). Lighter shades of gray mean smaller η_h; black means $\eta_h > 10$.

Vector fields

In contrast to scalars and fermions, we find no bound on the number of vector fields compatible with a viable gravitational fixed point. The effect of vector degrees of freedom is always to decrease $\tilde{G}_*$ and to increase $\tilde{\Lambda}_*$. The position of the fixed point and the values of the critical exponents and anomalous dimensions are shown in figs. 5.13,5.14, for $0 \leq N_V \leq 50$, covering all phenomenologically interesting models. The behavior is very smooth. From the point of view of the N_V-dependence, however, this is still a transient range. For very large N_V all quantities reach the following asymptotic values:

	$\tilde{G}_*$	$\tilde{\Lambda}_*$	θ_1	θ_2	η_h	η_c	η_V
$\lim_{N_V\to\infty}$	0	3/8	4	2	9/10	0	0

Table 5.2

This picture holds with small quantitative changes also when the RG improvement is taken into account, and with type Ia cutoff. The most significant difference lies in the fact that the vector anomalous dimension does not change sign even for large N_V, when the RG improvement is taken into account. We therefore believe that the existence of the fixed point is a true feature of gravity coupled to vector fields. It will be interesting to see whether the gauge coupling remains asymptotically free when Yang-Mills is coupled to gravity.

As a preliminary step, we consider the effect of gravitational fluctuations on the beta-function of the gauge coupling in the abelian case. In the context of asymptotic safety, this has been considered previously in [48, 56, 57]. In $d = 4$ the beta function is given by

$$\beta_g = \frac{1}{2}\eta_V g \approx \frac{g^3 N_D}{12\pi^2} - \frac{3}{8\pi} g \tilde{G} + \frac{3}{2\pi} g \tilde{G}\tilde{\Lambda}^2. \tag{5.42}$$

For a small value of the cosmological constant, we observe that gravitational fluctuations lead to an asymptotically free fixed point. Whether this behavior carries over to the QED coupling when defined as in [58], is an open question. As in [57], there is also a non-Gaußian fixed point, at which the QED coupling is irrelevant, and its value in the infrared can be predicted. A main difference to [57] lies in the $\tilde{\Lambda}$-dependence of our result, which is quadratic, instead of linear in $\tilde{\Lambda}$. For $|\tilde{\Lambda}| > \sqrt{0.4}$, the Gaußian and the non-Gaußian fixed point merge, and only a UV-repulsive Gaußian fixed point remains. For the matter content of the Standard Model, only the UV-repulsive noninteracting fixed point remains.

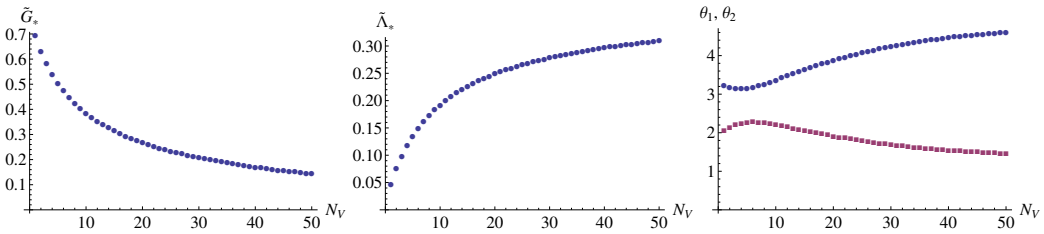

Figure 5.13: Position of the fixed point (left and middle) and critical exponents (right) as a function of number of vector fields.

Specific matter models

A viable gravitational fixed point exists for a small number of matter fields. Increasing the number of matter fields, two mechanisms can remove the fixed

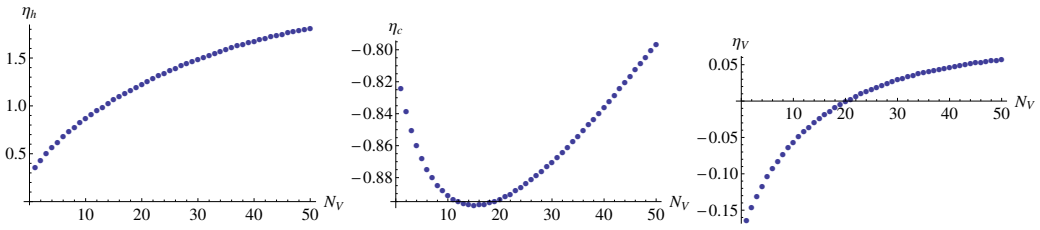

Figure 5.14: The graviton (left), ghost (middle) and vector (right) anomalous dimensions as functions of the number of vector fields.

point: A first possibility is for $\tilde{G}_*$ and/or $\tilde{\Lambda}_*$ to diverge. A second mechanism is the collision of fixed points: The beta functions admit several zeros, which move in the $\tilde{G}$-$\tilde{\Lambda}$ plane in dependence of the number of matter fields. These fixed points can collide, at which point they move off the real axis to complex values. These mechanisms are responsible for the existence of boundaries in the (N_S, N_D, N_V) space.

Before discussing the shape of the boundaries, we will investigate the compatibility of specific matter models with the asymptotic safety scenario. Note that our results rely on a particular truncation, thus extended truncations will most certainly result in quantitative changes. Recall also that we neglect all matter-self-interactions which are present in specific matter models. In particular we do not distinguish between abelian and non-abelian gauge bosons.

We begin with the standard model (in its original form excluding right-handed neutrinos). For reasons that have been discussed earlier, we take as our benchmark the one-loop results obtained with type II cutoff. These are reported in the first column of the following table.

	1L-II	full-II	1L-Ia	full-Ia
$\tilde{\Lambda}_*$	-2.399	-2.348	-3.591	-3.504
$\tilde{G}_*$	1.762	1.735	2.627	2.580
θ_1	3.961	3.922	3.964	3.919
θ_2	1.644	1.651	2.178	2.187
η_h	2.983	2.914	4.434	4.319
η_c	-0.139	-0.129	-0.137	-0.125
η_S	-0.076	-0.072	-0.076	-0.073
η_D	-0.015	0.004	-0.004	0.016
η_V	-0.133	-0.145	-0.144	-0.158

Table 5.3: Standard model matter

So the first and most important observation is that the matter content of the standard model is compatible with the existence of a fixed point. By first adding, one at the time, the vector fields, then the scalars, then the fermions, one can convince oneself that this fixed point is a continuous deformation of the one discussed in section IV.C.1. The second column shows the properties of the fixed point of the RG improved beta functions. They are not very different from the one loop results, as expected from the fact that the anomalous dimensions are not very large. The other two columns show the properties of the same fixed point when one uses a type Ia cutoff. As observed earlier, with this cutoff the allowed region is smaller, so the standard model is closer to the boundary and this explains why the couplings are larger. The variations are typical for the scheme dependence in this approach. All the evidence leads us to believe that this fixed point is a genuine feature of the theory and not an artifact of the truncation.

model	N_S	N_D	N_V	$\tilde{G}_*$	$\tilde{\Lambda}_*$	θ_1	θ_2	η_h
no matter	0	0	0	0.77	0.01	3.30	1.95	0.27
SM	4	45/2	12	1.76	-2.40	3.96	1.64	2.98
SM +dm scalar	5	45/2	12	1.87	-2.50	3.96	1.63	3.15
SM+ 3 ν's	4	24	12	2.15	-3.20	3.97	1.65	3.71
SM+3ν's + axion+dm	6	24	12	2.50	-3.62	3.96	1.63	4.28
MSSM	49	61/2	12	-	-	-	-	-
SU(5) GUT	124	24	24	-	-	-	-	-
SO(10) GUT	97	24	45	-	-	-	-	-

Table 5.4: Fixed-point values, critical exponents and anomalous graviton dimension for specific matter content.

Theories that go beyond the standard model contain more fields. So let us consider these models, starting from the ones with fewer fields. A very minimal extension is a single further scalar field, which can be viewed as a model of dark matter [59–62]. This has a small effect, as seen in the third row of table 5.4. In the fourth row we consider a model with three right-handed neutrinos, to account for neutrino masses. This has a somewhat larger effect but is still clearly compatible with asymptotic safety. In the fifth row we consider a model with three right-handed neutrinos and two scalars, one of which can be thought of as the axion [63–66], the other as dark matter. This model is still in the allowed region with the type II cutoff, but if one were to use the more stringent type Ia cutoff it would be quite close to the boundary.

This model is therefore nearly as extended as one can get without adding further gauge fields. The extent of the allowed region with $N_V = 12$ is shown in figure 5.15.

One important example of a model that is beyond the boundary is the MSSM. In the one loop approximation with type II cutoff there is actually no real solution with the matter content of the MSSM. In the RG improved equations, two real solutions with positive $\tilde{G}_*$ exist, but they have one positive and one negative critical exponent and are therefore not a continuous deformation of the no-matter fixed point. A similar situation holds with type Ia cutoff. Since they do not appear already in the one loop approximation they are likely to be truncation artifacts. We conclude that the matter content of the MSSM, again neglecting the non-abelian nature of the gauge bosons, is incompatible with the existence of a fixed point.

In the case of GUTs the fermion content is the same as the SM (typically with right-handed neutrinos included) and there are more gauge fields, so one may hope that they are compatible with a fixed point. In this case, however, it is the large number of scalars that poses a severe challenge. As examples we consider an $SU(5)$ and an $SO(10)$ model, both with minimal scalar sectors. In both cases the fermionic sector consists of three generations including right-handed neutrinos, *i.e.*, a total of 48 Weyl spinors, which count like 24 Dirac spinors. In the case of SU(5), we consider three scalar multiplets: one in the adjoint (24 real fields), one in the fundamental (5 complex fields) and one in the complex 45-dimensional representation. This sums up to $N_S = 124$. In the case of SO(10) a minimal scalar sector would contain the adjoint (45 real fields) two fundamental (10 real fields each) and one (complex) 16 [67] leading to $N_S = 97$.

The $SU(5)$ model actually has one fixed point with large $\tilde{G}_* = 37$, large critical exponents -80 and 38 with opposite signs, implying that it is not connected to the no-matter fixed point. Furthermore it has a huge anomalous dimension $\eta_h = 84$ which makes it rather unreliable. The RG improved beta functions again have a single real fixed point with positive $\tilde{G}_* = 0.21$, but in a very different position and with very different critical exponents -5.3 and 1.4 which make it impossible to identify it with the one of the one loop approximation. This strengthens the suspicion that they are both truncation artifacts. So while one cannot strictly exclude the existence of a fixed point for this particular matter content, it is beyond the boundary of our allowed region. In the case of the $SO(10)$ model this conclusion is even stronger, since there is no real nontrivial fixed point. Considering that realistic GUT models have many more scalars than the minimal models considered here, one can conclude with good confidence that GUTs with fundamental scalars are incompatible with a gravitational fixed point.

Technicolor-like models [68], which dispense with fundamental scalars, and instead introduce further fermions and gauge bosons, could very well be compatible with a fixed-point scenario for gravity, as larger numbers of vectors also imply a larger number of fermions compatible with the fixed point.

Fig. 5.15 shows the region in the N_S-N_D-plane where a fixed point exists with $\tilde{G}_* > 0$, $\theta_1, \theta_2 > 0$ for $N_V = 12$, at one loop and with type II cutoff. In comparison to the perturbative results, the inclusion of the anomalous dimensions leads to a more complicated shape of the boundary, but it remains true that continuous deformations of the fixed point without matter are only possible in a bounded domain of the plane. When one increases the number of scalars or fermions at fixed N_V one encounters a singularity, or the fixed point becomes complex.

The fixed points in the disconnected island on the right cannot be continuously deformed into the one without matter. Instead, they are the continuation of a fixed point that is complex in the permitted region connected to the origin, and becomes a pair of real fixed points for larger number of scalars. For small N_V the gap closes and there are combinations of matter fields such that the two fixed points are both real. This can be see in Fig. 5.16 which shows the exclusion plot in the plane $N_D = 0$. (No such phenomena occur in the $N_S = 0$ plane.) Since the second fixed point coexists with the one that we regard as physically significant in some region of the (N_S, N_D, N_V) space, it is probably an artifact of the truncation. Consequently, also in the rest of the space, its significance is doubtful. More detailed investigations will be necessary to clarify this point.

The shades of grey in figures 5.12, 5.15, 5.16 are related to the value of the graviton anomalous dimension, with darker tones indicating a larger anomalous dimension. We observe that η_h becomes very large ($O(10^3)$) at some points in the horn of fig. 5.12 and near the boundary, at small N_S. The restriction $\eta_h > -2$ is automatically satisfied everywhere and does not add significant restrictions, however the dark dots indicate that the truncation used is unreliable. Our graphs should therefore be taken with a grain of salt, as the shape and position of the boundary could change in an extended truncation.

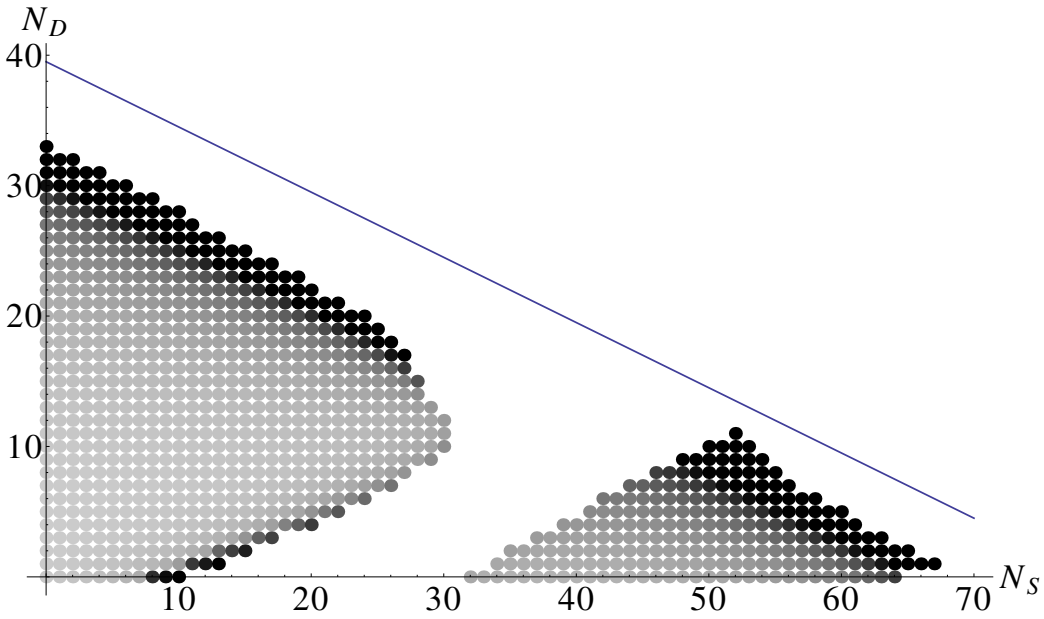

Figure 5.15: The region compatible with the existence of a gravitational fixed point with $\tilde{G}_* > 0$ and two attractive directions for $d = 4$, $N_V = 12$. The line represents the perturbative bound (5.27). Lighter shades of gray mean smaller η_h; black means $\eta_h > 10$.

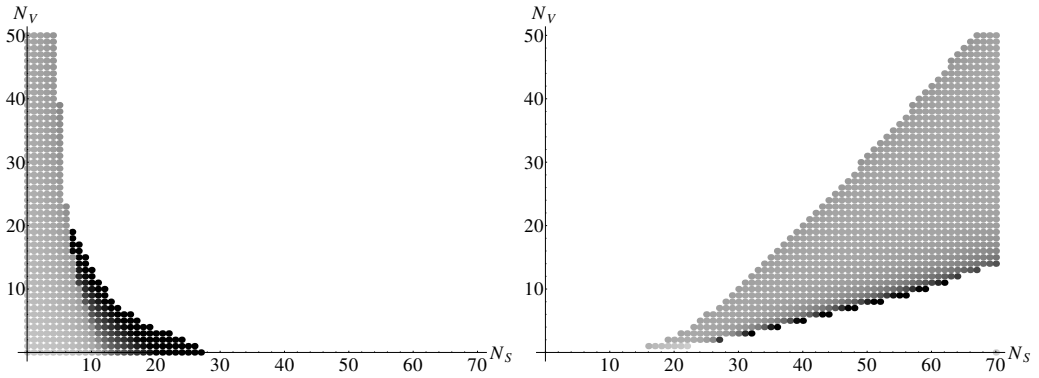

Figure 5.16: Left: existence region of the fixed point connected to the one without matter, in the plane $N_D = 0$. Middle: existence region of a second real fixed point with two relevant directions, in the same plane. The line $N_D = 0$ in fig. (5.15 corresponds to the line $N_V = 12$ in these two figures.

The overall conclusion of this brief investigation is that asymptotic safety puts very strong restrictions on the matter content. It is thus interesting to

observe that limited, observationally well-motivated extensions of the standard model are compatible with a fixed point for gravity, while models that demand a larger number of degrees of freedom for internal consistency reasons (such as supersymmetric models) are incompatible with the fixed-point scenario. The observation of many more fundamental particles at LHC or future accelerators could therefore pose a severe challenge to the asymptotic safety scenario.

5.3.4 The quantum gravity scale with matter

Although the asymptotic safety scenario aims at a construction of a continuum quantum gravity model, where no fundamental kinematical length scale exists, a quantum-gravity scale will emerge dynamically. This is very similar to QCD, where quantum fluctuations lead to the dynamical generation of Λ_{QCD}, which is a physical scale at which the behavior of the theory changes drastically. In quantum gravity the transition scale to the fixed-point regime is the dynamically generated quantum-gravity scale. There, the theory changes from the phase in which the dimensionful Newton coupling is constant, to a scale-free regime in which $G(k^2) \sim \frac{1}{k^2}$, which is conjectured to become visible, e.g., in graviton-mediated scattering cross sections [69–71]. A priori, this scale could take any value, but has been found to be close to the Planck scale in previous studies of the Einstein-Hilbert truncation [72]. Note that this notion of a quantum gravity scale differs from that discussed, e.g., in [73], where a quantum gravity scale is defined by $\tilde{G} \sim 1$. These two scales differ. The latter can be understood as a scale where quantum gravity effects in general become important. The former is a scale pertaining to the notion of asymptotic safety, and can be thought of as a scale at which predictions from asymptotic safety will differ from other quantum gravity theories.

Trajectories passing very closely to the Gaußian fixed point before approaching the UV fixed point [72] exist also under the inclusion of matter. We thus expect to find a fine-tuned trajectory where the gravitational couplings take on their measured values in the infrared. On trajectories similar to this highly fine-tuned one, all quantities then clearly show the dynamical emergence of a scale at which the fixed-point regime is reached. We fix the dimensionless Newton coupling and cosmological constant to fixed values $\tilde{G}_0, \tilde{\Lambda}_0$ at a given IR scale, and then numerically integrate the RG flow towards the UV. We observe that scalars seem to have little effect on the transition scale, whereas fermions shift this scale towards larger values. There are two competing effects at work here: If the fixed-point coordinates of the NGFP are further away from the GFP, the flow takes up more "RG-time" until it reaches the fixed point, if the critical exponents are un-

changed. If the critical exponents change also, they also alter the amount of "RG-time" necessary to reach the fixed point. Since the effect of fermions is to induce a considerable shift in the fixed-point values towards larger $\tilde{G}$ and more negative $\tilde{\Lambda}$, they shift the QG scale towards higher values. In the case of the Standard Model, the effect is less pronounced than in the case with fermions only. In our evaluation, we found a shift of the transition scale to the fixed-point regime by a factor of approximately 10.

Our study suggests that the dynamically generated quantum gravity scale is not independent of the existing matter degrees of freedom, as has also been observed in [73]. If a shift to higher scales is confirmed beyond our truncation, discovering phenomenological imprints of asymptotically safe quantum gravity might become even more challenging. It would be interesting to include the effect of the running Newton coupling into numerical calculations in the strong-gravity regime, such as those performed in [74]; see also [75, 76] for the discussion of black-hole production in asymptotic safety.

5.3.5 Higher-dimensional cases

Large extra dimensions have a number of theoretical motivations, and have been shown to be compatible with asymptotically safe gravity in the Einstein-Hilbert truncation [77] and under the inclusion of fourth-order derivative operators [78]. While extra dimensions are not necessary for the consistency of the model, they seem well compatible with it. Phenomenological implications have been studied in [69–71]. Experimentally, the best upper bounds on their radius come from recent LHC results, see, e.g., [79, 80].

While the extra dimensions have to be compactified in a realistic setting, we can neglect the effect of compactifications here: At momentum scales much higher than the inverse compactification radius, the difference between a continuum of momentum modes and a discrete set of Kaluza-Klein modes has no effect.

The allowed regions for $d = 5, 6$ and $N_V = 12$, at one loop and with type II cutoff, are shown in fig. 5.17. We see that the standard model would still be (barely) compatible with a fixed point in $d = 5$ but it is not in $d = 6$. It would be incompatible also in $d = 5$ if we used the type Ia cutoff. This case is therefore marginal and needs further investigation.

It appears that the existence of sufficiently many matter fields poses a new restriction on the number of dimensions compatible with asymptotic safety. While a pure gravitational fixed point exists in these dimensions, the observed matter degrees of freedom tend to destroy it, at least within our truncation. Whether this changes if only gravity can propagate into the extra dimensions would have to be re-examined.

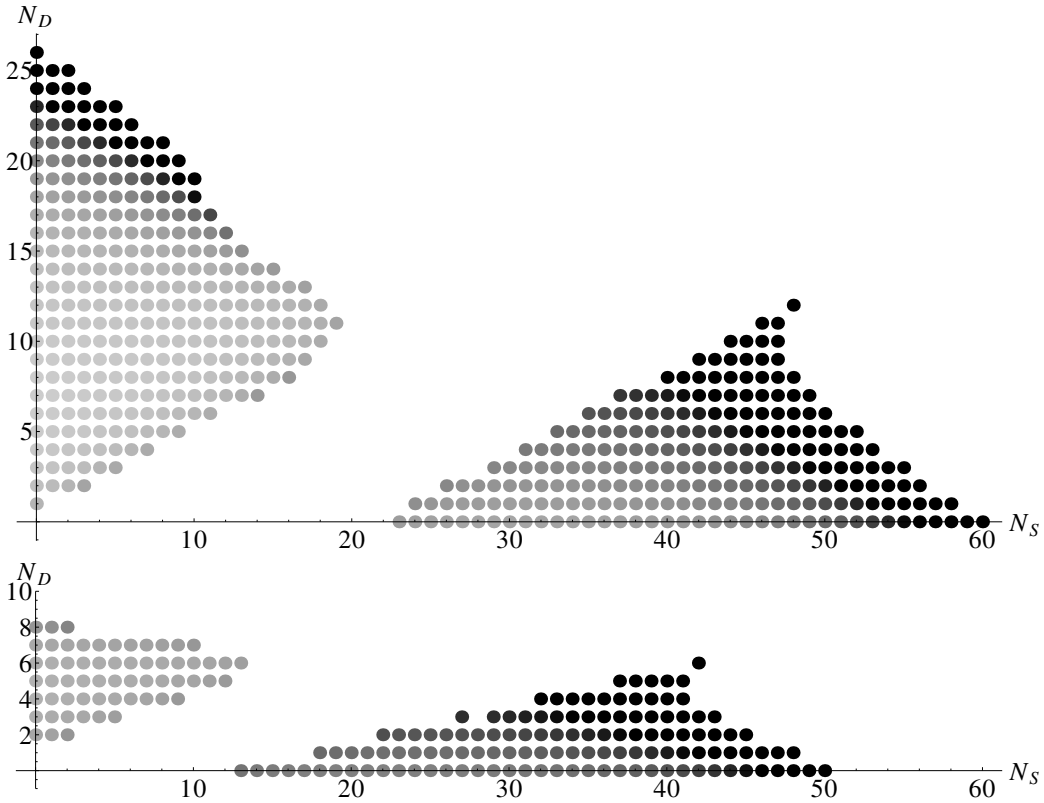

Figure 5.17: The region compatible with the existence of a gravitational fixed point with $\tilde{G}_* > 0$ and two attractive directions for $d = 5$ (top) and $d = 6$ (bottom) and $N_V = 12$. Lighter shades of gray mean smaller η_h; black means $\eta_h > 10$.

5.3.6 Anomalous dimension

In the scale-free fixed-point regime, the value of the anomalous dimension can be related to the momentum-dependence of the propagator as follows

$$P(p) \sim \frac{1}{(p^2)^{1-\eta/2}} \ . \tag{5.43}$$

It is interesting to observe that while a negative value of η implies a UV suppression of the propagator, a positive value corresponds to a UV-enhancement. For the background-field anomalous dimension, $\eta_N = -2$ arises as a fixed-point requirement, and could be read as a UV suppression. In contrast, the fluctuation field anomalous dimension without matter implies a rather weak UV enhancement of the graviton propagator. Scalar and fermion fields push η_h into the large positive region, and vectors also tend to increase it, at least

as long as N_V is not too large. The result is that for the Standard Model we have a rather large positive anomalous dimension, corresponding to a strong enhancement.

A large anomalous dimension η_h implies that for a more detailed understanding of the imprints of asymptotic safety on scattering cross sections in graviton-mediated scattering processes, the inclusion of vertex anomalous dimensions is necessary, as the UV scaling of the propagator alone implies an increase of the scattering cross section at high energies.

Quantitative changes are expected for η_h, when momentum-dependent higher-order correlation functions for the graviton are included in the truncation, and it remains to be investigated, whether $\eta_h < 0$ then, as one might naively expect for the unitarization. Making the simplifying assumption that graviton-matter vertices with one graviton and two matter fields do not get any explicit renormalization, the quantum-fluctuation-induced scaling of those vertices is determined purely by the anomalous dimensions. For instance, the dimensionless coupling $g_{h\phi\phi}$ of an operator of the form $h_{\mu\nu}\partial_\mu\phi\partial_\nu\phi$, will then scale as $g_{h\phi\phi} \sim k^{\eta_S+\frac{\eta_h}{2}}$. For graviton-mediated scattering processes, we encounter a divergence of the scattering cross section with the center-of-mass-energy at tree-level, if quantum-gravity-induced renormalization effects are not taken into account. Here we observe, that, upon an identification of k^2 with the center-of-mass energy s, we would conclude that a negative anomalous dimension for matter and gravity improves the situation, as there is the additional scaling $s^{2\eta_S+\eta_h}$. Additionally, the graviton propagator scales non-trivially with an additional $\frac{1}{p^{-\eta_h}}$. The combined effect could even lead to a fall-off of the scattering cross-section, depending on the size of the anomalous dimensions. Matter fluctuations tend to drive η_h to positive values, which is not the correct sign expected for the unitarization. Note that this expectation is subject to the scale identification $k \sim \sqrt{s}$, which might not capture the quantum effects correctly [81].

5.4 Computing the contribution of gravitinos

It is interesting to include also gravitino fields in the analysis of Section 5.3.3 at least a "one loop" level. The Rarita-Schwinger action[1] in four dimension is

$$S_{RS} = \frac{1}{2}\int d^4x\sqrt{g}\bar{\Psi}_\mu\gamma^{\mu\nu\rho}\nabla_\nu\Psi_\rho \ , \tag{5.44}$$

where $\gamma^{\mu\nu\rho}$ is the full antisymmetric product of three gamma matrices $\gamma^{[\mu}\gamma^\nu\gamma^{\rho]}$. It is convenient to decompose Ψ_μ into irreducible spin representation $((1\oplus 0)\otimes 1/2 = 3/2\oplus 1/2\oplus 1/2)$

$$\Psi_\mu = \Psi^T_\mu + \left(\nabla_\mu - \frac{1}{4}\gamma_\mu\gamma^\nu\nabla_\nu\right)\chi + \frac{1}{4}\gamma_\mu\psi \ , \tag{5.45}$$

where Ψ^T_μ satisfies $\gamma^\mu\Psi^T_\mu = \nabla^\mu\Psi^T_\mu = 0$. The decomposed action is

$$S_{RS} = \frac{1}{2}\int d^4x\sqrt{g}\left(\bar{\Psi}^T_\mu\not{\nabla}\Psi^T_\rho + \frac{3}{16}\bar{\chi}\left(-\nabla^2+\frac{R}{12}\right)\not{\nabla}\chi - \frac{3}{8}\bar{\psi}\left(-\nabla^2+\frac{R}{12}\right)\chi + \frac{3}{16}\bar{\psi}\not{\nabla}\psi\right) \ . \tag{5.46}$$

It's convenient to choose a gauge condition that eliminate the mixing between ψ and χ. This is achieved by the gauge fixing term

$$S_{GF\ RS} = \frac{3}{32\alpha'}\int d^4x\sqrt{g}\bar{F}\left(\not{\nabla}-2\rho\right)F \ , \tag{5.47}$$

where $F = \alpha'\psi + \left(\not{\nabla}+2\rho\right)\chi$ and $\rho = \sqrt{R/12}$. The local supersimmetry transformation that characterize the $N=1$ supergravity theory with parameter ϵ is

$$\delta e^a_\mu = \epsilon\gamma^a\Psi_\mu \ , \tag{5.48}$$

$$\delta\Psi_\mu = \nabla_\mu\epsilon \ , \tag{5.49}$$

performing the decomposition (5.45) one finds

$$\delta\psi = \not{\nabla}\epsilon, \qquad \left(-\nabla^2+\frac{R}{12}\right)(\delta\chi-\epsilon) = 0 \ . \tag{5.50}$$

Therefore the fermionic ghost action is given by

$$S_{gh,F} = \int d^4x\sqrt{g}\bar{\eta}\left[\alpha'\not{\nabla}+\left(\not{\nabla}+2\rho\right)\right]\eta \ . \tag{5.51}$$

[1] We refer to [82] for a Supergravity review.

Given that the gauge fixing involves the operator $\not{\nabla} - 2\rho$ we should also include the correspondent ghosts to ensure on-shell gauge independence. To do so we introduce the couple of ghost fields (Nielsen-Kallosh [83]) ω and γ, with action

$$S_{gh,NK} = \int d^4x\sqrt{g}\left[\bar{\omega}\left(\not{\nabla} - 2\rho\right)\omega + \bar{\gamma}\left(\not{\nabla} - 2\rho\right)\gamma\right] \ . \tag{5.52}$$

At this point is convenient to perform the redefinition $\sqrt{-\nabla^2 + \frac{R}{12}}\chi \to \chi$ whose Jacobian cancels that of the transformation (5.45). The total Rarita-Schwinger action including gauge fixing and ghost terms become

$$\begin{aligned} S_{RS} + S_{gh,F} + S_{gh,NK} = \frac{1}{2}\int d^4x\sqrt{g}\Bigg(&\bar{\Psi}^T_\mu \Delta_{RS}\Psi^T_\rho + \frac{3}{16}\frac{\alpha'+1}{\alpha'}\bar{\chi}\Delta_\chi\chi \\ &+ \frac{3}{16}(\alpha'+1)\bar{\psi}\Delta_\psi\psi + (\alpha'+1)\bar{\eta}\Delta_\eta\eta\Bigg) \ , \end{aligned} \tag{5.53}$$

where the operator Δs are

$$\Delta_{RS} = \not{\nabla} \qquad \Delta^2_{RS} = \Box + \frac{R}{3} \ , \tag{5.54}$$

$$\Delta_\chi = \not{\nabla} + 2\frac{\alpha'}{\alpha'+1}\rho \qquad \Delta^2_\chi = \Box + \frac{R}{4}\left(1 + \frac{4}{3}\left(\frac{\alpha'}{\alpha'+1}\right)^2\right) \ , \tag{5.55}$$

$$\Delta_\psi = \not{\nabla} - 2\frac{\alpha'}{\alpha'+1}\rho \qquad \Delta^2_\psi = \Box + \frac{R}{4}\left(1 + \frac{4}{3}\left(\frac{\alpha'}{\alpha'+1}\right)^2\right) \ , \tag{5.56}$$

$$\Delta_\eta = \not{\nabla} + 2\frac{1}{\alpha'+1}\rho \qquad \Delta^2_\eta = \Box + \frac{R}{4}\left(1 + \frac{4}{3}\frac{1}{(\alpha'+1)^2}\right) \ . \tag{5.57}$$

Finally we can compute the contribution of the fields Ψ^T_μ, χ, ψ and η and the Nielsen-Kallosh ghosts to the gravitational beta functions with a type II cutoff omitting all the anomalous dimensions:

$$\partial_t\Gamma_k = -\frac{1}{2}\mathrm{Tr}\frac{\partial_t R_k\left(\Delta_{RS}\right)}{P_k\left(\Delta_{RS}\right)} - \frac{1}{2}\mathrm{Tr}\frac{\partial_t R_k\left(\Delta_\chi\right)}{P_k\left(\Delta_\chi\right)} - \frac{1}{2}\mathrm{Tr}\frac{\partial_t R_k\left(\Delta_\psi\right)}{P_k\left(\Delta_\psi\right)} \tag{5.58}$$

$$+ \frac{1}{2}\mathrm{Tr}\frac{\partial_t R_k\left(\Delta_\eta\right)}{P_k\left(\Delta_\eta\right)} + \frac{1}{2}\mathrm{Tr}\frac{\partial_t R_k\left(\Delta_\omega\right)}{P_k\left(\Delta_\omega\right)} + \frac{1}{2}\mathrm{Tr}\frac{\partial_t R_k\left(\Delta_\gamma\right)}{P_k\left(\Delta_\gamma\right)} \ . \tag{5.59}$$

In the $\alpha' = 1$ gauge all the squared operators becomes equal to $\Box + R/3$ then it is easy to compute

$$\partial_t\Gamma_k = -\frac{N_{RS}}{2}\frac{1}{(4\pi)^2}\mathrm{Tr}\left[4k^4 - \frac{4}{3}k^2R\right] \ . \tag{5.60}$$

Moreover we can look at the "perturbative" beta functions to get a grasp on the effect of adding minimally coupled spin 3/2 fields to the theory.

$$\beta_{\tilde{G}} = 2\tilde{G} + \frac{\tilde{G}^2}{6\pi}\left(N_S + 2N_D - 4N_V + 4N_{RS} - 46\right) , \tag{5.61}$$

$$\begin{aligned}\beta_{\tilde{\Lambda}} &= -2\tilde{\Lambda} + \frac{\tilde{G}}{4\pi}\left(N_S - 4N_D + 2N_V - 4N_{RS} + 2\right) \\ &\quad + \frac{\tilde{G}\tilde{\Lambda}}{6\pi}\left(N_S + 2N_D - 4N_V + 4N_{RS} - 16\right) .\end{aligned} \tag{5.62}$$

We can notice the Rarita-Schwinger fields give a contribution similar to the fermions. Thus we can safely claim that adding too many of these fields can destroy the gravitational fixed point.

We will limit ourself to a "one loop" computation so we will not compute the anomalous dimension of the spin 3/2 field. Nevertheless it can be interesting to explore within this approximation some explicit matter models as we did in Section 5.3.3. In particular we will look at Supergravity models

model	N_S	N_D	N_V	N_{RS}	$\tilde{G}_*$	$\tilde{\Lambda}_*$	θ_1	θ_2	η_h
SUGRA	0	0	0	1	0.758	0.089	-3.18	-2.17	0.411
mSUGRA	49	61/2	12	1	-	-	-	-	-

Table 5.5: Fixed-point values, critical exponents and anomalous graviton dimension for specific matter content.

As we expected from the one loop analysis the minimal SUper GRAvity model result not compatible within our analysis with the existence of the gravitational fixed point. The Supergravity model sits near the pure gravity fixed point in the number of fields parameter space thus in this case a gravitational FP can be found.

5.5 Running graviton "mass"

In the asymptotic safety framework the effective action at a scale k, where degrees of freedom of momenta higher than k have been integrated out, depends on the background metric and the fluctuation metric, i.e., $\Gamma_k = \Gamma_k[h_{\mu\nu}; \bar{g}_{\mu\nu}]$. Crucially, this dependence is such that one cannot recombine $\bar{g}_{\mu\nu}$ and $h_{\mu\nu}$ to give the full metric, i.e., the effective action is not symmetric under the shift $\bar{g}_{\mu\nu} \to \bar{g}_{\mu\nu} - \gamma_{\mu\nu},\ h_{\mu\nu} \to h_{\mu\nu} + \gamma_{\mu\nu}$.

Two types of terms break this shift symmetry: The first is a regulator term, that is introduced into the path integral to implement a momentum-shell-wise integration: It acts as a mass-like term for fluctuations of low momenta and therefore has the structure $h_{\mu\nu} R_k^{\mu\nu\rho\sigma}\left(\bar{\Delta}\right) h_{\rho\sigma}$, where $\bar{\Delta}$ denotes an operator constructed with the background metric only that include the background-covariant Laplacian. The cutoff function R_k appearing here should not be confused with the Riemann tensor. The second is the gauge fixing term, where the fluctuations are gauge-fixed with respect to the background (3.10). Accordingly, couplings of background operators and fluctuation operators do not share the same beta function. For instance, one can define a Newton coupling from the prefactor of the $\bar{R}$ term in the effective action as we did in the previous chapters, or from the momentum-squared part of the graviton three- or four point function. These three definitions of the Newton coupling obey a different Renormalization Group running.

First explorations of the bimetric structure in asymptotically safe quantum gravity have indicated that the evidence for asymptotic safety from the single-metric approximation is still present when resolving this approximation [22–24, 44, 51]. One should note that at this stage, only few couplings have been considered in a bimetric setting, and higher-order truncations could yield different results. In particular, investigations of quantum gravity coupled to dynamical matter show that significant differences arise between the two treatments [28, 29, 84]. As discussed in [85] using the example of a scalar field, a single-metric approximation can result in spurious fixed points, and a treatment of the full bimetric structure is crucial.

In this Section, we will make a further step forward in disentangling the running of fluctuation and of background couplings by distinguishing the role of the cosmological term in the background and in the two point function.

We will study the following truncation

$$\begin{aligned}\Gamma_k &= \Gamma_{\rm EH} + S_{\rm gf} \\ &= \frac{1}{16\pi G}\int d^dx\sqrt{\bar g}\left(-\bar R + 2\Lambda\right) \\ &\quad + \frac{Z_h}{2}\int d^dx\sqrt{\bar g}\, h_{\mu\nu}K^{\mu\nu\alpha\beta}((-\bar D^2 + M^2)\mathbf{1}^{\rho\sigma}_{\alpha\beta} + W^{\rho\sigma}_{\alpha\beta})h_{\rho\sigma}\ .\end{aligned} \tag{5.63}$$

Here and elsewhere $\mathbf{1}$ is the identity in the space of the fields (in this instance, symmetric tensors), K is given by (5.1).

This truncation goes beyond the approximation $-2\bar\Lambda = M^2$, that was used in in the previous chapters.

The appropriate ghost term for the gauge fixing are the same used in Section 3.2.

Our main new result is the β function for the graviton mass, which reads

$$\begin{aligned}&\beta_{\tilde M^2} \\ &= -2\tilde M^2 + \eta_h\,\tilde M^2 - \frac{2^{9-d}d\,\pi^{1-\frac{d}{2}}\tilde G(6+d-\eta_c)}{(4+d)\,(6+d)\,(-2+3d)\Gamma(d/2)} \\ &\quad + \frac{2^{-d}\pi^{1-\frac{d}{2}}\tilde G}{(d-2)(-2+3d)(1+\tilde M^2)^2\Gamma(3+d/2)}\cdot \\ &\qquad \Big(\tilde\Lambda\cdot(2+d-\eta_h)\Big[-16+d(28+d(44+d(-29+3d)))\Big] \\ &\qquad\quad +(d-2)\,(d(d-1)(72+d(-38+3d)))\,(4+d-\eta_h)\Big) \\ &\quad + \frac{2^{-d}\pi^{1-\frac{d}{2}}\tilde G}{(d-2)(-2+3d)(1+\tilde M^2)^3\Gamma(4+d/2)}\cdot \\ &\quad \cdot\Big(\tilde\Lambda^2(2+d-\eta_h)2(4+d)(6+d)(d^4-19d^3+40d^2+12d-16) \\ &\qquad +\tilde\Lambda(4+d-\eta_h)2(d-2)(d-1)d(6+d)\,(52+d(d-20)) \\ &\qquad +(6+d-\eta_h)\frac{d-2}{2}(d-1)d(2+d)\,(60+d(d-22))\Big)\ .\end{aligned} \tag{5.64}$$

The computation is performed on flat background by setting to zero the external momenta of diagrams 5.1 and 5.2.

The other beta functions can be deduced from the beta functions and anomalous dimensions given in [84], with the replacement $\tilde\Lambda \to -\frac{1}{2}\tilde M^2$. Note that we make the following approximation here: while all n graviton vertices and graviton-matter vertices have their own, independent couplings, in a first step we will identify these with the background couplings. Accordingly, the

momentum-independent 3- and 4-graviton vertices are $\sim \tilde{\Lambda}$, which explains the occurrence of $\tilde{\Lambda}$ in the numerator of the β functions.

As a first major result we find that the interacting fixed point found in previous calculations exists under the extension of the graviton mass: We find two interacting fixed points, one of which is clearly an extension of the well-known one. This fixed point (which we call FP1) has three relevant directions, cf. tab. 5.6, and is connected to the Gaussian fixed point by a separatrix. The other fixed point has two relevant directions, but is not connected to the Gaussian fixed point. We conclude that only the first fixed point features a trajectory emanating from it, which connects this UV-completion to a classical regime, where G and Λ assume their measured values.

The fixed-point values and critical exponents are close to those reported in [52].

Here and in the following, we will mainly focus on the "one-loop" form of the beta functions, which simply implies that we neglect terms $\sim \eta$ on the right-hand-side of the equations for the anomalous dimensions. The main reason is that the full RG-improved structure of the equations can induce further fixed points, that are not present in the one-loop equations, and are induced purely by the RG-improvement. Since the RG-improvement arises from a particular choice of regulator, where R_k depends on the wave-function renormalization, any fixed point induced by that particular structure is presumably spurious. In cases where the fixed point exists in both the one-loop and the RG-improved equations, and $\eta < 1$, the RG-improved result is expected to be quantitatively more precise.

As is to be expected from the fact that the fixed point called FP2 has an irrelevant direction, there is a trajectory emanating from FP1 and hitting FP2 in the infrared. This trajectory is both UV and IR complete, and could in principle define a complete quantum theory of gravity. However it is easy to see that it does not feature a semi-classical regime, where both G and Λ assume their measured value. This complete trajectory is therefore ruled out experimentally.

	$\tilde{G}_*$	$\tilde{\Lambda}_*$	$\tilde{M}_*^2$	θ_1	θ_2	θ_3	η_h	η_c
FP1 full	0.622	0.051	-0.341	3.92	1.37 + i 0.93	1.37 - i 0.93	0.53	-1.26
FP2 full	0.52	0.08	-0.58	4.10	1.71	-3.64	1.30	-2.17
FP1 one-loop	0.62	0.05	-0.33	3.94	1.39 + i 0.91	1.39 - i 0.91	0.50	-1.26
FP2 one-loop	0.52	0.075	-0.56	4.22	1.70	-3.57	1.25	-2.24

Table 5.6: Fixed-point values and critical exponents of the two interacting fixed points in the one-loop approximation and the full system.

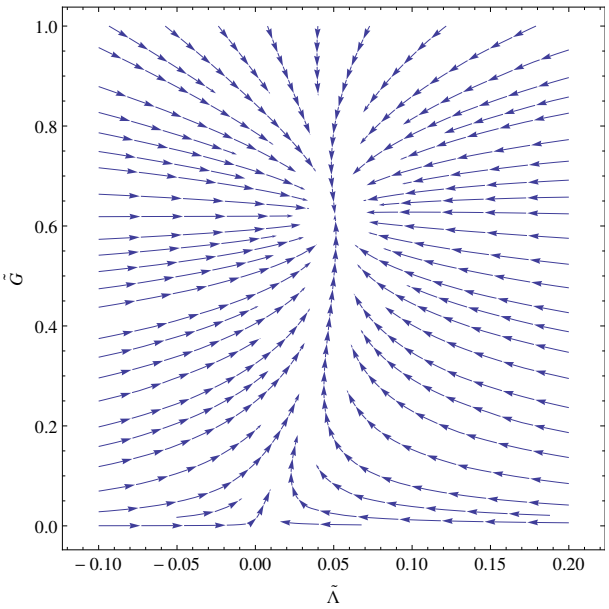

Figure 5.18: The flow near the FP1 in the $\tilde{\Lambda}\tilde{G}$ plane at fixed $\tilde{M}^2 = -0.341$.

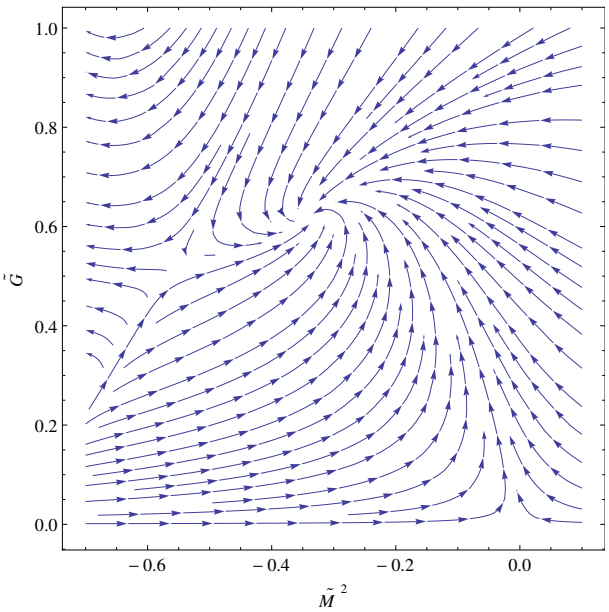

Figure 5.19: The flow near FP1 in the $\tilde{M}^2\tilde{G}$ plane at fixed $\tilde{\Lambda} = 0.05$. The "FP" on the far left is what will become FP2 for $\tilde{\Lambda} = 0.075$

In Fig. 5.18 we can look at the RG flow in the $\tilde{\Lambda}$-$\tilde{G}$ plane. The critical exponent in this plane are real similarly of what is seen in [44] while in the $\tilde{M}^2 - \tilde{G}$ plane they are complex as often seen in the literature results where $\Lambda \sim M^2$.

In comparison to the result in of Section 5.1.1, where the graviton mass was identified with the background cosmological constant, the fixed-point values and critical exponents change quantitatively, but not qualitatively. Lifting the approximation $\Lambda \sim M^2$ also implies that there is no longer a singularity in the Renormalization Group flow at $\tilde{\Lambda} = \frac{1}{2}$. As for any massive field, there is now a singularity at $\tilde{M}^2 = -1$.

To analyze the RG flow of the mass in the infrared, we can use a perturbative approximation in the vicinity of the Gaussian fixed point:

$$\beta_{\tilde{M}^2} = -2\tilde{M}^2 - \frac{87}{40\pi}\tilde{G} + \frac{59}{30\pi}\tilde{G}\,\tilde{M}^2 + \frac{12}{5\pi}\tilde{G}\,\tilde{\Lambda} - \frac{27}{10\pi}\tilde{G}\,\tilde{\Lambda}\tilde{M}^2 \ . \qquad (5.65)$$

For the "RG trajectory of our universe" [72], $\tilde{G}$ runs to very small values in the infrared. Although $\tilde{\Lambda}$ grows, such that $\Lambda \approx$ constant, this running only has a negligible influence on M^2, as all non trivial terms in (5.65) are proportional to at least one power of $\tilde{G}$. Accordingly we observe that the running of $\tilde{M}^2$ is driven mostly by the term arising from the canonical dimensionality, which simply reflects the rescaling of $\tilde{M}$ under a redefinition of scale. For the separatrix we have correctly that $M \to 0$ in the IR.

5.6 Tetrad gravity revisited

It is worth now to go back to the analysis of Chapter 4 on the stability of the gravitational fixed point in the tetrad formalism using the expression of the gravitational anomalous dimensions computed in Section 5.1.1. Since the graviton is not decomposed in our previous computations we will look only at the type Ia cutoff in the $\alpha = 1$ gauge (analysed in [36]) and at the type IIa cutoff. Since we are fixing the gauge to a specific value we have to limit ourselves just to the analysis the dependence of the FP on the $O(d)$ ghost mass parameter.

In Section 4.3 we reviewed the analysis performed with a type Ia cutoff and completely neglecting the Lorentz ghosts ($\tilde{\mu} \to \infty$). The existence of a non-Gaussian fixed point for any value of the dimensionless constant $\tilde{\mu}$ was found: for small values of $\tilde{\mu}$ the FP is UV attractive with two real critical exponents, which then turn into a complex conjugated pair as $\tilde{\mu}$ increases and for a critical value of $\tilde{\mu} \approx 1.35$ the FP changes its character and becomes UV repulsive in both directions. It was also noted the presence of a limit circle around the FP [36].

Then we looked at the type IIa case. A nontrivial FP exists and has complex critical exponents for all values of $\tilde{\mu}$ greater than a critical value $\tilde{\mu}_c \approx 0.748$ for $\alpha = 1$. For small $\tilde{\mu}$ the FP moves towards negative values of $\tilde{\Lambda}$. For large $\tilde{\mu}$ the fixed point remains UV attractive, in contrast to the result found in [36] with the type Ia cutoff scheme.

It is interesting to check if lifting the approximation $\eta_h = \partial_t \log G_k$, using the prescription presented in Section 5.1.1, we can find a different dependence on $\tilde{\mu}$ of the FP. We performed the computation using (5.2) and (5.6) in the "one loop" approximation.

The result are more stable with respect to the old "RG-improved" scheme. A nontrivial FP exists and has real critical exponents for all values of $\tilde{\mu}$, the value of the cosmological constant $\tilde{\Lambda}$ at the FP is always slightly negative.

In Fig. 5.20 to 5.21 we plot the dependence on the dimensionless parameter $\tilde{\mu}$ of the critical exponents. It is interesting to compare these figures with the corresponding one computed before Fig. 4.3 Fig. 4.4.

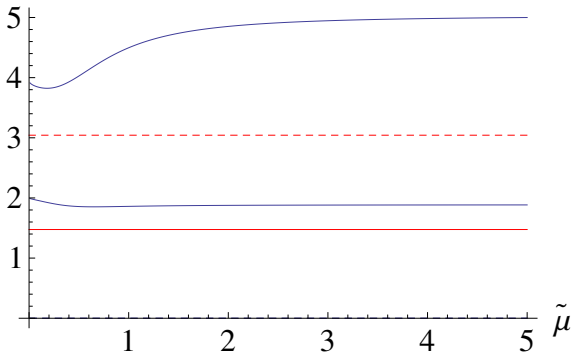

Figure 5.20: Critical Exponents as functions of the $\tilde{\mu}$ parameter for type Ia cutoff. The continuous line is the real part of the critical exponent, the dashed line the imaginary part of the critical exponent. In red the metric case is given for reference.

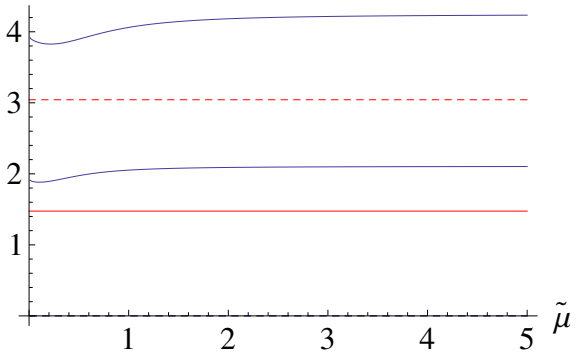

Figure 5.21: Critical Exponents as functions of the $\tilde{\mu}$ parameter for type IIa cutoff. The continuous line is the real part of the critical exponent, the dashed line the imaginary part of the critical exponent. In red the metric case is given for reference.

Conclusion

In this thesis we have mostly reviewed and extended recent work on the asymptotic safety approach to quantum gravity coupled to matter fields. In this approach, the metric (or the d-bein) is taken seriously as the carrier of the fundamental degrees of freedom and one remains within the well tested framework of QFT. The central hypothesis to make this procedure work in spite of the well-known difficulties is the existence of a nontrivial FP for gravity, having finitely many UV-attractive directions. In this way one can obtain a well-defined UV scaling limit which is not seen in perturbation theory and retain predictivity, which is lost in perturbation theory due to the necessity of introducing an infinite number of counterterms. In particular we have focussed on three topics.

How to build a good cutoff term for fermion fields. The implementation of the FRGE in the presence of fermions and gravity presents some subtleties that had not been fully appreciated until recently. The sign ambiguity of the fermionic contribution to the running of Newton's constant had been known for a while, but it was regarded as just another aspect of the scheme dependence that is intrinsic to applications of the FRGE, albeit a particularly worrying one. Although a completely satisfactory understanding can come only from a treatment of physical observables, we have argued in the first half of Chapter 4 that the correct treatment of fermion fields, when the Dirac operator is squared, is to use a cutoff that depends on $-D^2 + \frac{R}{4}$ (type II cutoff). There also follows from our discussion that using a cutoff that depends on $-D^2$ (type I cutoff) may give physically incorrect results.

What are the correct fundamental degrees of freedom to describe gravity in presence of fermions? In the second half of Chapter 4 we studied the RG flow of gravity in the tetrad formulation, extending the analysis initiated in [36] by using a different cutoff (type Ib and IIb vs. type Ia) which allowed us to keep the diffeomorphism gauge parameter α arbitrary. We have found that the results for the running couplings using the tetrad

formalism are qualitatively similar to those of the metric formalism, with some quirks.

In the metric formalism the type IIb cutoff with generic α had never been used before and the results obtained here are new. We have shown that for $\alpha = 1$ they coincide with the ones for the type IIa cutoff. For other values of α they differ only marginally from those obtained with other cutoff types and confirm the stability of the fixed point in the metric formalism. Type II cutoffs have the attractive feature that they lead to somewhat more compact expressions for the beta functions.

In the tetrad formalism a new ambiguity appears in the definition of the ghost sector: it can be parametrized by a mass μ that appears in the mixing between diffeomorphism and Lorentz ghosts, or by the corresponding dimensionless parameter $\tilde{\mu} = \mu/k$. This parameter is *a priori* arbitrary, but in order not to introduce additional mass scales into the problem it is natural to assume that it is of order one. On the other hand we recall that in perturbation theory and in the chosen gauge the Lorentz ghosts are neglected, since they do not propagate. This corresponds to taking $\tilde{\mu} = \infty$. It would be natural to treat μ as a running coupling; we show in Appendix of Chapter 4 that in the approximations used here its beta function vanishes. Thus $\tilde{\mu}$ would tend to infinity for $k \to 0$ (which agrees with the standard perturbative prescription) and to zero for $k \to \infty$. It is conceivable that the presence of more complicated ghost interactions, whose existence has been discussed in [42], could generate a nontrivial fixed point for $\tilde{\mu}$.

If one uses a type Ia cutoff and completely neglects the Lorentz ghosts, there is no attractive FP for positive G [36]. Instead, one finds a UV repulsive fixed point surrounded by a UV attractive limit cycle. This is not the case when one imposes the cutoff separately on each spin component, as we did here. We find that with both type Ib and IIb cutoffs an attractive FP with complex critical exponents is present also when Lorentz ghosts are neglected, for both $\alpha = 1$ and $\alpha = 0$. This is reassuring because in the metric formalism the fixed point can be found even using the perturbative one loop beta functions.

If the contribution of Lorentz ghosts is added, as advocated in [36], its effect is weighted by the parameter $\tilde{\mu}$: it is strong for small $\tilde{\mu}$ and weak for large $\tilde{\mu}$. Since the ghosts are fermions, the fixed point is shifted toward negative Λ for decreasing $\tilde{\mu}$. In addition, they have a systematic effect on the critical exponents, in the $\alpha = 1$ gauge the modulus of the imaginary part decreases with decreasing $\tilde{\mu}$ and there is a critical value $\tilde{\mu}_c$ under which the critical exponents become real, in the $\alpha = 0$ gauge the real part of the critical exponents becomes negative for $\tilde{\mu} \approx 1.4$, and this marks the appearance of the limit cycle. With the type II cutoffs discussed here the effect is much

weaker and the fixed point becomes only slightly less attractive even in the limit $\tilde{\mu} \to \infty$ in both gauges.

Using type b cutoffs has the advantage that one can keep the diffeomorphism gauge parameter α arbitrary. The gauge dependence of the critical exponents is similar to what had been observed previously in the metric formalism, as long as α is not too much greater than one.

On the other hand for α somewhat larger than one the fixed point becomes either complex or repulsive. All these phenomena are probably unphysical artifact of the identification of η_h with η_G. This is supported by the discussion in Section 5.6 where we have seen that if we use the gravitational anomalous dimensions computed from the two point functions the interacting FP always exist and become almost insensitive to the value of $\tilde{\mu}$.

In conclusion, let us comment on the use of tetrad versus metric variables. Since fermions exists in nature, it may seem in principle inevitable that gravity has to be described by tetrads. This would complicate the theory significantly. Every diffeomorphism–invariant functional of the metric can be viewed as a diffeomorphism and local Lorentz–invariant functional of the tetrad, but in the bimetric formalism there are many functionals of two tetrads that cannot be viewed as functionals of two metrics. Therefore, as already noted in [36], the tetrad theory space is much bigger than the metric theory space.

The necessity of using tetrads should, however, not be taken as a foregone conclusion. First of all, it is possible that the fermions occurring in nature are Kähler fermions. This would completely remove the argument for the use of tetrads, even in principle. Whether this is the case is a difficult issue that should be answered experimentally.

Using Dirac-Kähler fermions is possible to formulate extension of the Standard Model based on Dirac-Kähler spinors [86]. One Dirac-Kähler fermion correspond to the degree of freedom of four Dirac fermion fields. This extra fermion field is interpreted as a new flavor. The observation of a 4th generation would boost the prospects of this model. Non-observation pushes the limits of the masses of the fourth generation. Current observations are against the realization in Nature of this model.

For the time being one might just consider the use of Kähler fermions as a computational trick. Second, even if we stick to spinor matter, by squaring the Dirac operator and using a type II cutoff one can calculate many quantum effects due to fermions without ever having to use tetrad fields.

Does matter matter in asymptotically safe quantum gravity? In Chapter 5 of this thesis we have re-examined the compatibility of minimally

coupled matter degrees of freedom with the asymptotic safety scenario for gravity. This issue had been addressed before [28, 29], but advances in our understanding in the intervening ten years lead to corrections and improvements. Our present treatment differs in two crucial ways. One is the way the cutoff is implemented on fermions: In accord with our discussion in Chapter 4 the cutoff is chosen to be of type II (a function of $-\Box + \frac{R}{4}$) while in [28,29] the cutoff was chosen to be a function of $-\Box$ (so-called type I cutoff).

The second difference is in the treatment of the anomalous dimension of the graviton. In order to close the flow equations, the approximation $\eta_h = \eta_N \equiv \partial_t G/G$ was often made earlier. However, the effective average action $\Gamma_k(h_{\mu\nu}; \bar{g}_{\mu\nu})$ is a functional of two fields: the background metric and the fluctuation, and the wave function renormalization of the fluctuation has a different scale dependence from $1/G$, which appears as a prefactor in the background part of the action. We have followed here the calculation of the graviton anomalous dimension of [44], but adopting a slightly different definition of the anomalous dimension. Additionally, we have explicitly calculated the matter anomalous dimensions, which also enter the gravitational beta functions. As a result of these changes, the allowed region in the (N_S, N_D, N_V) space is quite different from that of [28, 29].

Our main finding is that within the Einstein-Hilbert truncation for the gravitational degrees of freedom, and with minimally coupled matter, there are upper limits on the allowed number of scalar and fermionic degrees of freedom. Increasing the number of vector fields leads to weaker bounds. Focusing on models of particular interest, we find that the standard model matter content is compatible with an appropriate fixed point.

Small extensions of the SM, e.g., the inclusion of right-handed neutrinos, an axion and a scalar dark matter particle, are still compatible, but big enlargements are highly problematic. In spite of the increase in the number of gauge fields, realistic GUTs have too many scalars. Things would improve assuming that the gauge symmetry is broken dynamically, but we are not aware of detailed models of this type. The MSSM does not show a viable fixed point within our approximations. Models with a larger number of vector degrees of freedom, such as technicolor models, can accommodate a larger number of fermions and still be compatible with the existence of the fixed point.

Including gravitinos does not help the existence of the FP, their effect is similar to the one of fermion and scalar fields. A suitable fixed point exist in the simple $N = 1$ SUGRA, it does not exist in mSUGRA.

Going to a larger number of dimensions, we find that the allowed region for the matter content shrinks, and there is no viable gravitational fixed point compatible with the standard model matter content in $d = 6$, while the case

$d = 5$ is in the balance. This indicates that while the gravitational dynamics allows for a fixed point in any number of dimensions [77,78], matter dynamics is sensitive to the dimensionality, and tend to destroy the gravitational fixed point above $d = 4$. Extrapolating the trend from d=4, 5, 6, we do not expect that the standard model is compatible with a nontrivial gravitational fixed point in any number of extra dimensions. Our work thus indicates that a realistic model of asymptotically safe gravity, which includes dynamical matter, disfavors scenarios with universal extra dimensions. In the future, it could be interesting to examine this in extended truncations, and to study different models for extra dimensions. For instance, our conclusion could change if only gravity can propagate into the extra dimensions, but matter fields cannot.

We also examined the effect of matter degrees of freedom on the quantum gravity scale. In the asymptotic safety scenario this is the dynamically generated transition scale to the fixed-point regime. Physical observables will presumably exhibit a change of behavior at this scale, even though there is not strictly speaking a phase transition. We find that, fixing the IR value of the Newton coupling and the cosmological constant to small positive values and integrating toward the UV, the fixed-point scale is moved to higher values under the inclusion of matter, e.g., in the standard model case. We trace this back to the fact that for the standard model, the fixed-point coordinates are further away from the Gaussian fixed point, in the vicinity of which the RG flow towards the UV starts at low scales. Having a higher transition scale implies that effects of asymptotic safety might become more challenging to detect,

We will discuss now what are the limit of our results due to the approximations we adopted.

First of all, we have restricted ourselves to the cosmological and Newton coupling. This is partly justified by the fact that in extended truncations they are confirmed to be the most relevant ones. Perhaps some further support for this approximation comes from one loop calculations, where the (universal) four-derivative terms do not yield new constraints on matter, and where there exists at least one cutoff scheme where the same is true of all higher derivative terms.

Our calculations involve rather large uncertainties, so most results should be taken as broad trends rather than precise statements. The beta functions are obtained by off-shell calculations and are gauge-dependent. We have used throughout the Feynman-de Donder gauge $\alpha = 1$. Regarding the "scheme"-dependence, most results have been given at one loop and with a type II cutoff on all degrees of freedom, but we have thoroughly studied also the case with a type Ia cutoff on the gravitons, and (with both cutoffs) the RG-improved

flow equations.

In the perturbative approximation we have found that using the type Ia cutoff leads to a restriction of the allowed region by 12 Dirac fields or 24 scalar fields. This can be taken as a typical theoretical uncertainty in this type of calculation. Having given the results for the less restrictive type II cutoff, it is likely that we have erred by allowing models that are forbidden, rather than the converse. Detailed calculations with different schemes and/or different gauges will be necessary to sharpen the boundary of the allowed region.

Another strong limitation is the truncation on the gravitational action. Even within the context of terms with two derivatives only, due to the natural bi-metric dependence of the effective average action, there is a difference between the cosmological and Newton couplings that multiply the background field terms, and the coefficients of the terms involving powers of the fluctuation $h_{\mu\nu}$. In most of the literature, the coefficients of the fluctuation terms have been treated as in the expansion of the Einstein-Hilbert action, thus identifying them with the cosmological and Newton coupling. Here we have made a first distinction between the background Newton coupling and the coefficient of the p^2h^2 term, which we called Z_h and a distinction between the background Cosmological constant and the coefficient of the h^2 term, which we called M^2 "mass" term.

Perhaps most importantly, we have neglected all matter self-interactions. From [41] it is known that quantum gravity fluctuations induce momentum-dependent matter self-interactions, which couple back into the anomalous dimensions. We expect that our boundaries in the (N_S, N_D, N_V)-space will change under a corresponding extension of the truncation.

In spite of these limitations, this work clearly shows that "matter matter" in asymptotically safe quantum gravity. Asymptotic safety might not be compatible with arbitrary extensions of the Standard Model; e.g., supersymmetric extensions and higher dimensions seem to be disfavoured. This opens a new route to obtain experimental guidance in the construction of a viable model of quantum gravity: The discovery of many new fundamental matter fields at the LHC or future colliders could potentially lead to a situation that is theoretically inconsistent with asymptotic safety.

Bibliography

[1] G. 't Hooft and M. J. G. Veltman, Annales Poincare Phys. Theor. A **20** (1974) 69.

[2] M. H. Goroff and A. Sagnotti, Phys. Lett. B **160** (1985) 81.

[3] M. H. Goroff and A. Sagnotti, Nucl. Phys. B **266** (1986) 709.

[4] J. Polchinski, Cambridge, UK: Univ. Pr. (1998) Vol ! and 2

[5] C. Rovelli, Living Rev. Rel. **11** (2008) 5.

[6] S. Weinberg, *In *Hawking, S.W., Israel, W.: General Relativity*, 790-831* (Cambridge University Press, Cambridge, 1980).

[7] K. G. Wilson, Phys. Rev. B **4**, 3174 (1971);
K. G. Wilson, Phys. Rev. B **4**, 3184 (1971);
K. G. Wilson and J. B. Kogut, Phys. Rept. **12** (1974) 75;
K. G. Wilson, Rev. Mod. Phys. **47**, 773 (1975).

[8] C. Wetterich, 'Phys. Lett. B **301**, 90 (1993).

[9] T. R. Morris, Int. J. Mod. Phys. A **9** (1994) 2411 [hep-ph/9308265].

[10] B. Delamotte, arXiv:cond-mat/0702365

[11] D. F. Litim, Phys. Rev. D **64**, 105007 (2001) [hep-th/0103195].

[12] S.M. Christensen and Michael J. Duff (1978).Phys. Lett. B **79**, 213.

[13] R. Gastmans, R. Kallosh and C. Truffin (1978). Nucl. Phys. B **133**, 417.

[14] M. Reuter, Phys. Rev. D **57**, 971 (1998) [hep-th/9605030].

[15] M. Reuter and C. Wetterich, Nucl. Phys. B **417** (1994) 181.

[16] M. Reuter and C. Wetterich, Nucl. Phys. B **427** (1994) 291.

[17] I. L. Buchbinder, S. D. Odintsov and I. L. Shapiro, Bristol, UK: IOP (1992) 413 p

[18] A. Codello, R. Percacci and C. Rahmede, Annals Phys. **324**, 414 (2009) [arXiv:0805.2909 [hep-th]].

[19] D. Dou and R. Percacci, Class. Quant. Grav. **15** (1998) 3449 [hep-th/9707239].

[20] P. Donà and R. Percacci, Phys. Rev. D **87**, no. 4, 045002 (2013) [arXiv:1209.3649 [hep-th]].

[21] F. Larsen and F. Wilczek, Nucl. Phys. B **458** (1996) 249 [hep-th/9506066].

[22] E. Manrique and M. Reuter, Annals Phys. **325**, 785 (2010) [arXiv:0907.2617 [gr-qc]].

[23] E. Manrique, M. Reuter and F. Saueressig, Annals Phys. **326**, 440 (2011) [arXiv:1003.5129 [hep-th]].

[24] E. Manrique, M. Reuter and F. Saueressig, Annals Phys. **326**, 463 (2011) [arXiv:1006.0099 [hep-th]].

[25] E. Kähler, *Rendiconti di Matematica (3-4)* **21**, 425 (1962).

[26] W. Graf, Annales Poincare Phys. Theor. **29** (1978) 85.

[27] I. M. Benn and R. W. Tucker, Commun. Math. Phys. **89** (1983) 341.

[28] R. Percacci and D. Perini, Phys. Rev. D **67**, 081503 (2003) [hep-th/0207033].

[29] R. Percacci and D. Perini, Phys. Rev. D **68**, 044018 (2003) [hep-th/0304222].

[30] G. Narain and R. Percacci, Classical Quantum Gravity **27**, 075001 (2010); G. Narain and C. Rahmede, Classical Quantum Gravity **27**, 075002 (2010).

[31] D. Benedetti, P. F. Machado and F. Saueressig, Nucl. Phys. B **824** (2010) 168 [arXiv:0902.4630 [hep-th]].

[32] R. Percacci, Phys. Rev. D **73**, 041501 (2006) [hep-th/0511177].

[33] O. Zanusso, L. Zambelli, G. P. Vacca and R. Percacci, Phys. Lett. B **689**, 90 (2010) [arXiv:0904.0938 [hep-th]].

[34] A. Rodigast and T. Schuster, Phys. Rev. Lett. **104** (2010) 081301 [arXiv:0908.2422 [hep-th]].

[35] G. P. Vacca and O. Zanusso, Phys. Rev. Lett. **105**, 231601 (2010) [arXiv:1009.1735 [hep-th]].

[36] U. Harst and M. Reuter, JHEP **1205**, 005 (2012) [arXiv:1203.2158 [hep-th]].

[37] O. Lauscher and M. Reuter, Phys. Rev. D **65**, 025013 (2002).

[38] C. Rahmede, Ph.D. thesis, SISSA. 2008.

[39] A. Eichhorn and H. Gies, New J. Phys. **13**, 125012 (2011) [arXiv:1104.5366 [hep-th]].

[40] H. Gies and S. Lippoldt, arXiv:1310.2509 [hep-th].

[41] A. Eichhorn, Phys. Rev. D **86**, 105021 (2012) [arXiv:1204.0965 [gr-qc]].

[42] A. Eichhorn, Phys. Rev. D **87**, 124016 (2013) [arXiv:1301.0632 [hep-th]].

[43] M. Shaposhnikov and C. Wetterich, Phys. Lett. B **683**, 196 (2010) [arXiv:0912.0208 [hep-th]].

[44] A. Codello, G. D'Odorico and C. Pagani, arXiv:1304.4777 [gr-qc].

[45] A. Eichhorn and H. Gies, Phys. Rev. D **81**, 104010 (2010) [arXiv:1001.5033 [hep-th]].

[46] R. P. Woodard, Phys. Lett. B **148**, 440 (1984).

[47] P. van Nieuwenhuizen, Phys. Rev. D **24**, 3315 (1981).

[48] J. -E. Daum, U. Harst and M. Reuter, JHEP **1001**, 084 (2010) [arXiv:0910.4938 [hep-th]].

[49] K. Groh and F. Saueressig, J. Phys. A **43**, 365403 (2010) [arXiv:1001.5032 [hep-th]].

[50] I. Donkin and J. M. Pawlowski, arXiv:1203.4207 [hep-th].

[51] N. Christiansen, D. F. Litim, J. M. Pawlowski and A. Rodigast, Phys. Lett. B **728**, 114 (2014) [arXiv:1209.4038 [hep-th]].

[52] N. Christiansen, B. Knorr, J. M. Pawlowski and A. Rodigast, arXiv:1403.1232 [hep-th].

[53] M. Reuter and F. Saueressig, Phys. Rev. D **65**, 065016 (2002) [hep-th/0110054].

[54] G. Narain and R. Percacci, Acta Phys. Polon. B **40**, 3439 (2009) [arXiv:0910.5390 [hep-th]].

[55] K. Falls, D. F. Litim, K. Nikolakopoulos and C. Rahmede, arXiv:1301.4191 [hep-th].

[56] S. Folkerts, D. F. Litim and J. M. Pawlowski, Phys. Lett. B **709**, 234 (2012) [arXiv:1101.5552 [hep-th]].

[57] U. Harst and M. Reuter, JHEP **1105**, 119 (2011) [arXiv:1101.6007 [hep-th]].

[58] D. J. Toms, Phys. Rev. D **84**, 084016 (2011).

[59] J. M. Cline, K. Kainulainen, P. Scott and C. Weniger, Phys. Rev. D **88**, 055025 (2013) [arXiv:1306.4710 [hep-ph]].

[60] V. Silveira and A. Zee, Phys. Lett. B **161**, 136 (1985).

[61] J. McDonald, Phys. Rev. D **50**, 3637 (1994) [hep-ph/0702143 [HEP-PH]].

[62] C. P. Burgess, M. Pospelov and T. ter Veldhuis, Nucl. Phys. B **619**, 709 (2001) [hep-ph/0011335].

[63] R. D. Peccei and H. R. Quinn, Phys. Rev. Lett. **38**, 1440 (1977); Phys. Rev. D **16**, 1791 (1977).

[64] S. Weinberg, Phys. Rev. Lett. **40**, 223 (1978);

[65] F. Wilczek, Phys. Rev. Lett. **40**, 279 (1978).

[66] R. Essig, J. A. Jaros, W. Wester, P. H. Adrian, S. Andreas, T. Averett, O. Baker and B. Batell *et al.*, arXiv:1311.0029 [hep-ph].

[67] S. Bertolini, L. Di Luzio and M. Malinsky, Phys. Rev. D **80**, 015013 (2009) [arXiv:0903.4049 [hep-ph]].

[68] F. Sannino, Acta Phys. Polon. B **40**, 3533 (2009) [arXiv:0911.0931 [hep-ph]].

[69] D. F. Litim and T. Plehn, Phys. Rev. Lett. **100**, 131301 (2008) [arXiv:0707.3983 [hep-ph]].

[70] E. Gerwick, D. Litim and T. Plehn, Phys. Rev. D **83**, 084048 (2011) [arXiv:1101.5548 [hep-ph]].

[71] B. Dobrich and A. Eichhorn, JHEP **1206**, 156 (2012) [arXiv:1203.6366 [gr-qc]].

[72] M. Reuter and H. Weyer, JCAP **0412**, 001 (2004) [hep-th/0410119].

[73] X. Calmet, S. D. H. Hsu and D. Reeb, Phys. Rev. Lett. **101**, 171802 (2008) [arXiv:0805.0145 [hep-ph]].

[74] W. E. East and F. Pretorius, Phys. Rev. Lett. **110**, no. 10, 101101 (2013) [arXiv:1210.0443 [gr-qc]].

[75] S. Basu and D. Mattingly, Phys. Rev. D **82**, 124017 (2010) [arXiv:1006.0718 [hep-th]].

[76] K. Falls, D. F. Litim and A. Raghuraman, Int. J. Mod. Phys. A **27**, 1250019 (2012) [arXiv:1002.0260 [hep-th]].

[77] P. Fischer and D. F. Litim, Phys. Lett. B **638**, 497 (2006) [hep-th/0602203].

[78] N. Ohta and R. Percacci, arXiv:1308.3398 [hep-th].

[79] G. Aad *et al.* [ATLAS Collaboration], JHEP **1304**, 075 (2013) [arXiv:1210.4491 [hep-ex]].

[80] G. Aad *et al.* [ATLAS Collaboration], New J. Phys. **15**, 043007 (2013) [arXiv:1210.8389 [hep-ex]].

[81] M. M. Anber and J. F. Donoghue, Phys. Rev. D **85**, 104016 (2012) [arXiv:1111.2875 [hep-th]].

[82] P. Van Nieuwenhuizen, Phys. Rept. **68** (1981) 189.

[83] N. K. Nielsen, Nucl. Phys. B **140** (1978) 499.

[84] P. Donà, A. Eichhorn and R. Percacci, Phys. Rev. D **89** (2014) 084035 [arXiv:1311.2898 [hep-th]].

[85] I. H. Bridle, J. A. Dietz and T. R. Morris, JHEP **1403** (2014) 093 [arXiv:1312.2846 [hep-th]].

[86] A. N. Jourjine, arXiv:0804.2102 [hep-ph].
A. N. Jourjine, Phys. Lett. B **693** (2010) 149 [arXiv:1005.3593 [hep-ph]].
A. N. Jourjine, Phys. Lett. B **695** (2011) 482 [arXiv:1011.0382 [hep-ph]].
A. N. Jourjine, arXiv:1101.2993 [hep-ph].